

---

**Pacific Northwest  
National Laboratory**

Operated by Battelle for the  
U.S. Department of Energy

## Detection of Periodic Beacon Loads in Electrical Distribution Substation Data

D.J. Hammerstrom  
R.T. Guttromson  
N. Lu  
P.A. Boyd

D.J. Trudnowski  
D.P. Chassin  
C.A. Bonebrake  
J.M. Shaw

May 2006



Prepared for  
U.S. Department of Energy  
Under Contract DE-AC05-76RL01830

---

## DISCLAIMER

This report was prepared as an account of work sponsored by an agency of the United States Government. Neither the United States Government nor any agency thereof, nor Battelle Memorial Institute, nor any of their employees, makes **any warranty, express or implied, or assumes any legal liability or responsibility for the accuracy, completeness, or usefulness of any information, apparatus, product, or process disclosed, or represents that its use would not infringe privately owned rights.** Reference herein to any specific commercial product, process, or service by trade name, trademark, manufacturer, or otherwise does not necessarily constitute or imply its endorsement, recommendation, or favoring by the United States Government or any agency thereof, or Battelle Memorial Institute. The views and opinions of authors expressed herein do not necessarily state or reflect those of the United States Government or any agency thereof.

PACIFIC NORTHWEST NATIONAL LABORATORY  
*operated by*  
BATTELLE  
*for the*  
UNITED STATES DEPARTMENT OF ENERGY  
*under Contract DE-AC05-76RL01830*

Printed in the United States of America

Available to DOE and DOE contractors from the  
Office of Scientific and Technical Information,  
P.O. Box 62, Oak Ridge, TN 37831-0062;  
ph: (865) 576-8401  
fax: (865) 576-5728  
email: reports@adonis.osti.gov

Available to the public from the National Technical Information Service,  
U.S. Department of Commerce, 5285 Port Royal Rd., Springfield, VA 22161  
ph: (800) 553-6847  
fax: (703) 605-6900  
email: orders@ntis.fedworld.gov  
online ordering: <http://www.ntis.gov/ordering.htm>



This document was printed on recycled paper.

# **Detection of Periodic Beacon Loads in Electrical Distribution Substation Data**

D.J. Hammerstrom  
R.T. Guttromson  
N. Lu  
P.A. Boyd

D.J. Trudnowski  
D.P. Chassin  
C.A. Bonebrake  
J.M. Shaw

May 2006

Prepared for  
the U.S. Department of Energy  
under Contract DE-AC05-76RL01830

Pacific Northwest National Laboratory  
Richland, Washington 99352



## Executive Summary

A study was undertaken to investigate whether periodic “beacon loads” could be detected from available substation feeder data of the type and quality available from utility SCADA. The detection of such beacons could provide power system utilities with a mechanism for various loads to send messages over their distribution lines to the substations at no cost, using existing SCADA infrastructure.

The implications of such a unique communications scheme are that the utility can gain detailed knowledge of system load status without the need for an external communications system in place. Such communications would primarily benefit applications such as demand-side management or infrastructure diagnostic indicators, such as overloaded capacity indications.

This study has revealed several unique and pertinent properties of power system load feeder data. It is important to recognize that the conclusions are based on the data analyzed and observed through laboratory simulation and a specific field study.

1. Initial beacon simulations demonstrated the potential for using statistical spectral analysis to detect a periodic beacon. Both the power spectral density and correlation of time-separated signals proved to detect beacon signals.
2. There is no significant difference in the noise content of the phase current when comparing seasons (winter, spring, summer, and fall) based on the analyses of Vista and Benton City substation data that represent commercial and residential feeders. We lack adequate data to make this claim for agricultural or industrial feeders.
3. All noise tends to roll off at a rate of approximately  $-20\text{dB/decade}$  in the power spectrum. This finding was remarkably constant for all feeder data analyzed.
4. There is only a slight difference in the normalized noise content during light loading conditions versus heavy loading. Therefore, it is likely that if one can detect a beacon having a peak power  $0.05\%$  of the feeder’s loading under a heavy loaded condition, then one could also detect a comparable beacon under a light loaded condition.
5. There is no significant difference between workday and weekend noise content for the analyzed feeders. This finding was unexpected.
6. When comparing time of day loading, the noise tends to be significantly less during the evening or nighttime hours. Therefore, smaller beacons could be detected during the nighttime hours.
7. At higher frequency, the phases tend to have significant common-mode noise. Calculating a phase difference or sum using  $I_A - 0.5I_B - 0.5I_C$  or  $I_A - I_B$  seems to provide the improved common-mode rejection. During field testing, it was observed, however, that the successful

- application of these differences depended upon transformer configurations between the substation and beacon. Beacon signals can be canceled too if the beacon appears on two phase currents because of a delta-wye transformer connection. Then the sum  $I_A+I_B$  becomes promising. Almost all combinations would need to be tried by trial and error unless one possesses detailed information about the exact phase connections in the feeder.
8. There is no measurable correlation between significantly time-shifted versions of the phase current. The time shift needs to be several hours. Because of this property, coherency analysis between time-shifted versions of the data may be an excellent detection tool. The use of coherency was not yet adequately assessed in laboratory simulations or field experiments.
  9. The two analyzed substations have very similar noise amplitudes when comparing the normalized phase currents. After normalization of the feeder currents, the differences between feeders by type, season, and time-of-day will likely become unimportant. Only the relative magnitude of the beacon load and its frequency are then important.
  10. There is a trade off between the length data being analyzed versus the amplitude of the beacon that can be detected. For simulations conducted on the Vista substation data, a beacon amplitude of 0.02 - 0.05% of the feeder's average load is detectable if a one-half to one full day of data is collected and analyzed. But, if the analysis data is reduced to 6 hours or less, beacon powers in this range are difficult or impossible to detect. This observation, based on analysis, was later tested and proven using the full-scale beacon in the field.
  11. We were able to obtain 1-s data bandwidth for load currents sampled at 3 of the 4 substations where we collected data. This data sample rate was perhaps 5 times faster than the rate that would be available centrally through existing SCADA. At the residential Benton City substation, data collection was limited to about 0.05 Hz by other communications equipment at the substation that was competing for metering resources.
  12. A switched beacon load as small as 750 W, representing approximately 0.02% of the feeder load, was detected from substation data in the field using 6 – 12 hours of phase current data. As suggested by analysis, detection of this beacon became questionable as the data duration and beacon magnitude were reduced.
  13. Beacons having cycle periods 5 and 10 seconds were detected in the field. Contrary to prediction, there was no clear benefit for using the higher frequency beacon load.
  14. Based on laboratory simulation, the distance between the substation and beacon load does not seem to influence the beacons observability. There is some evidence that the beacon load current will not be appreciably coupled from one phase to another simply by distribution line magnetic coupling over distance.

## **Acknowledgments**

The authors acknowledge the assistance received from Bryan Coyne, Dave Colby, and their employer, Benton PUD of Kennewick, Washington. These individuals installed metering equipment in their electrical distribution substations for us and otherwise facilitated our field data collection and field experimentation. This contract and report would not have been so successful and interesting without their involvement.

We also acknowledge that report author D. J. Trudnowski is a consultant and professor of electrical engineering at Montana Tech in Butte, Montana. His valuable capabilities in the areas of power spectral density and coherency analysis were greatly utilized in the research conducted.



# Contents

Executive Summary .....	iii
Acknowledgments.....	v
1.0 Problem Statement .....	1
2.0 Distribution Feeder Noise .....	3
2.1 What is Distribution Feeder Noise?.....	3
2.2 Available Feeder Electrical Measurements .....	4
3.0 Definition of Periodic Beacon Load .....	5
3.1 Defining the Beacon Load.....	5
3.2 Limitations Placed on the Beacon Load .....	5
3.3 Strategies Considered for Beacon Detection .....	6
4.0 Feeder Field Data Collection .....	7
4.1 Data Collection Process and Methods .....	7
4.2 Types of Feeder Data Needed .....	8
4.2.1 Agricultural .....	8
4.2.2 Commercial .....	8
4.2.3 Industrial .....	9
4.2.4 Residential.....	9
4.3 Quality, Precision, and Accuracy of Collected Data .....	10
5.0 Analysis Methods .....	17
5.1 Time Domain.....	17
5.2 Frequency Domain .....	17
5.3 Spectral computation in Matlab.....	18
5.4 Spectral Content of a Beacon .....	19
6.0 Field Data Analysis.....	23
6.1 Analysis Approach .....	23
6.2 Vista Analysis.....	24
6.3 Benton Substation Analysis.....	35
6.4 Riverfront Substation Analysis.....	42
7.0 Beacon Simulation and Detection.....	45
7.1 Beacon Simulation.....	45
7.2 December 1, 2004.....	54
8.0 Laboratory Feeder Simulation .....	57
8.1 Laboratory Feeder Model .....	57
8.2 Data Collection .....	59
8.3 Laboratory Simulation Results .....	61
9.0 Field Beacon Load Tests.....	69
9.1 The Field Beacon.....	69
9.2 Data Collection.....	71
9.3 Field Results .....	72
10.0 Conclusions.....	81
11.0 Recommendations.....	83
12.0 References.....	85
Distribution .....	Distr.1

## Figures

Figure 4.1. Configuration and relative positions of field data collection sites.....	8
Figure 4.2. Picture of Vista substation.....	9
Figure 4.3. One day of Benton City $I_A$ current data showing invalid data points .....	11
Figure 4.4. One day of Whitcomb $I_A$ data .....	12
Figure 4.5. Zoomed version of Figure 4.4 that shows data discretization quality .....	13
Figure 4.6. One day of Vista $I_A$ data. ....	14
Figure 4.7. Zoomed version of Figure 4.6 showing good data resolution .....	14
Figure 5.1. Estimated PSD of a single sinusoid signal .....	20
Figure 5.2. Estimated PSD of a two sinusoid signal.....	21
Figure 5.3. Estimated PSD of a square-wave signal .....	21
Figure 6.1. Vista substation $I_A$ for fall 2004 (13 days of complete data).....	24
Figure 6.2. Vista $I_A$ for winter 2004/5 (35 days of complete data) .....	25
Figure 6.3. Vista $I_A$ for spring 2005 (nine complete days of data).....	25
Figure 6.4. Vista substation difference $I_A-I_B$ for fall 2004 .....	26
Figure 6.5. Vista substation PSD of $I_A$ for all fall days except holidays (13 days analyzed in Nov. 2004) .....	27
Figure 6.6. Vista substation PSD of $I_A$ for all winter days except holidays and Dec. 1, 2004 (34 days analyzed Dec. 2004 - Jan. 2005).....	27
Figure 6.7. Vista substation PSD of $I_A$ for all spring days except holidays (nine days analyzed Apr. 2005 – May 2005).....	28
Figure 6.8. Vista substation comparison of mean PSD of $I_A$ , for fall, winter, and spring.....	29
Figure 6.9. Vista substation mean PSD of $I_A$ for winter, light vs. heavy loading (34 days analyzed Dec. 2004 – Jan. 2005).....	30
Figure 6.10. Vista substation mean PSD of $I_A$ for winter, workday vs. weekend (Dec. 2004 – Jan. 2005) .....	31
Figure 6.11. Vista substation mean PSD of $I_A$ for winter, time-of-day comparison (34 days analyzed Dec. 2004 – Jan. 2005).....	32
Figure 6.12. Vista substation coherency between $I_A$ and $I_B$ for winter (35 days Dec. 2004 – Jan. 2005)..	33
Figure 6.13. Vista substation mean PSD for winter, $I_A$ versus phase-difference currents (61 days Dec. 2004 – Jan. 2005).....	33
Figure 6.14. Vista substation coherency of $I_A$ for the 1 <sup>st</sup> -half of the day versus the 2 <sup>nd</sup> -half of the day for fall (13 days Nov. 2004) .....	34
Figure 6.15. Vista substation coherency of $I_A$ for the 1 <sup>st</sup> -half of the day versus the 2 <sup>nd</sup> -half of the day for winter (35 days Dec. 2004 – Jan. 2005).....	34
Figure 6.16. Vista substation coherency of $I_A$ for the 1 <sup>st</sup> -half of the day versus the 2 <sup>nd</sup> -half of the day for spring (9 days Apr. 2005 – May 2005).....	35
Figure 6.17. Benton substation $I_A$ for fall (9 days analyzed Oct. 2004).....	36
Figure 6.18. Benton substation $I_A$ for winter (17 days analyzed Jan. 2005 – Feb. 2005) .....	36
Figure 6.19. Benton substation $I_A$ for spring (51 days analyzed Mar. 2005 – May 2005).....	37
Figure 6.20. Benton substation $I_A$ for summer (29 days analyzed Jun. 2005 – Jul. 2005).....	37
Figure 6.21. Benton substation mean PSD of $I_A$ , season comparison (all available days Oct. 2004 – Jul. 2005).....	38
Figure 6.22. Benton substation mean PSD of $I_A$ for winter, light vs. heavy loading (51 days May 2005 – May 2005).....	38
Figure 6.23. Benton substation mean PSD of $I_A$ for summer for workday, weekend (Jun. – Jul. 2005) ...	39

Figure 6.24. Benton substation mean PSD of $I_A$ for winter by time-of-day (17 days Jan. – Feb. 2005)....	40
Figure 6.25. Benton mean PSD for summer, $I_A$ versus phase-difference currents (5 days Jun. – Jul. 2005) .....	40
Figure 6.26. Benton substation coherency of $I_A$ for the 1st-half of the day versus the 2nd-half of the day for spring (51 days Mar. – May 2005).....	41
Figure 6.27. Mean PSD of $I_A$ , for Benton versus Vista substations (winter 2004 – 2005) .....	42
Figure 6.28. PSD of Riverfront substation phase currents (full day, Sep. 21, 2005).....	43
Figure 7.1. Beacon square-wave at 3 cycles per minute, beacon amplitude = 1% of average.....	45
Figure 7.2. Beacon simulation $I_A$ with and without beacon signal (beacon amplitude = 1% average load , Dec. 4, 2005, Vista substation) .....	46
Figure 7.3. PSD of beacon alone and $I_A$ with the beacon added (beacon amplitude = 1%, 24 hours of analyzed data, Dec. 5, 2004, Vista).....	47
Figure 7.4. PSD of $I_A$ with and without beacon signal (beacon amplitude = 1%, 24 hours of analyzed data, Dec. 5, 2004, Vista).....	47
Figure 7.5. PSD of $I_A-I_B$ with and without beacon signal (beacon amplitude = 1%, 24 hours of analyzed data, Dec. 5, 2004, Vista).....	48
Figure 7.6. Coherency of $I_A-I_B$ for the 1st-half of the day versus the 2nd-half of the day for the beacon simulation example (beacon amplitude = 1%, 24 hours of analyzed data, Dec. 5, 2004) .....	48
Figure 7.7. PSD of $I_A-I_B$ with and without the beacon signal (beacon amplitude = 0.05%, 24 hours of analyzed data, Dec. 5, 2004, Vista).....	49
Figure 7.8. Coherency of $I_A-I_B$ for the 1st-half of the day versus the 2nd-half of the day for the beacon simulation example (beacon amplitude = 0.05%, 24 hours of analyzed data, Dec. 5, 2004, Vista) .....	50
Figure 7.9. PSD of $I_A-I_B$ with and without beacon signal (beacon amplitude = 0.02%, 6 hours of analyzed data, Dec. 5, 2004, Vista).....	50
Figure 7.10. Coherency of $I_A-I_B$ for the 1st-half of the day versus the 2nd-half of the day for the beacon simulation example (beacon amplitude = 0.02%, 24 hours of analyzed data, Dec. 5, 2004, Vista) .....	51
Figure 7.11. PSD of $I_A-I_B$ with and without beacon signal (beacon amplitude = 0.05%, 12 hours of analyzed data, Dec. 5, 2004, Vista).....	52
Figure 7.12. Coherency of $I_A-I_B$ for the 1st-half of the data versus the 2nd-half of the data for the beacon simulation example (beacon amplitude = 0.05%, 12 hours of analyzed data, Dec. 5, 2004, Vista) .....	52
Figure 7.13. PSD of $I_A-I_B$ with and without beacon signal (beacon amplitude = 0.05%, 6 hours of analyzed data, Dec. 5, 2004, Vista).....	53
Figure 7.14. Coherency of $I_A-I_B$ for the 1st-half of the data versus the 2nd-half of the data for the beacon simulation example (beacon amplitude = 0.05%, 6 hours of analyzed data, Dec. 5, 2004, Vista) .....	53
Figure 7.15. Coherency of $I_A-I_B$ for the 1st-half of the data versus the 2nd-half of the data for the beacon simulation example (beacon amplitude = 0.02%, 48 hours of analyzed data, Dec. 5 – 6, 2004, Vista) .....	54
Figure 7.16. Normalized $I_A$ for Vista on December 1-3, 2005.....	55
Figure 7.17. PSD of Vista $I_A$ , Dec. 1, 2004.....	55
Figure 8.1. Laboratory feeder model line diagram .....	58
Figure 8.2. Laboratory equipment diagram for the scaled laboratory emulation of power grid beacon production and detection.....	60
Figure 8.3. Laboratory PSD of b-phase data with a 0.1-Hz beacon load and 1 mile of simulated distribution line.....	61
Figure 8.4. Laboratory PSD using differences of phase currents with 0.1-Hz beacon load and 1 mile of simulated distribution line.....	62
Figure 8.5. Laboratory PSD of phase data with a 0.1-Hz beacon load and 5 miles of simulated distribution line .....	63

Figure 8.6. Laboratory PSD using differences of phase currents with 0.1-Hz beacon load and 5 miles of simulated distribution line.....	64
Figure 8.7. Laboratory PSD of b-phase current with a 0.2-Hz beacon load and 5 miles of simulated distribution line .....	65
Figure 8.8. Laboratory PSD using differences of phase currents with a 0.2-Hz beacon load and 5 miles of simulated distribution line.....	66
Figure 9.1. Original field beacon circuit with IGBT switch .....	70
Figure 9.2. Final beacon load switch with function generator, electronic relay, and portable heater load .....	70
Figure 9.3. Picture of opened field-scale beacon load controller showing ac load plugs .....	71
Figure 9.4. PSD of Vista field current data for each of the three phase currents without a beacon load (12-hour duration, March 11, 2006) .....	72
Figure 9.5. PSD of differential currents at Vista substation without a beacon load (24 hour duration, Mar. 11, 2006) .....	73
Figure 9.6. PSD of Vista substation currents with 1500-W, 0.1-Hz beacon load revealed on a- and b-phases (12-hour duration, Feb. 24, 2006) .....	74
Figure 9.7. PSD of various phase current differences at Vista substation with a 1500-W, 0.1-Hz beacon load (24-hours duration, Feb. 24, 2006).....	74
Figure 9.8. PSD for phase currents at Vista substation using a 750-W beacon at 0.1 Hz (12-hour duration, Mar. 18, 2006).....	75
Figure 9.9. PSD for phase currents at Vista substation using a 750-W beacon at 0.1 Hz (12-hour duration, Mar. 19, 2006).....	76
Figure 9.10. PSD for phase currents at Vista substation using a 750-W beacon at 0.1 Hz using reduced data collection duration (6-hour duration, Mar. 19, 2006).....	77
Figure 9.11. PSD for phase currents at Vista substation using a 750-W beacon at 0.1 Hz using reduced data collection duration (3-hour duration, Mar. 19, 2006).....	77
Figure 9.12. PSD for Vista substation currents using a 750-W, 0.2-Hz beacon load (12-hour duration, Mar. 22, 2006).....	78
Figure 9.13. PSD for Vista substation currents using a 750-W, 0.2-Hz beacon load and reduced data collection duration (6-hour duration, Mar. 22, 2006) .....	79
Figure 9.14. PSD for Vista substation currents using a 750-W, 0.2-Hz beacon load and reduced data collection duration (3-hour duration, Mar. 22, 2006) .....	79

## **1.0 Problem Statement**

We pose the problem statement as follows: Can the presence of a small, periodically-actuated load be detected at an ac feeder substation that serves the load? If so, what are the characteristics of such a “beacon load” that determine whether it can be detected? And can the beacon load be detected with the typical data collection metering that could be anticipated to be found installed at electrical power substations?

This report describes the designs of and results from theoretical, laboratory simulation, and field experiments that were formulated to answer this problem statement.



## 2.0 Distribution Feeder Noise

### 2.1 What is Distribution Feeder Noise?

A feeder is a set of three-phase conductors that terminate and are metered at a distribution substation. Most feeders are fed by only one substation; however, throw over switches on the feeder often permit the reconfiguration of the feeder circuit. Very large commercial loads are fed by all three feeder phases. Smaller residential loads are serviced by at least one, and sometimes two, of the three phase conductors of a feeder, depending on the configuration of the distribution transformers that supply the load.

The electrical background signal within which we are challenged to detect a single signal consists of two components: The first component is what is classically referred to as measurement noise, including discretization errors, aliasing, temperature effects, and sensor non-linearity. These effects are unavoidable but relatively innocuous for our research challenge. The second and overwhelming component is the sum of all load currents measured on a given distribution feeder during a given time interval. We feel justified calling this current signal “noise” because it is the unpredictable signal within which we try to identify our desired, deterministic signal. Using this terminology, the term “signal-to-noise-ratio” accepts its useful and standard definition.

Each time a load cycles on, or each time a person flips a light switch on a feeder, the new load is added to or removed from the summation of the feeder’s load current. While each such event is fully deterministic, the sum of the many such loads on a feeder is described statistically. The seasonal, weekly, and daily loads can be described by their averages and by patterns within the durations. We can attribute some of the patterns to the actuation of certain loads only on a statistical basis. For example, summer peak loads can be attributed to the combined periodic operation of many air conditioners cycling on and off during the hottest part of mid-day.

Careful analysis of feeder currents in the frequency domain reveals further details about the loads (again, only on a statistical basis). If the on/off events of all the individual loads were truly random, the frequency representation of feeder load would be disinteresting, like that of white noise. In fact, we know that many of the loads cycle with some predictable or limited period. Good examples of such loads include heating and air conditioning loads and refrigeration loads. We humans too affect the frequency spectrum on a feeder by our habits. The frequency with which we open the refrigerator, the minimum time we leave room lights on, and even the frequency with which we bath all contribute to trends that are observable in the frequency domain. Otherwise unobservable load trends and cycles become emphasized in the frequency domain.

Self and cross-correlation of the load also reveals patterns that cannot be seen in the time domain. Basically, correlation emphasizes cyclical trends and de-emphasizes truly random behaviors. (Might point out what is shown in correlation that is not evident in Fourier.)

The components of our “noise” that are not caused by the switching of feeder loads constitute measurement noise. No experiment was found to differentiate the effects of switching and measurement noises in real feeder data. However, the effects of aliasing and discretization can be analytically addressed if one knows enough about the sensors being used to collect the feeder data. Discretization error usually places a hard lower limit on the observability of weak signals, but the analysis of the effects of discretization must be addressed more carefully in our case where we are able to view and analyze a long duration of data and possibly see trends in that data that are smaller in magnitude than the measurement discretization.

All of these properties will be used to characterize load data at various seasons, days, and times of days. We also will use these characterizations to differentiate the data that one should anticipate at various types of feeders.

## **2.2 Available Feeder Electrical Measurements**

At substations, phase currents and voltages are scaled down to measurable magnitudes by instrument transformers. The signals are further scaled and digitized by system control and data acquisition, or SCADA, systems. Other system quantities, including real, apparent, and reactive electrical powers are derived from these measured quantities. SCADA will usually communicate these measurements at 15-second intervals or slower to centralized control centers. We observed several makes and qualities of available SCADA at different substations within the same utility area. The SCADA remote terminal units manufactured by DAQ which we encountered we were able to connect directly into a data stream via a laptop computer’s serial connection. Obtaining data at other substations was not so straightforward.

The DAQ units we connected to permitted us to obtain approximately 1-second interval data at the substations; we would have been limited to 15-second data had we relied on the central reporting from that same DAQ unit to the utility’s control room, as it was configured.

Increasingly, intelligent electronic devices, or *IEDs*, are surpassing the substation SCADA in their abilities to obtain fast, accurate data. Where available, these IEDs could be used to obtain data far superior to SCADA data that we were able to obtain at the substations where we collected field data.

We could seek a hidden signal in any of the feeder measurements available at a substation. However, we quickly focused on the available feeder current signals. On an ac electrical power signal, the voltage is usually considered the cause, and the current is the result of applying that voltage to a load. The voltage magnitude remains virtually constant except when the very largest loads are switched onto a feeder. Load signals only appear in feeder voltage where the feeder is connected to transmission voltages through relatively high series impedance, as can occur when a large load is attached to a feeder far from its substation transformer. Because voltage remains mostly unaffected, the calculated power signal is similar to the measured current signal for its information content.

## 3.0 Definition of Periodic Beacon Load

### 3.1 Defining the Beacon Load

For the purpose of this report, we define a *beacon load* as a controlled load that can be periodically modulated on and off. The word *beacon* refers to our interest in detecting this signal on an electric power distribution system. Our understanding is that the only communication performed by the beacon load is to “broadcast” its unique carrier signal frequency. Only the presence or absence of the carrier signal is of interest. No further modulation of the carrier signal was investigated.

### 3.2 Limitations Placed on the Beacon Load

We will address only beacon loads that have a predominantly real power consumption and will be either fully turned on or off to create an approximate square current wave shape. The effect of power factor of the beacon load will be considered for its effect on the beacon’s observability, but the power factor of the beacon load is not assumed to be independently controllable.

The magnitude of beacon load is preferably on the order of a small appliance load, say 1 kW or less, of the types that would be anticipated in residential and small commercial, single-phase, low voltage distribution systems. However, one goal of this report is to identify the necessary magnitude of the beacon load for its observability, regardless of that magnitude.

While beacon load energy could be more finely focused on a single frequency by modulating the beacon load sinusoidally, doing so will not likely be practicable. Consequently, we accept some frequency domain spreading of the beacon load’s signal energy that is caused by square-wave modulation. Because the beacon load is effectively a square-wave, the frequency spreading will occur at the known odd harmonics. It is therefore theoretically possible to use this knowledge when detecting the presences of a beacon load. That is, the energy of the odd harmonics can theoretically be added to that of the fundamental harmonic to enhance its detectability.

The practical frequency at which the beacon load may be modulated will also be limited. The lowest modulation frequency will be determined by our need to detect such a beacon on a distribution system within a reasonable time period—say, two days. Because the proposed analysis method for detecting a beacon is statistical signal processing, the actual beacon frequency should be much faster than the two-day detection window. This will allow for spectral averaging which improves the detection algorithm performance. The beacon load’s fastest practicable modulation frequency will be limited by the sampling frequency available for the detection of the beacon load at substations, sampling which now occurs at 1 to 15-second intervals by substation SCADA. Maximum beacon frequency also could be limited, of course, by the available means of actuating such a beacon load. For this study, we did not assume that actuation of the beacon would create an upper frequency limitation. Applying these likely upper and lower bandwidth limitations results in a beacon frequency range from about 6 cycles-per-hour to 30 cycles-per-minute range. A preferred, perhaps optimal, switching frequency exists within this broad frequency range. A later analysis will show that the upper end of this frequency range is preferred.

### **3.3 Strategies Considered for Beacon Detection**

The primary focus of this study is the detection of the fundamental switching frequency from available SCADA substation data. SCADA data at substations normally report feeder line currents and feeder phase voltage magnitudes at 1 to 15-second intervals. Other quantities, like real and reactive power and power factor, can be calculated from and by the SCADA system. We observed during this study that slightly faster sampled data can be had at the substation than might be reported by the SCADA to central control stations. Therefore, one may be able to detect a beacon at the substation that cannot be detected from reported SCADA data.

The small beacon loads of interest will never be detectable in the time domain in this data, but the beacon load may be detected in the frequency domain. Additionally, it was found during this research that self- and cross-correlation methods were useful for concentrating the energy from the beacon loads into an observable signal. Furthermore, certain preconditioning operations on the raw current data, like subtracting data from the remaining phase or phases were beneficial. We believe such preconditioning effectively removed common-mode load “noise” allowing the beacon load to be more observable.

## 4.0 Feeder Field Data Collection

### 4.1 Data Collection Process and Methods

We were fortunate to obtain the cooperation of Benton PUD, Benton County, Washington State, for the collection of SCADA data from four of their substations. The processes by which data became available to us took anywhere from 10 minutes to several months to implement. The shortest time was needed for a substation having an existing DAQ data collection system, for which we needed only to complete a serial port connection between a DAQ system port and our laptop computer. This connection took only minutes once we obtained access to the substation.

Much longer setup times were needed where different, or no, SCADA equipment existed. At two of the four substations, we installed DAQ systems in parallel with the existing SCADA, and at a fourth substation, we installed current monitoring where none had previously existed. At these locations, we were required to coordinate our installation activities with utility personnel who provided access and assistance with the equipment wiring.

In two of the four substations, we successfully established wireless radio communications from the substation data collection to our laboratory, where the data was archived. The wireless connection required installation of a repeater station atop Badger Mountain south of Tri-Cities, Washington. With repeater, we are able to collect data from the two substations that are 12 and 10 miles from the data collection site at Pacific Northwest National Laboratory. Weather conditions created data latency over this distance as the weather improved or degraded. The relative positions of the data collection sites is shown in Figure 4.1.

A third substation was too far from our repeater. However, similar wireless communication equipment allowed us to collect our data periodically and wirelessly from outside the perimeter of the substation without bothering the PUD personnel. The data was quickly downloaded to our laptop computer while we sat in the substation parking lot. A modest-sized computer within the substation could store over a month's data until it could be later downloaded via the wireless connection.

A fourth substation required that access be provided us into the substation by PUD personnel for direct connection and download of stored data to a portable laptop computer. Regrettably, this substation is remotely located and was inconvenient to visit for both utility personnel and us.

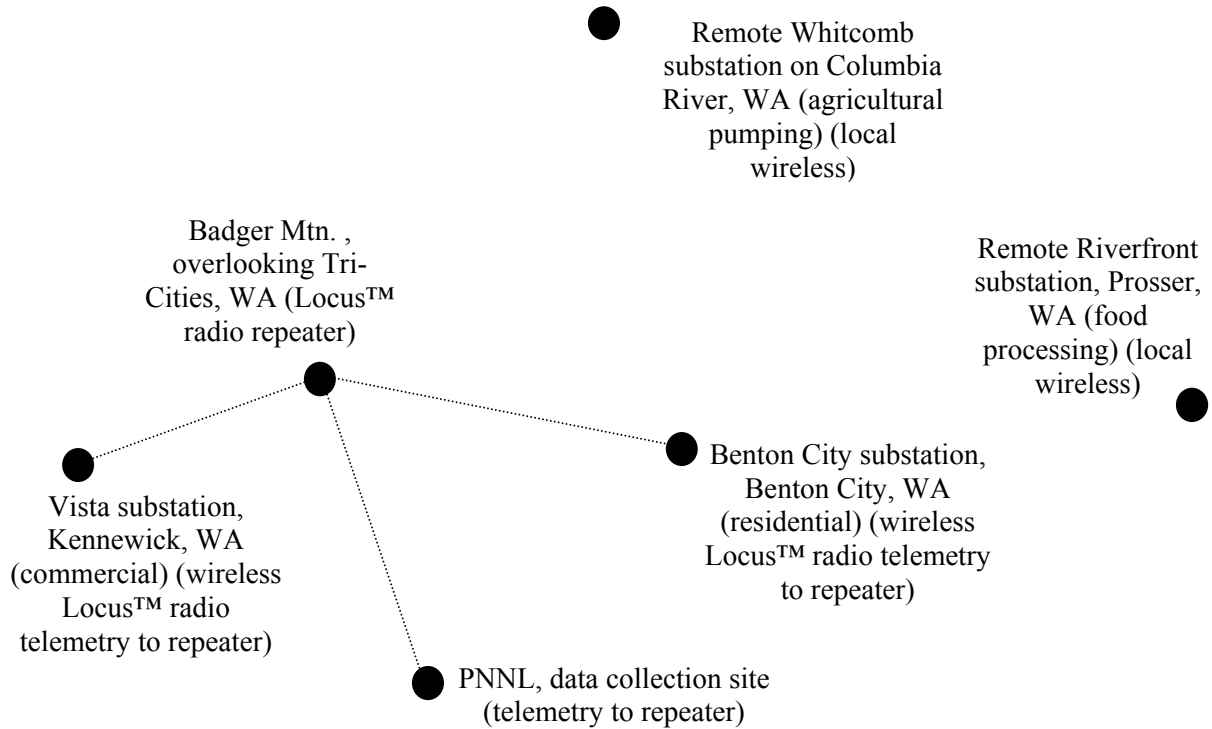


**Figure 4.1.** Configuration and relative positions of field data collection sites

The data was collected at PNNL into a MySQL database from the radio telemetry, from where it could later be ported into analysis tools like Matlab®.

## 4.2 Types of Feeder Data Needed

### 4.2.1 Agricultural

Whitcomb substation serves an agricultural water pumping load of several megawatts.

### 4.2.2 Commercial

Vista substation feeder #1 serves Columbia Center Mall, which houses a mixture of small commercial apartment stores, special interest mall shops, a restaurant, theater, and a food court.



**Figure 4.2.** Picture of Vista substation

### **4.2.3 Industrial**

The Prosser substation primarily serves a food processing facility.

### **4.2.4 Residential**

Benton City is a small community West of Tri-Cities, Washington. The Benton City substation serves the city with two feeders.

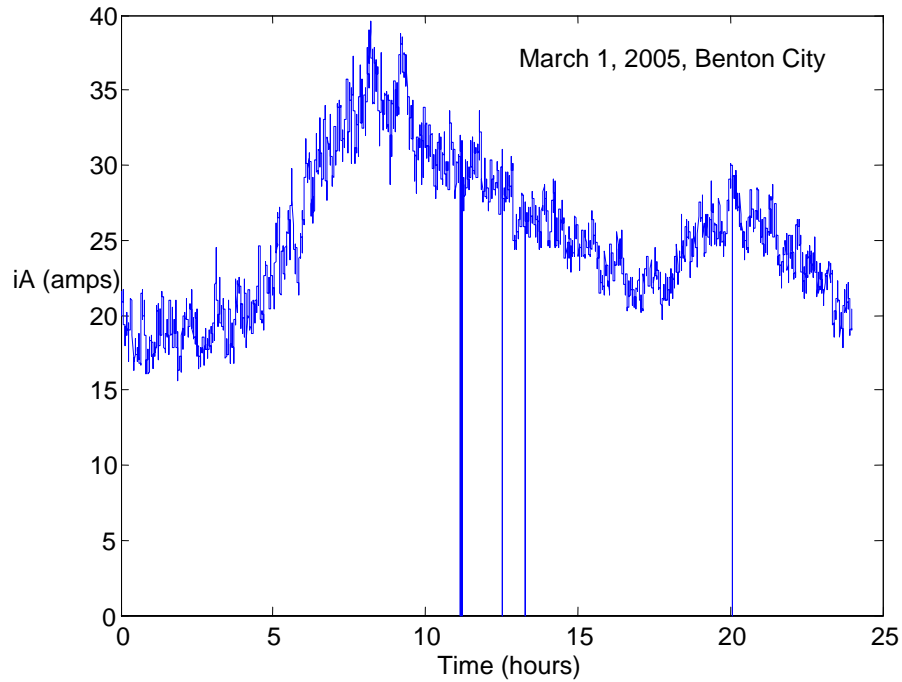
**Table 1.** Summary of substations and their types and properties

	<b>Benton City</b>	<b>Vista</b>	<b>Riverfront</b>	<b>Whitcomb</b>
type	residential (mostly single dwelling)	small commercial (shopping mall)	small industrial (food processing plant)	agricultural (pumping)
location	Benton City, WA	Kennewick, WA	Prosser, WA	South of Tri-Cities, WA
No. feeders monitored	2	1	1	2
primary voltage (kV)	7.2	7.4	7.2	4.16
existing SCADA	DAQ with Cooper recloser using DNP 3.0	QEI	QEI	DAQ
project data collection method	remote wireless via existing DAQ and Locus HSE wireless remote connection	remote wireless via added DAQ and Locus HSE wireless remote connection	added DAQ, accessible locally via Locus HSE wireless connection	DAQ serial comm.. to laptop
A/D bit precision	16/12	12	12	12
local data collection rate (s <sup>-1</sup> )	0.04 – 0.5 (DNP 3.0 communications slowed data collection here)	1.0	1.0	1.0
central existing remote SCADA data collection rate (s <sup>-1</sup> )	~0.03 @ 1.2 kbaud	0.05 - 0.07 @ 1.2 kbaud	0.05 - 0.07 @ 1.2 kbaud	0.05 - 0.07 @ 9.4 kbaud

### 4.3 Quality, Precision, and Accuracy of Collected Data

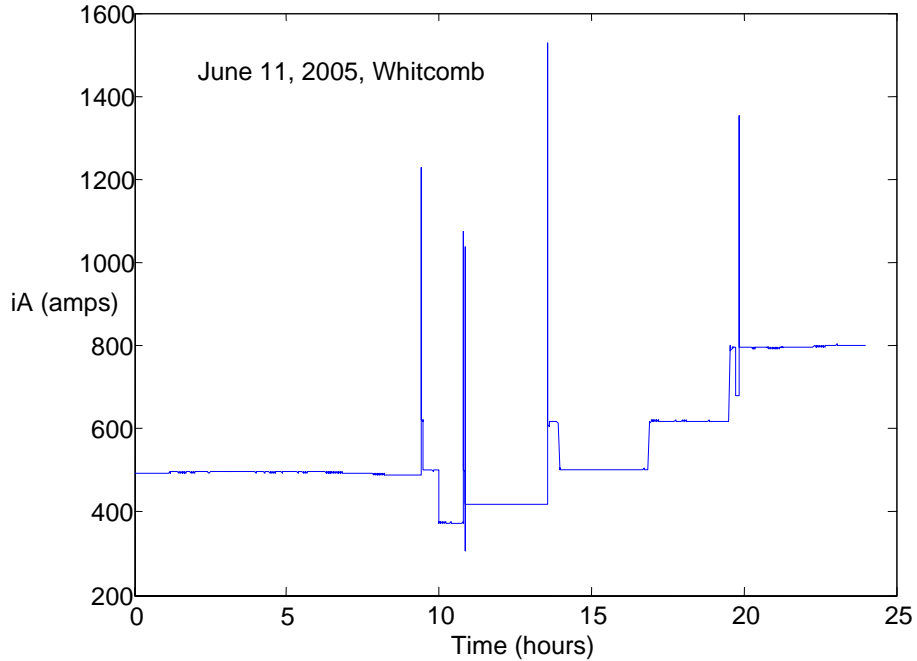
Three critical issues were encountered when evaluating and analyzing the field collected data: quality; resolution; and bandwidth.

To conduct the spectral analysis presented in this report, a full day of quality data is required. For many days in the provided data sets, several hours are invalid or missing; therefore, that entire day of data cannot be used for spectral analysis. If the invalid data is limited to approximately an hour or less scattered throughout the day, interpolation is used to fill the missing data. For example, consider the a-phase current data collected at Benton on March 1, 2005 shown in Figure 4.3. As can be seen, the data is invalid at 4 points in the day where it goes to zero. Prior to analysis, these points are interpolated to the previous valid data point.



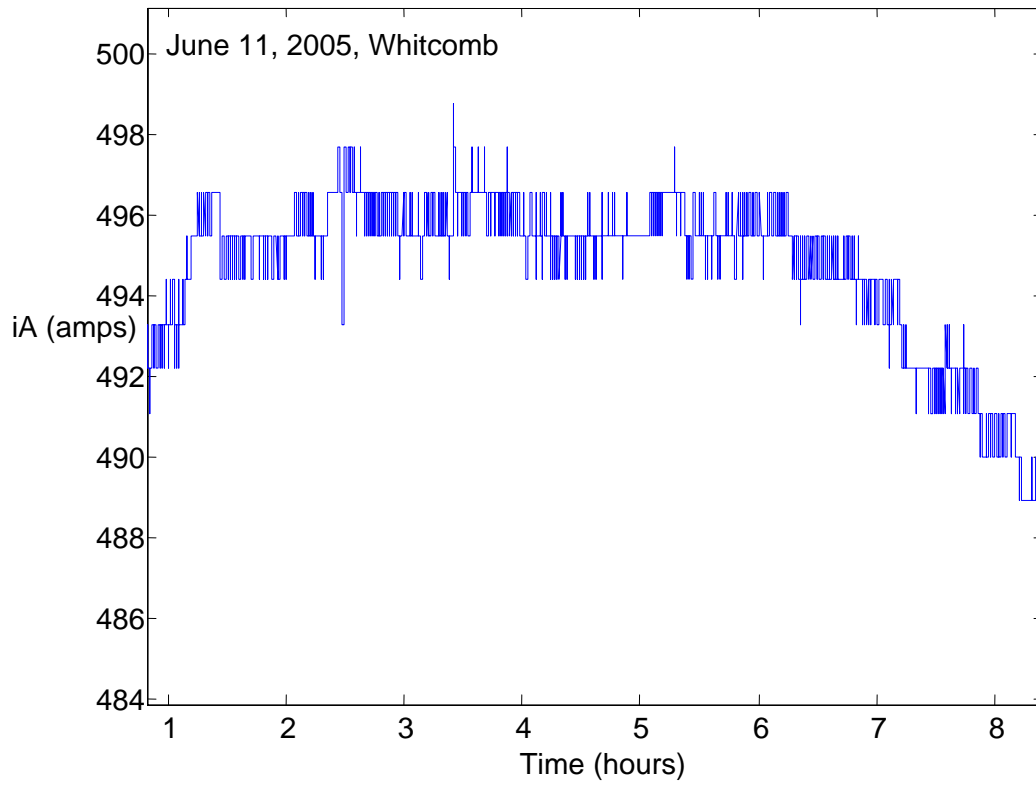
**Figure 4.3.** One day of Benton City  $I_A$  current data showing invalid data points

All three feeders were collected using 16-bit digital precisions. But, the least-significant 4 bits for the Vista and Whitcomb data were truncated in the collection process of the SCADA units. The variation of the Vista data is well above the resolution limits; therefore, the data is of acceptable quality. Unfortunately, this is not also true for the Whitcomb data. Figure 4.4 shows one day of the Whitcomb data. As seen, the data is characterized by relatively steady-state values coupled with large current transients (likely due to large induction motor load startup).



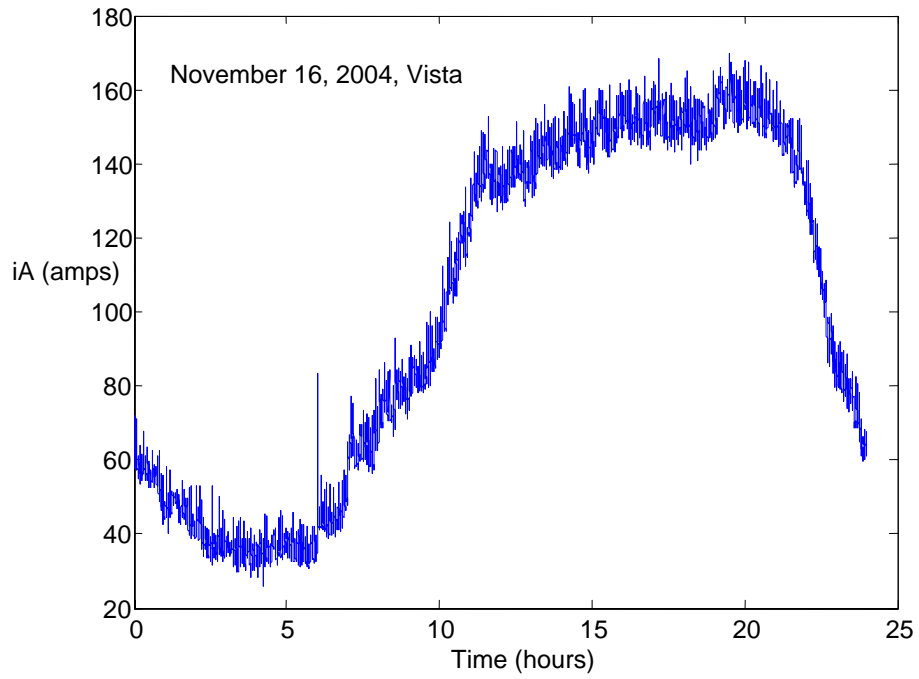
**Figure 4.4.** One day of Whitcomb  $I_A$  data

Figure 4.5 shows the same day but zoomed into the data centered on the 5-hour point. As seen in Figure 4.5, the resolution of the data is very poor. Therefore, it was judged that the Whitcomb data should not be used for spectral analysis. It is safe to assume that one could detect a beacon signal in the Whitcomb data if the beacon amplitude is larger than the resolution of the measurement system. That is, the resolution of the measurement system is the primary limiting factor for detecting a beacon in the Whitcomb data instead of the power system effects. Evaluating the power system effects would require improved resolution measurement.



**Figure 4.5.** Zoomed version of Figure 4.4 that shows data discretization quality

Figure 4.6 and Figure 4.7 show similar plots for the Vista data; as seen in Figure 4.7, the data has very good resolution properties.



**Figure 4.6.** One day of Vista  $I_A$  data.

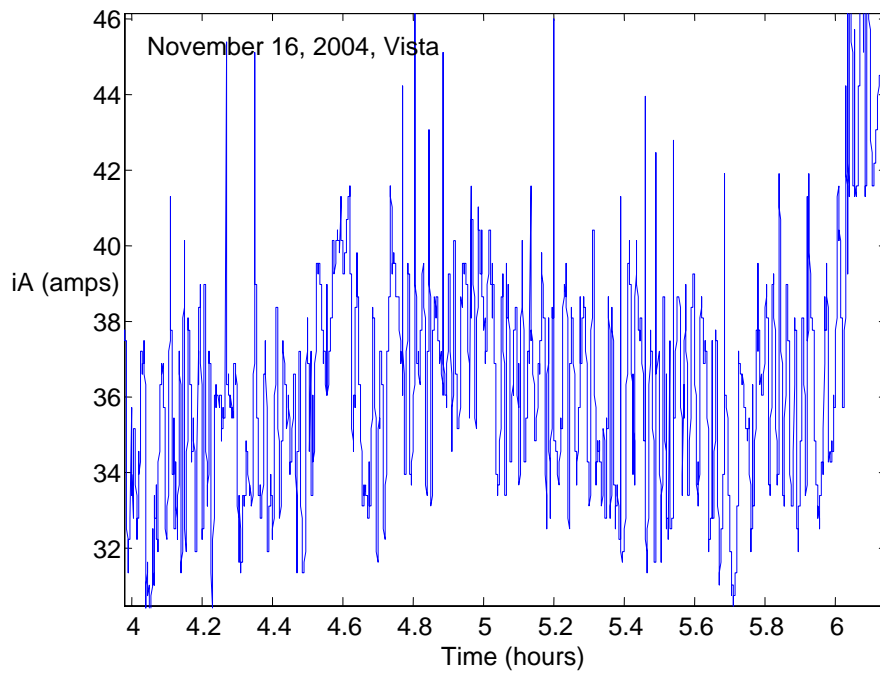


**Figure 4.7.** Zoomed version of Figure 4.6 showing good data resolution

The third issue relates to the bandwidth of the data. No information was provided concerning the bandwidth of the data acquisition system used to collect the data. All data was collected with a sample rate of 1.05 seconds for the Benton City and Vista data, and 1.08 seconds for the Whitcomb data. It is assumed that the bandwidth of the data acquisition system was from 0 Hz to the Nyquist frequency. All conclusions provided in this report use this assumption. If future analysis indicates that the data is band limited by the data acquisition, then the conclusions should be similarly modified.



## 5.0 Analysis Methods

### 5.1 Time Domain

Each set of substation data and the simulated substation data from laboratory experiments was first observed in the time domain as a set of sequential data samples. Observation in the time domain proved useful for assessing the general quality of the data. For example, missing data and erroneous data are readily detected in a time series. As one would expect, beacons that had a magnitude comparable to the resolution of the metering equipment and smaller were not observable in the time domain.

### 5.2 Frequency Domain

Because of the highly random nature of the feeder load data, statistical spectral analysis methods should be employed. Such methods remove the highly random components leaving the underlying spectral structure of the data. The statistical spectral analysis methods commonly used are the auto-spectrum or power spectral density (PSD) and coherency calculations [Bendat].

Power-system feeder load is typically characterized by two properties in the current: slowly-changing deterministic diurnal variations; and faster-changing random variations. For example, consider the single day of commercial feeder load shown in Figure 4.6. As can be seen, the variation can be broken into a 24-hour diurnal cycle superimposed with a higher-frequency random component. The residential load in Figure 4.3 has a similar characteristic. The agricultural load in Figure 4.4 does not contain the diurnal effect; but, it too can be broken into a deterministic component coupled with a random component (unfortunately, the resolution is too poor to effectively measure the random component). Because the slowly-changing deterministic components tend to vary much slower than the expected beacon load, the goal is remove the deterministic effect from the data. This is accomplished by detrending the data prior to analysis.

One definition of the PSD of a random signal  $y_1$  is

$$S_{11}(\omega) = E\{Y_1^*(\omega)Y_1(\omega)\} \quad (1)$$

where  $E\{ \}$  is the “expectation” operation (or average),  $Y_1(\omega)$  is the Fourier transform of  $y_1(t)$  at frequency  $\omega$ , and  $Y_1^*(\omega)$  is the conjugate of  $Y_1(\omega)$ . We must use the expectation operation because all signals are random. That is to say, the Fourier transformed signal  $Y_1(\omega)$  will be random, but, through the expectation operation we can examine the “average” or expected effect. Basically, the PSD provides the average power-per-frequency of a signal as a function of frequency.

The coherency is a measure of correlation between two signals in the frequency domain. It is computed from the PSD and the cross spectral density (CSD). Say one is given two signals,  $y_1$  and  $y_2$ ; the CSD is defined to be

$$S_{12}(\omega) = E\{Y_1^*(\omega)Y_2^*(\omega)\} \quad (2)$$

The coherency-squared between  $y_1$  and  $y_2$  is then defined by

$$\gamma_{12}^2(\omega) = \frac{|S_{12}(\omega)|^2}{S_{11}(\omega)S_{22}(\omega)} \quad (3)$$

Effectively,  $\gamma_{12}^2(\omega)$  is a measure of percentage correlation between  $y_1$  and  $y_2$ . It is bound between 0 and 1. If it is near 0, the two signals are not correlated and have no common component. If it is unity, the two signals are 100% correlated and share the same component at that frequency.

Hypothetically, the coherency is a valuable tool for beacon detection under two possible conditions. First, consider the case where a random signal of time length  $L$  is broken into two sections of length  $L/2$ . If the signal is truly random and  $L$  is considerably long relative to the frequency content of the signal, the coherency between the two sections converges to zero. If we now add a beacon signal to the original random signal, the coherency will converge to unity at the beacon frequency because the beacon is present in both sections. Therefore, one is left with a normalized spectral plot with peaks at the beacon frequency.

The second condition relates to what is termed here as phase-difference currents. For example, consider the case where the beacon is present in the a-phase current ( $I_A$ ) and not present in the b-phase current ( $I_B$ ). If the two phase currents have relatively high common-mode noise, then  $I_A - I_B$  will reduce the noise level while preserving the beacon amplitude. Therefore,  $I_A - I_B$  provides improved signal-to-noise ratio for beacon detection. Cross-correlation via the coherency between  $I_A$  and  $I_B$  provides information on the level of common-mode noise reflecting the potential of phase-difference analysis.

### 5.3 Spectral computation in Matlab

The common method for estimating the PSD and CSD is Welch's periodogram averaging. Essentially, this estimation is calculated with a sliding window fast Fourier transform (fft). The computer analysis software package Matlab® was used to conduct all spectral analysis for this report. In version 7 of Matlab® (with the signal processing toolbox), the key functions are "pwelch" for the PSD and "cpsd" for the CSD. In versions prior to version 7, the functions are termed "psd" and "csd."

There are four key parameters to select when using the pwelch and cpsd functions: (1) the fft window size; (2) the amount to overlap the fft windows; (3) the type of window to use to avoid spectral leakage; and (4) the total data used in the analysis. Using the Matlab help on pwelch and cpsd, the variable names are NFFT, NOVERLAP, and WINDOW. Unless otherwise stated, the following parameters were selected throughout this report:

NFFT = fft window size = 1 hour.

NOVERLAP = 80% of NFFT = 0.8 \* NFFT.

WINDOW = hanning(NFFT).

Prior to spectral processing, all time-domain data is pre-processed using the “detrend” function in Matlab. Detrending removes the least-squares straight-line fit from the data. On the one-hour processing window, this effectively removes all the deterministic diurnal components of the data leaving the random components for spectral processing.

The fft window size is selected to be one hour. This provides a frequency resolution of 1/60 cycles-per-minute in the frequency plots allowing one to characterize the data for beacons as slow as one switching cycle per hour. A larger window size would allow one to characterize the data for slower effects, but at the cost of poorer statistical smoothing. The larger the overlap, the more “averaging” one will have in the results; thus removing the random effects. In general, the results do not improve with an overlap greater than 80%.

The purpose of the window is to remove spectral leakage due to data truncation. Because a very large data window is being used (1 hour of data), very little spectral leakage is expected. Experiments with the data show nearly no noticeable difference when comparing various windowing methods. A Hanning window was used because it is typically used in the signal processing industry. All other common windowing methods provide the same conclusions, including a box-car window.

The sample period for the data is either 1.05 seconds or 1.08 seconds. This places the Nyquist frequency at approximately 30 cycles-per-minute. Due to aliasing, it is typically recommended that the data be analog filtered prior to sampling. For typical measurement systems, this places the bandwidth of the data below and satisfies the Nyquist criterion. No information was provided on the true bandwidth of the data acquisition systems employed for this study. Therefore, it was assumed the bandwidth was effectively up to the Nyquist frequency. Some of the higher-frequency roll-off effects observed in the data may be caused by the analog filtering of the data.

The total data used in a given analysis depends on the goal of the analysis. Increasing the amount of data provides more averaging and removal of random effects (often termed “data smoothing”). Once adequate data smoothing is achieved, more data provides little added value. Several experiments were conducted to determine adequate overall data sizes for a given analysis. The majority of the PSD analyses that follow use a full day of data, while some use as little as six hours of data. Data lengths less than size hours were judged inadequate.

To achieve the equivalent smoothing from a coherency analysis as for a given PSD calculation requires double the data length. When conducting the coherency analyses that follow, each day is broken into two half-days (midnight to noon versus noon to midnight). The cross correlation is then conducted using one-hour blocks using the Matlab “cpsd” function.

## **5.4 Spectral Content of a Beacon**

The ambient data (i.e., data containing no beacon) characterization that follows this section should be interpreted in the context of a hypothetical beacon signal. Spectral analysis provides the advantage that the PSD of substation data containing a beacon is the superposition of the ambient signal and the beacon. Therefore, we can study the two separately. Using the PSD to characterize the ambient data raises the question: what is the PSD of a beacon signal?

The PSD provides the average power-per-frequency of a signal as a function of frequency. The integral of the PSD is the power contained in the signal over the range of integration. Therefore, if a signal contains only one frequency, the theoretical PSD consists of a delta spike at that frequency and zero at all other frequencies. The width of the spike is infinitely small and the height of the spike will be infinitely high. The area under the spike equals the power in the beacon sinusoid; that is, the RMS amplitude squared. This high-spiking property makes the PSD advantageous for signal detection.

Estimating the PSD using a finite amount of data with fft averaging causes the delta spike to become finite width and height. As an example, consider the following 1-Hz signal  $y(t) = \sin(2\pi t)$  -- a one-half watt signal if the signal were passed thru a 1- $\Omega$  resistor as a current. We sample the signal at a 10-Hz rate for 20 seconds. We then calculate the PSD using Welch's method with a window size of 10 seconds and a box-car window. The resulting PSD is shown in Figure 5.1. As seen in the figure, the area under the spike is 0.5 watts.

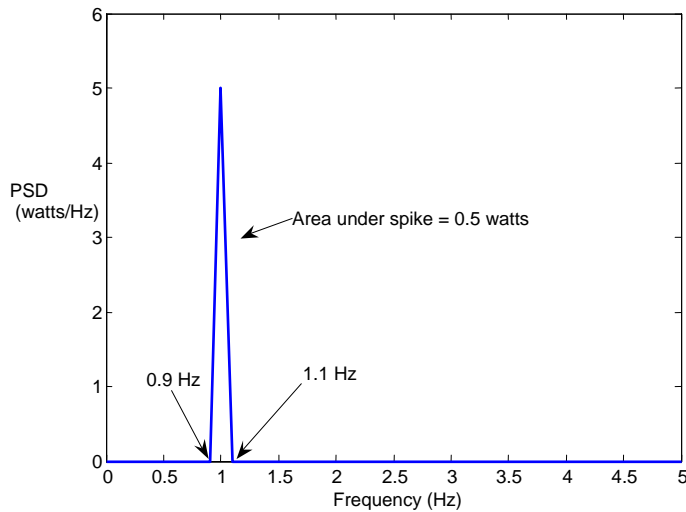
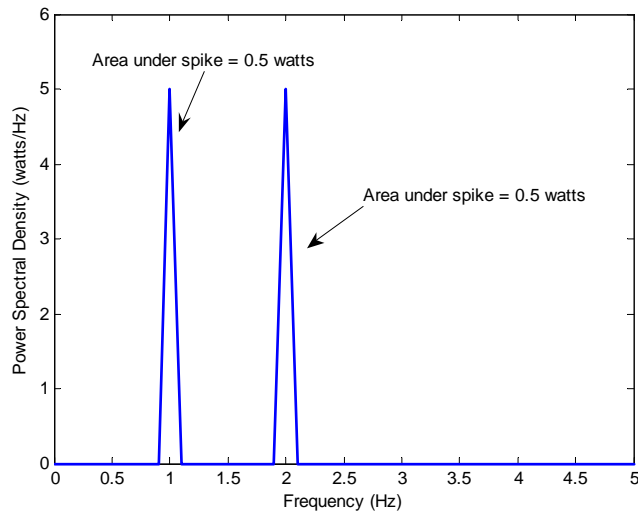


Figure 5.1. Estimated PSD of a single sinusoid signal

We now repeat the example, but now the signal consists of two sinusoids at 1-Hz and 2-Hz of equal amplitude —  $y(t) = \sin(2\pi t) + \sin(4\pi t)$ . The resulting estimated PSD is shown in Figure 5.2. Because each sinusoid has unity amplitude, the power (or area under the estimated PSD) is 0.5 watts for both spikes.



**Figure 5.2.** Estimated PSD of a two sinusoid signal

In reality, a beacon signal will likely be closer to a square-wave signal depicting an on/off switching load. The square-wave has a similar PSD shape as the sinusoid except for some spectral leakage to the higher harmonics of the switching frequency. As an example, consider the case where the signal is a 1-Hz square wave with amplitudes 0 and 1 and 50% duty cycle. The total true power in the signal is 0.5 watts; 0.25 watts at DC and 0.25 watts at the AC components. We estimate the PSD using the same parameters as above with the results shown in Figure 5.3. As seen, the area under the first-harmonic 1-Hz spike is approximately 0.2 watts. The remaining 0.05 watts of AC power is spread over the other frequencies contained in the signal at the higher harmonics. In this simple example, the peak at 3 Hz is the third harmonic. When evaluating a beacon signal, it may be advantageous to detect not only the fundamental harmonics but also the higher frequency terms.

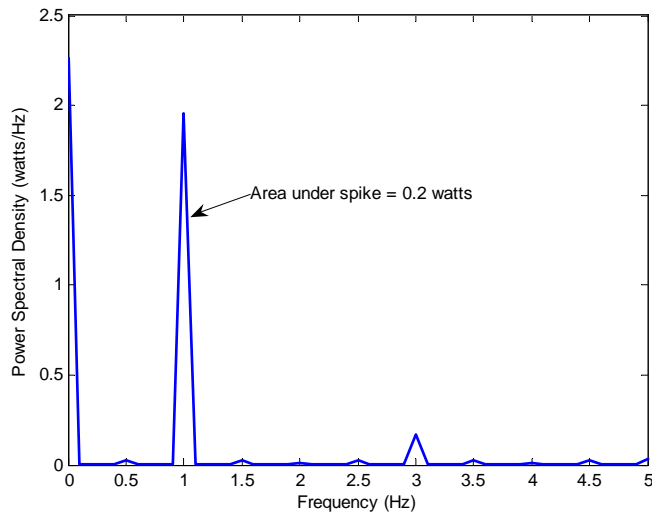


**Figure 5.3.** Estimated PSD of a square-wave signal



## 6.0 Field Data Analysis

The goal of the analysis is to characterize properties of the data to help design and evaluate detection methods of a periodic beacon load on the feeder. Auto-spectrum and cross-spectrum analysis are used to examine the data.

### 6.1 Analysis Approach

Several months of ambient data were collected from each substation. Prior to spectral analysis, all data is normalized by the daily average and detrended, as was described in Section 5.3. The unit of measurement for the normalized current is “per unit” or pu. This allows one to compare the spectral content from different, dissimilar substations. Data is characterized from the following perspectives.

- Season:
  - Fall – September, October, November;
  - Winter – December, January, February;
  - Spring – March, April, May;
  - Summer – June, July, August.
- Light-loading vs. heavy loading:
  - Heavy loading – hourly average is above the daily average;
  - Light loading – hourly average is below the daily average.
- Workdays (Monday thru Friday) vs. weekends.
- Time of day:
  - Morning – 12AM to 6AM;
  - Mid-morning – 6AM to 12PM;
  - Afternoon – 12PM to 6PM
  - Evening – 6PM to 12AM.
- Phase difference:
  - $I_A - I_B$  (A-phase current magnitude – B-phase current magnitude).
  - $I_A - 0.5I_B - 0.5I_C$

Phase-difference currents are evaluated as it has been hypothesized that a large portion of the current noise may be common mode. Therefore, subtracting the two phases will remove common-mode noise thus making single-phase beacon detection more feasible. Another alternative considered is subtracting half the b- and c-phase currents from the a-phase current.

For all the analysis to follow, holidays are removed from the data where the following were considered holidays: January 1, July 4, November 25, and December 25. Also, all frequency-domain plots are shown using a decibel (dB) scale for the PSD to allow a very large range of activity to be shown on one plot, and the frequency scale is shown logarithmically to allow for a large range of frequencies.

## 6.2 Vista Analysis

Figure 6.1 through Figure 6.3 show the normalized  $I_A$  used for analysis from the Vista substation. Thirteen days of data are available for fall 2004, 35 days of data are available for Winter 2004/5, and 9 days of data are available for spring 2005.

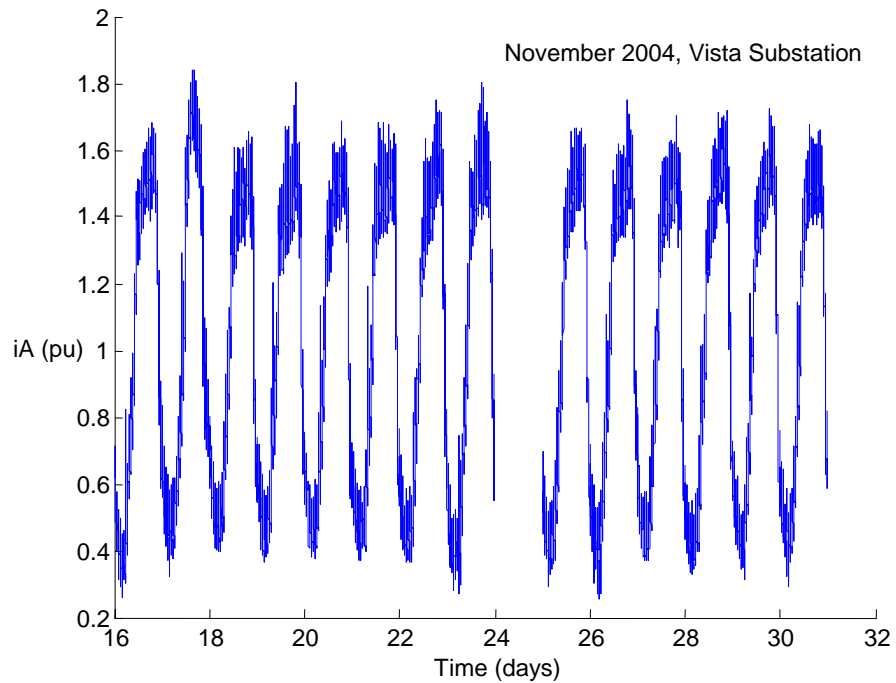


**Figure 6.1.** Vista substation  $I_A$  for fall 2004 (13 days of complete data)

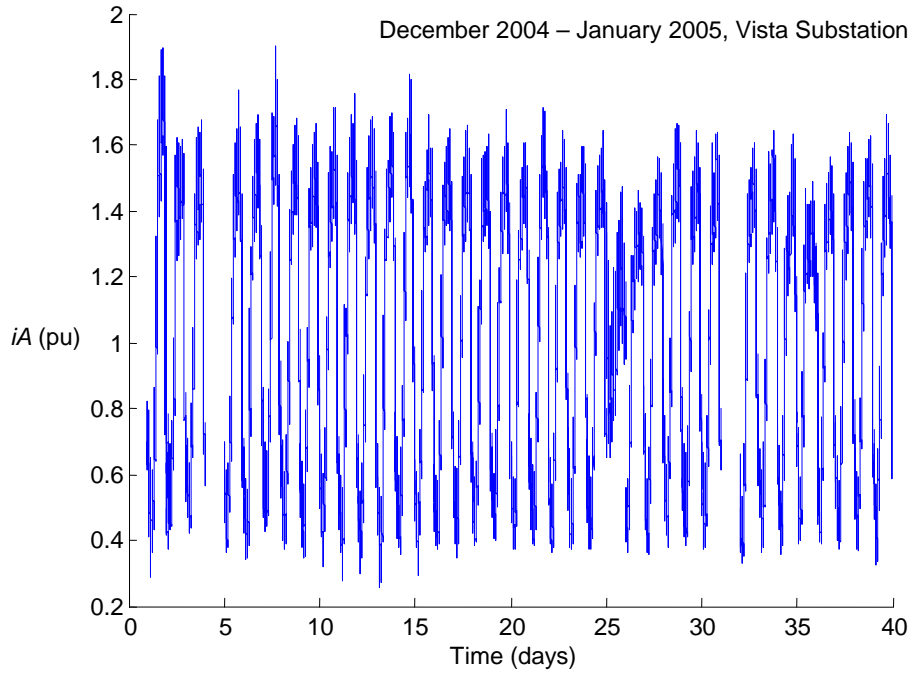


**Figure 6.2.** Vista  $I_A$  for winter 2004/5 (35 days of complete data)

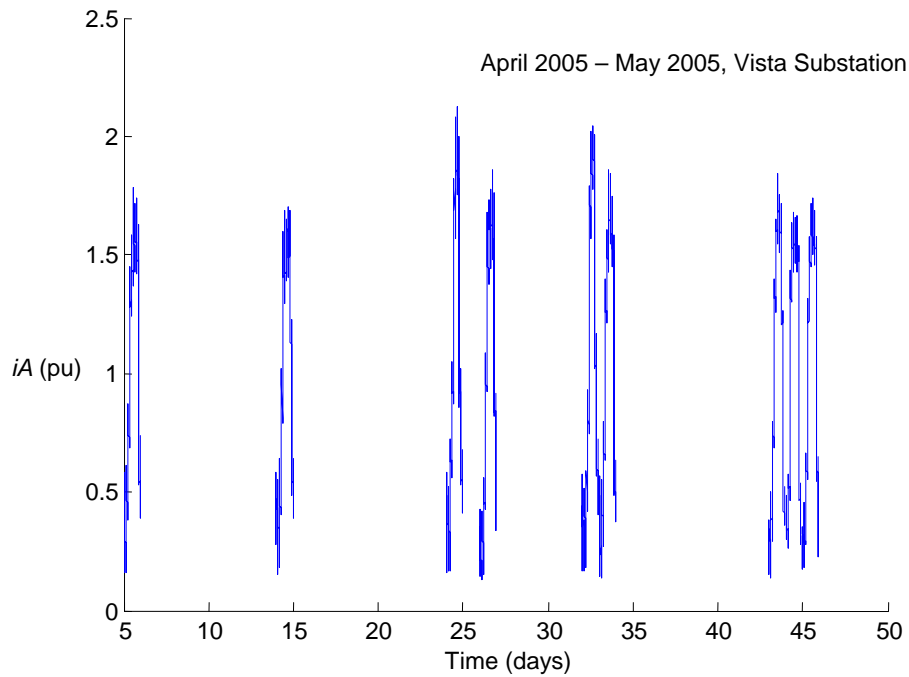


**Figure 6.3.** Vista  $I_A$  for spring 2005 (nine complete days of data)

The phase-difference current for fall 2004 is shown in Figure 6.4 (winter and spring phase-difference data are not shown here but have a similar appearance). We observe that, as expected, per unit range of current data is greatly reduced by the removal of the common mode currents in the a- and b-phases.

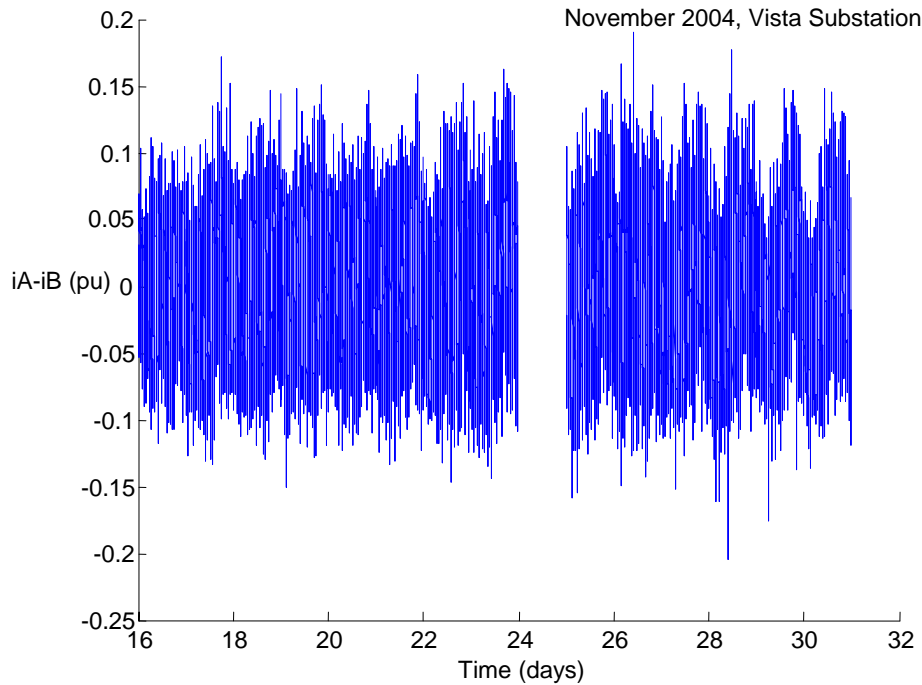


**Figure 6.4.** Vista substation difference  $I_A-I_B$  for fall 2004

The PSD analyses for all days are summarized in Figure 6.5 through Figure 6.7. For each plot, four curves are shown: the mean; the median; the maximum; and the minimum power spectral densities. For example, in Figure 6.5, 13 days of data were analyzed resulting in one PSD for each day. For each frequency bin, the mean, median, maximum, and minimum of the PSDs of the 13 days is shown. Note that the min/max bounds tend to be relatively tight to the mean and median. This property was found to be consistent throughout the Vista substation and Benton substation data.

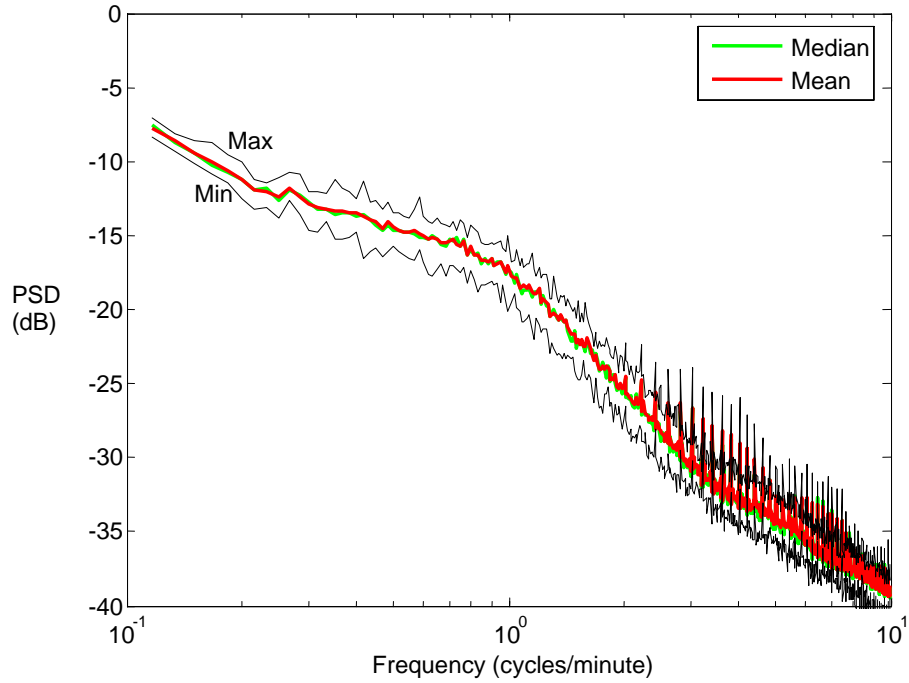


**Figure 6.5.** Vista substation PSD of  $I_A$  for all fall days except holidays (13 days analyzed in Nov. 2004)

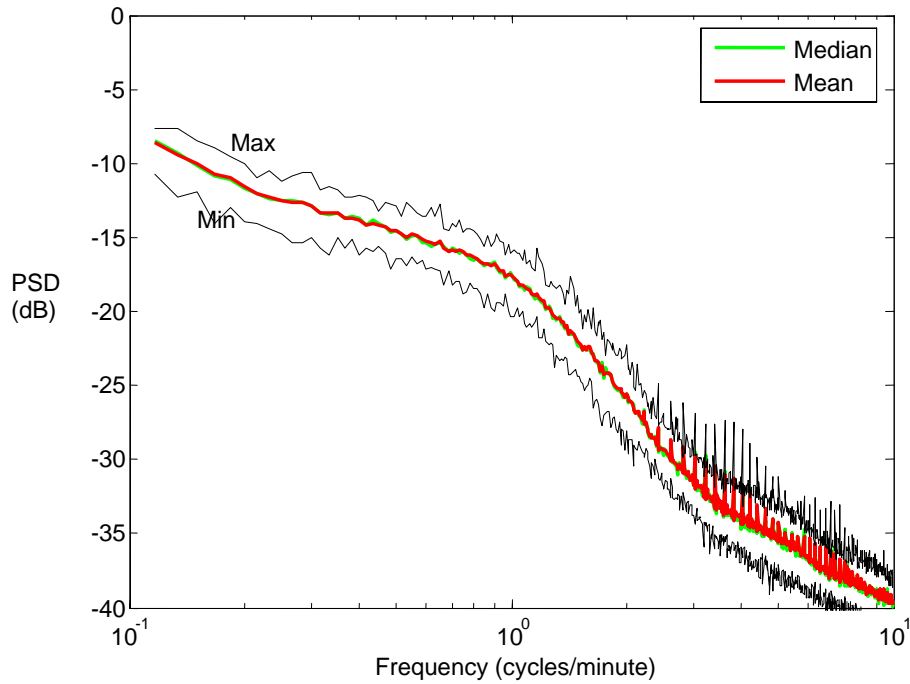


**Figure 6.6.** Vista substation PSD of  $I_A$  for all winter days except holidays and Dec. 1, 2004 (34 days analyzed Dec. 2004 - Jan. 2005)

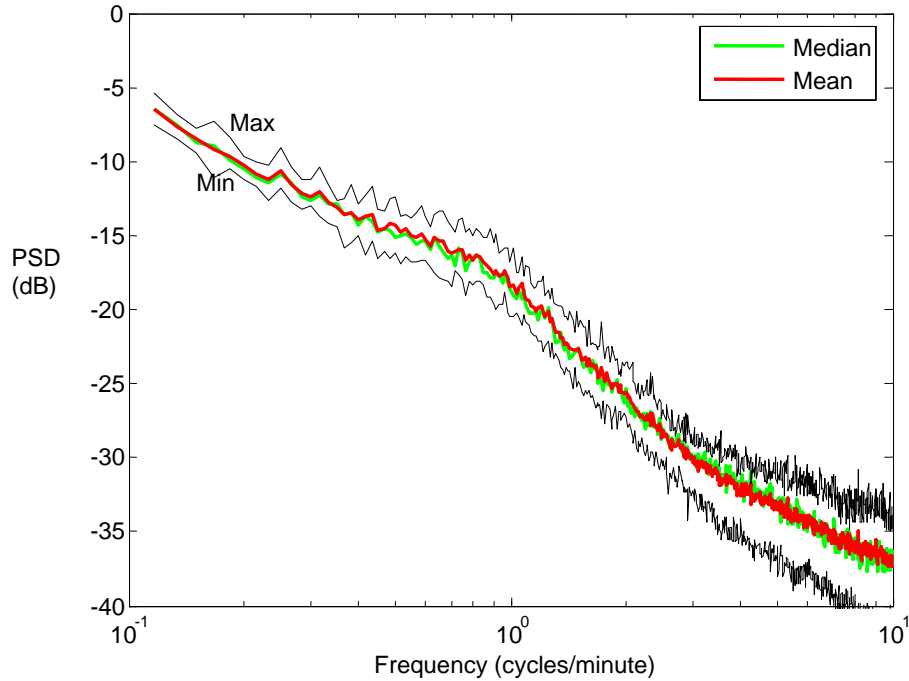


**Figure 6.7.** Vista substation PSD of  $I_A$  for all spring days except holidays (nine days analyzed Apr. 2005 – May 2005)

A comparison of the three seasons is shown in Figure 6.8. As can be seen, all three seasons have very similar characteristics and noise levels. The noise has a consistent roll-off with respect to frequency with an increased roll-off rate starting at 1 cycle-per-minute. The cause of the patterns for the characteristic shape of the PSD of the deterministic noise at this commercial substation cannot be ascribed. The consistent roll-off of the data implies that a beacon frequency should be as high as possible given the bounds of the data acquisition system.

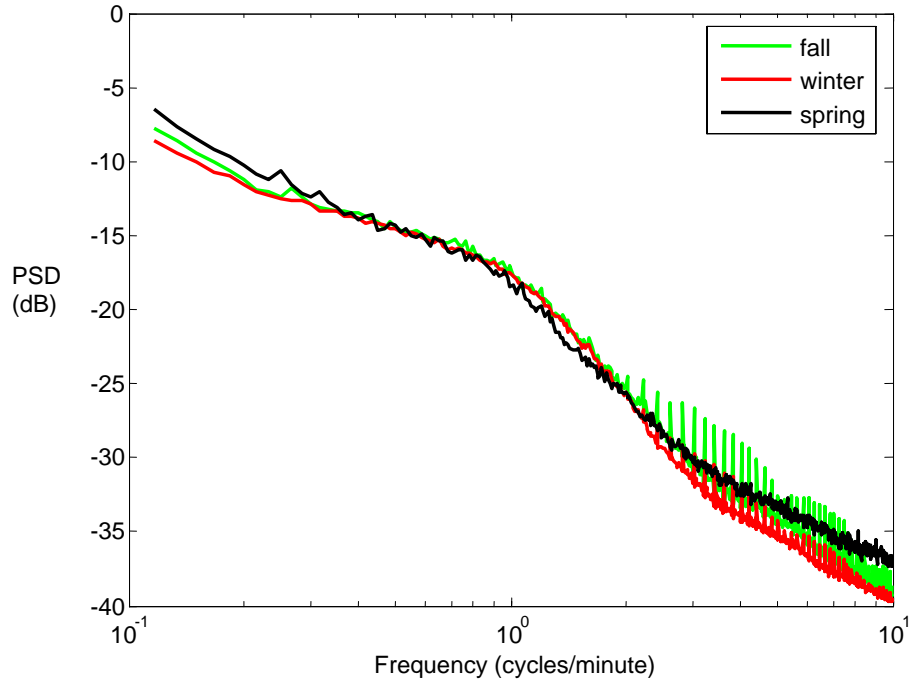


**Figure 6.8.** Vista substation comparison of mean PSD of  $I_A$ , for fall, winter, and spring

Surprisingly, the comparison of light loading versus heavy loading conditions as well as workday loading versus weekend loading indicates little difference between the noise content. Figure 6.9 compares the PSD for the light loading portion of the day versus the heavy loading portion of the day for the winter season. One can observe a difference in the shape of the two PSD as a function of loading, and the heavy loading curve displays a series of spikes at higher frequencies that is not observed for light loading. The two curves are otherwise similar.

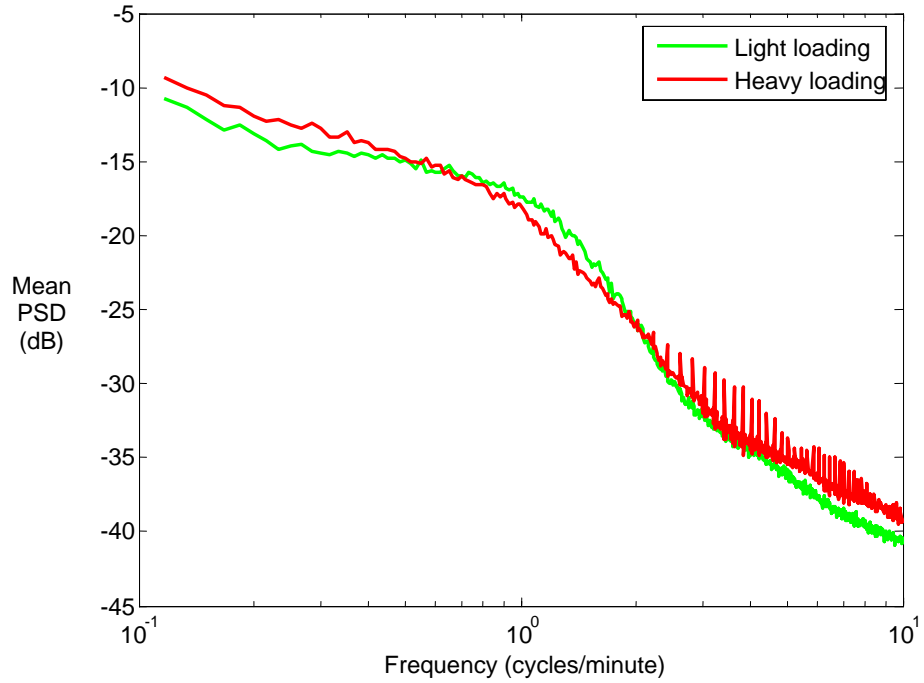


**Figure 6.9.** Vista substation mean PSD of  $I_A$  for winter, light vs. heavy loading (34 days analyzed Dec. 2004 – Jan. 2005)

The workday versus weekend loading for the winter season is shown in Figure 6.10; as seen, the two are very similar. Similar observations were observed to occur for the fall and spring data.

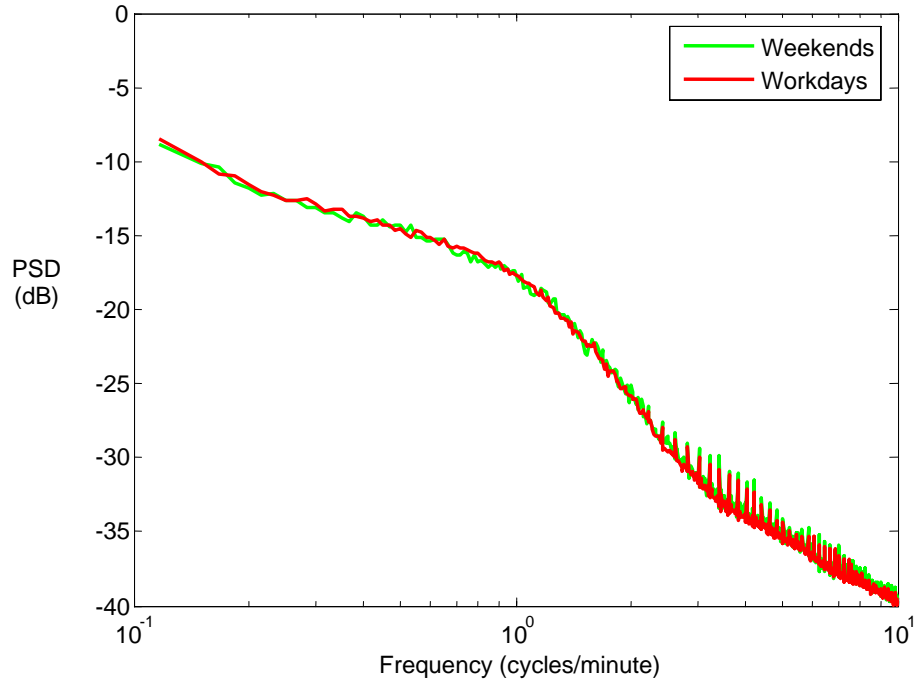


**Figure 6.10.** Vista substation mean PSD of  $I_A$  for winter, workday vs. weekend (Dec. 2004 – Jan. 2005)

Time of day loading shows that noise conditions tend to be significantly lower in the evening hours. This is indicated in Figure 6.11. The evening load noise is consistently 5 dB below the afternoon noise. This indicates that a beacon might be more detectable in the evening hours.

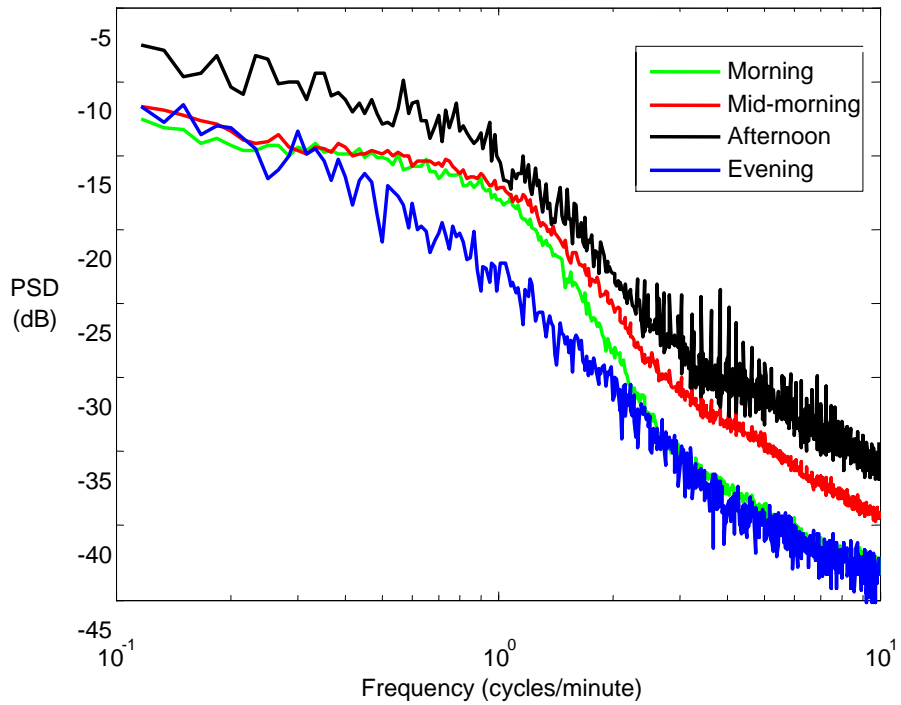


**Figure 6.11.** Vista substation mean PSD of  $I_A$  for winter, time-of-day comparison (34 days analyzed Dec. 2004 – Jan. 2005)

Phase-difference currents proved to have considerably less noise than  $I_A$  alone for frequencies above 2 cycles per minute. This is demonstrated in Figure 6.12 and Figure 6.13 for the winter season. The coherency tending toward unity at the higher frequencies in Figure 6.12 indicates that at the higher frequencies (above 2 cycles per minute) there is a relatively large amount of common-mode noise between  $I_A$  and  $I_B$ . Similar information is conveyed in Figure 6.13 which shows the PSD for  $I_A$  versus the phase-difference currents. Spring and fall season results are similar to the winter results shown in Figure 6.12 and Figure 6.13. These results indicate that the phase-difference currents are good candidates for beacon detection if the beacon frequency is in the range of the common-mode noise (above 2 cycles per minute for the Vista data).

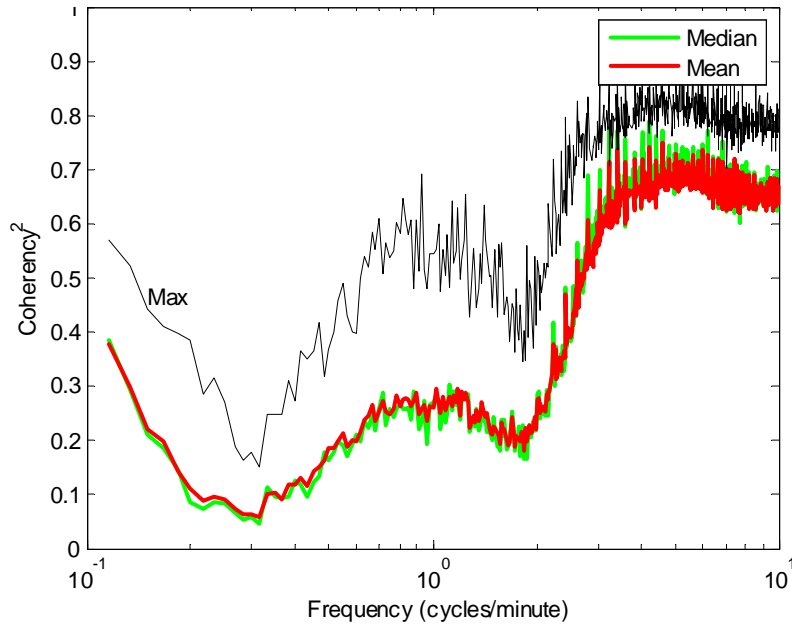


**Figure 6.12.** Vista substation coherency between  $I_A$  and  $I_B$  for winter (35 days Dec. 2004 – Jan. 2005)

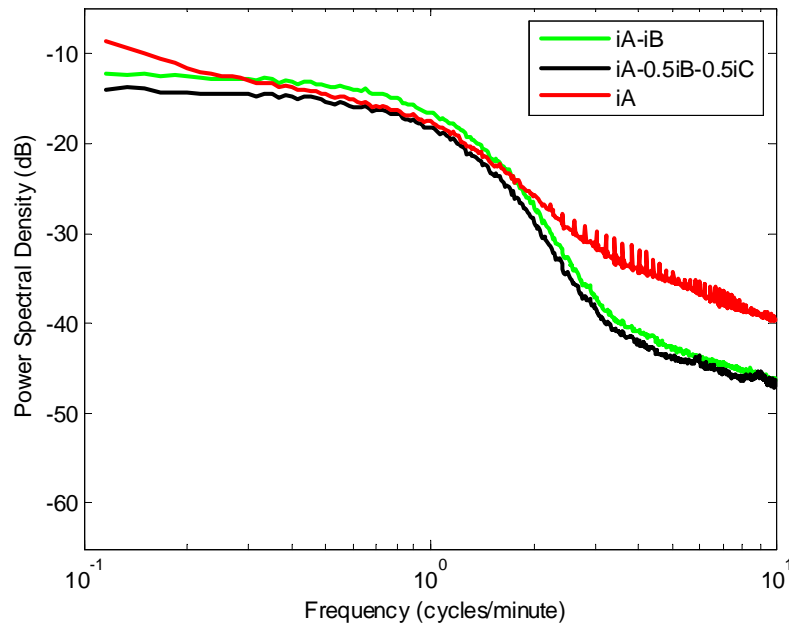


**Figure 6.13.** Vista substation mean PSD for winter,  $I_A$  versus phase-difference currents (61 days Dec. 2004 – Jan. 2005)

Coherency analyses between the 1<sup>st</sup>-half of a day versus the 2<sup>nd</sup>-half of the day are presented in Figure 6.14 through Figure 6.16. Because the coherency is very close to zero for all seasons, the data is highly uncorrelated over time. This indicates good potential for beacon detection using cross-correlation between independent time periods.

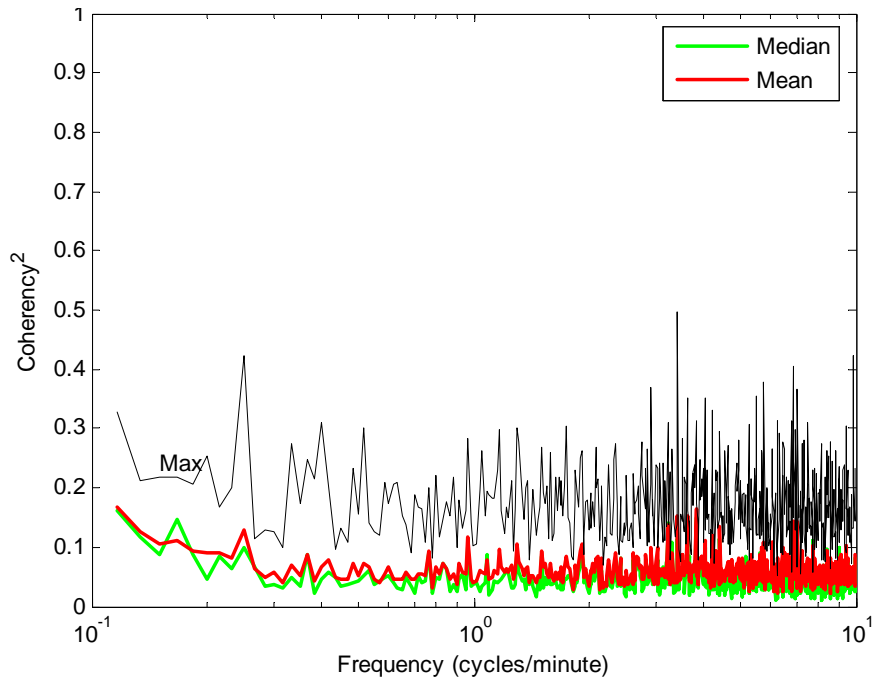


**Figure 6.14.** Vista substation coherency of  $I_A$  for the 1<sup>st</sup>-half of the day versus the 2<sup>nd</sup>-half of the day for fall (13 days Nov. 2004)

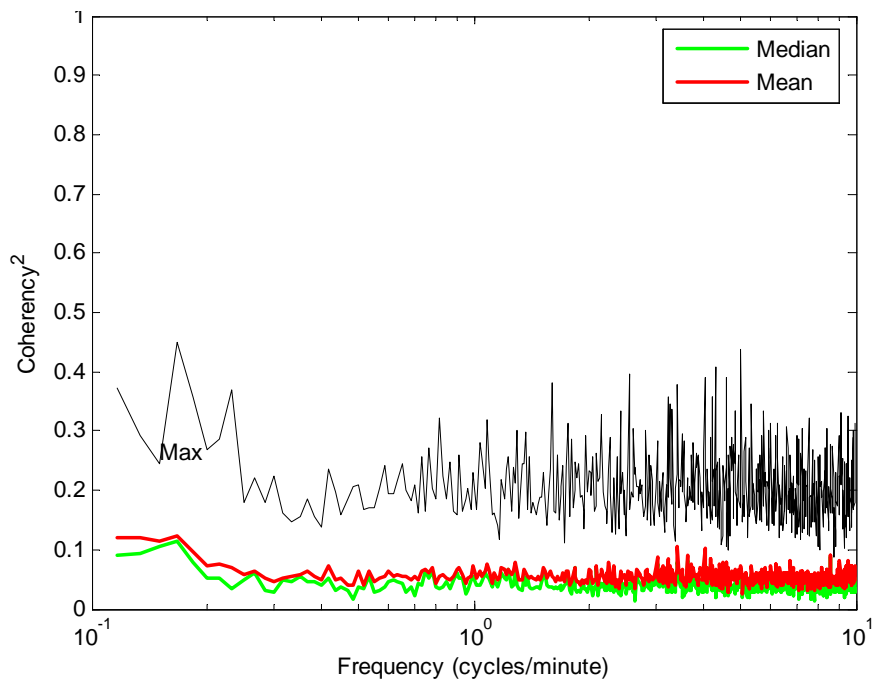


**Figure 6.15.** Vista substation coherency of  $I_A$  for the 1<sup>st</sup>-half of the day versus the 2<sup>nd</sup>-half of the day for winter (35 days Dec. 2004 – Jan. 2005)

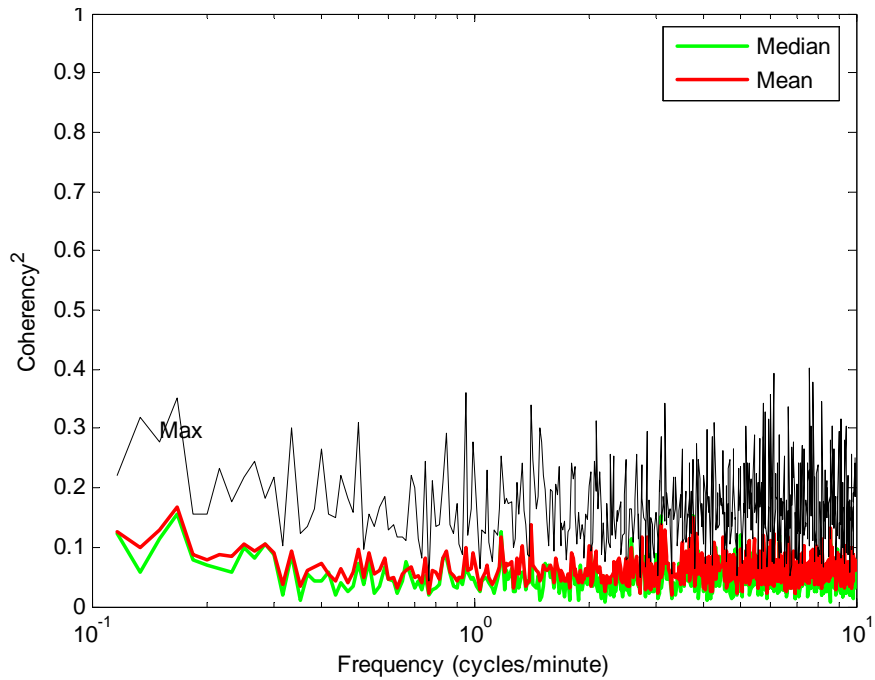


**Figure 6.16.** Vista substation coherency of  $I_A$  for the 1<sup>st</sup>-half of the day versus the 2<sup>nd</sup>-half of the day for spring (9 days Apr. 2005 – May 2005)

### 6.3 Benton Substation Analysis

Figure 6.17 through Figure 6.20 show the normalized  $I_A$  used for analysis from the Benton substation. Nine days of data is available for fall 2004, 17 days of data is available for winter 2004/5, 51 days of data are available for spring 2005, and 29 days of data are available for summer 2005.

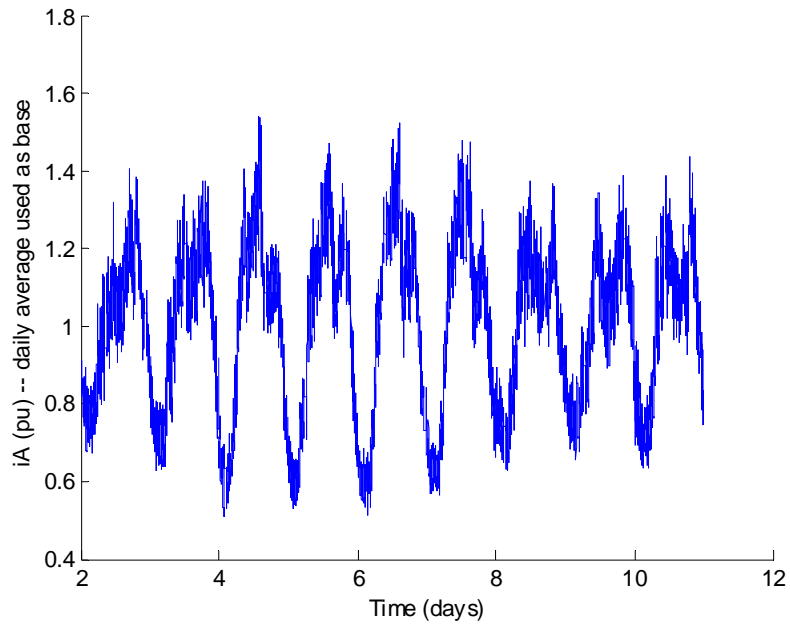


**Figure 6.17.** Benton substation  $I_A$  for fall (9 days analyzed Oct. 2004)

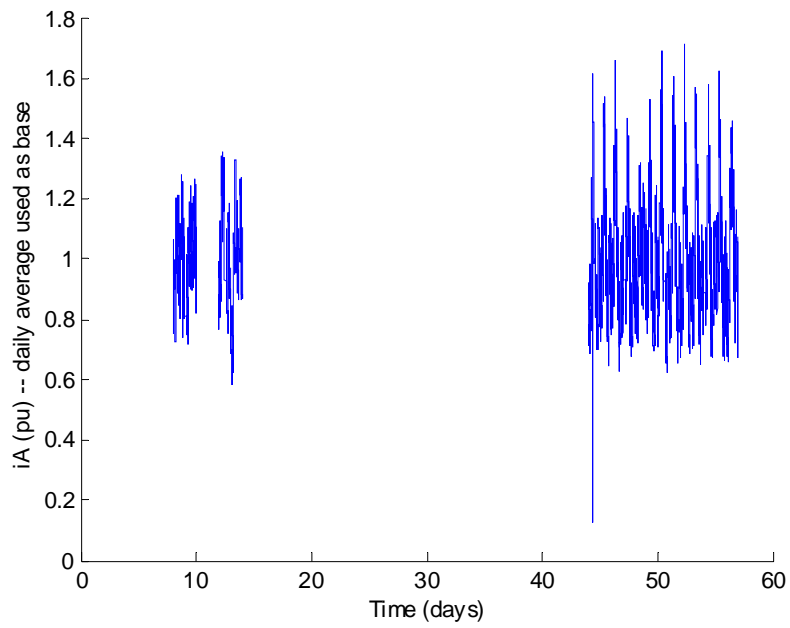


**Figure 6.18.** Benton substation  $I_A$  for winter (17 days analyzed Jan. 2005 – Feb. 2005)

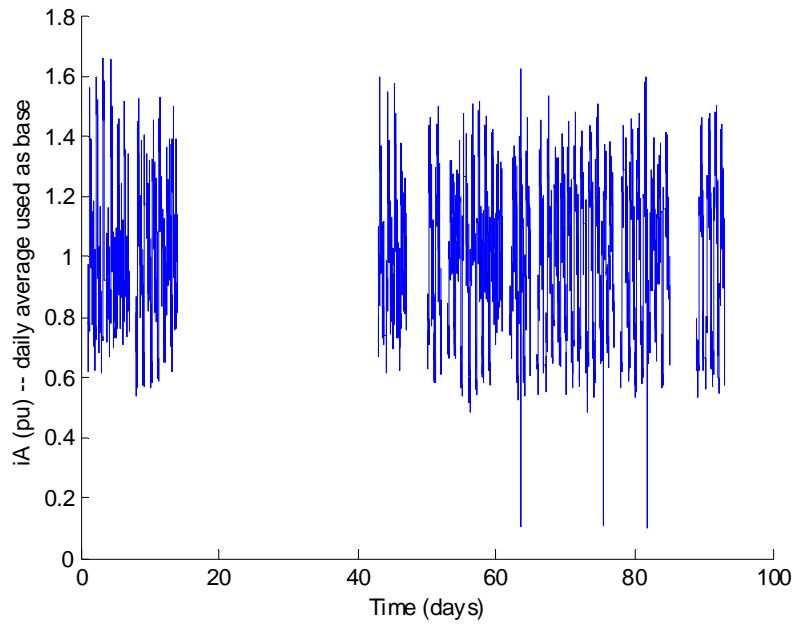


**Figure 6.19.** Benton substation  $I_A$  for spring (51 days analyzed Mar. 2005 – May 2005)

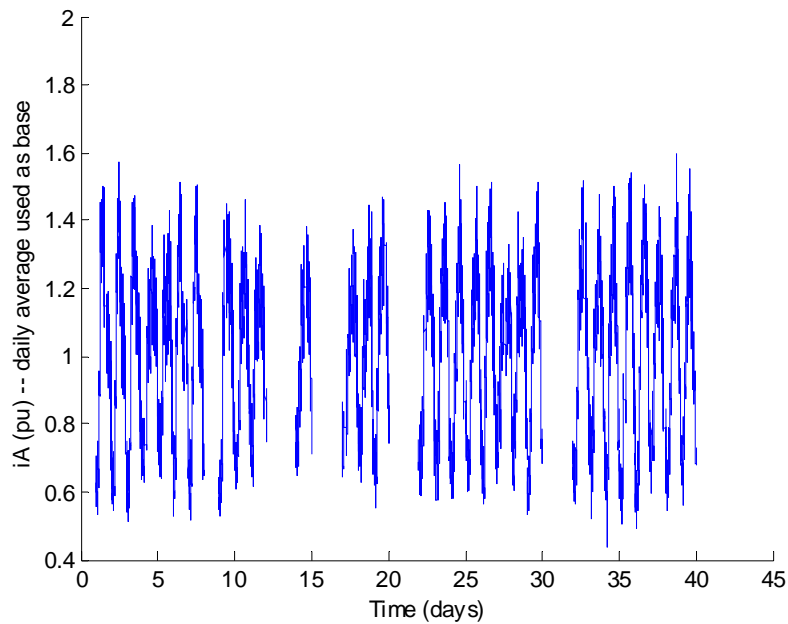


**Figure 6.20.** Benton substation  $I_A$  for summer (29 days analyzed Jun. 2005 – Jul. 2005)

A comparison of all four seasons is shown in Figure 6.21. Just as in the Vista data, all seasons have very similar characteristics and noise levels. The noise has a consistent roll-off with respect to frequency. But, the roll-off rate does not increase with frequency as in the Vista data. This implies again that a beacon frequency should be as high as possible for a residential feeder given the bounds of the data acquisition system.

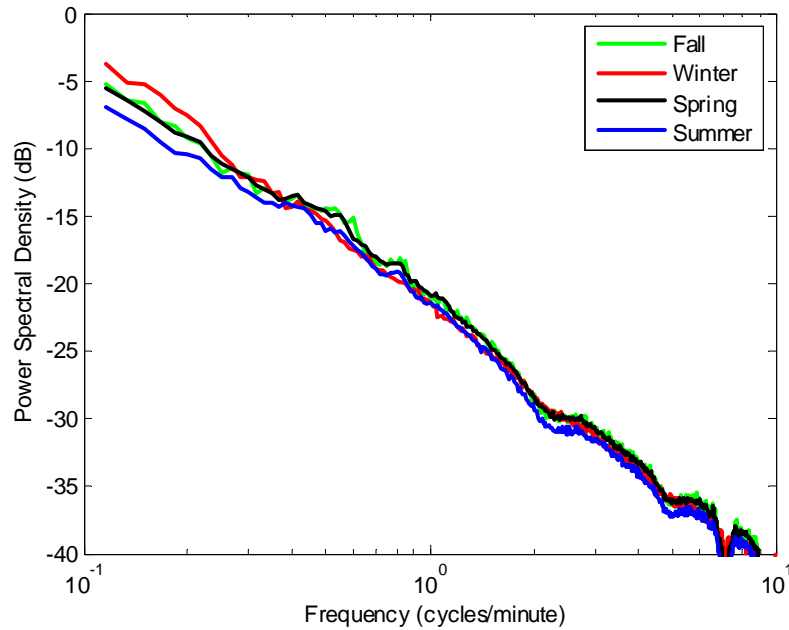


**Figure 6.21.** Benton substation mean PSD of  $I_A$ , season comparison (all available days Oct. 2004 – Jul. 2005)

Unlike the Vista data, the light-loading condition for Benton had lower PSD for all seasons when compared to the heavy loading portion of the day. This is demonstrated in Figure 6.22 for the winter season. As seen in the figure, the light-loading condition has approximately 3 dB lower noise.

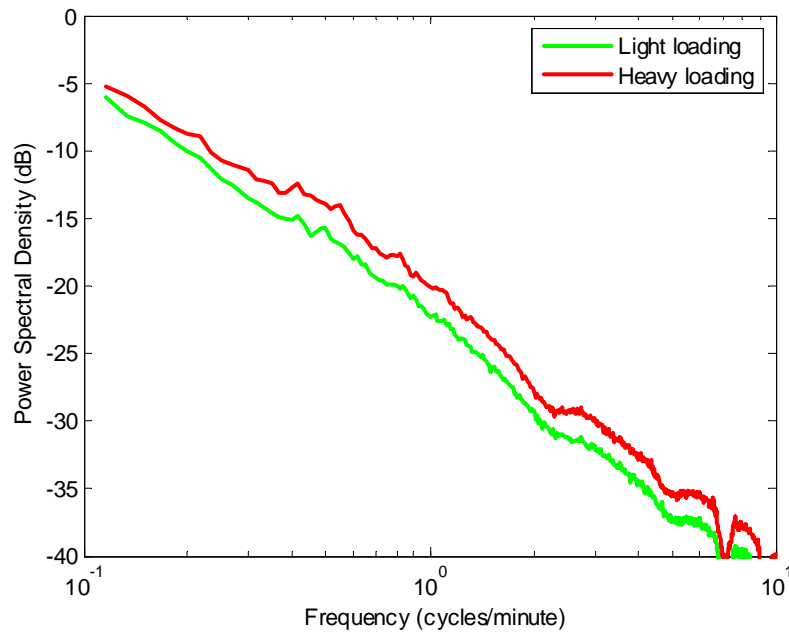


**Figure 6.22.** Benton substation mean PSD of  $I_A$  for winter, light vs. heavy loading (51 days May 2005 – May 2005)

The daily properties of the Benton data have the same properties as the Vista data. There is very little difference between the workday and weekend PSD for all seasons in the Benton data; this is reflected in Figure 6.23.

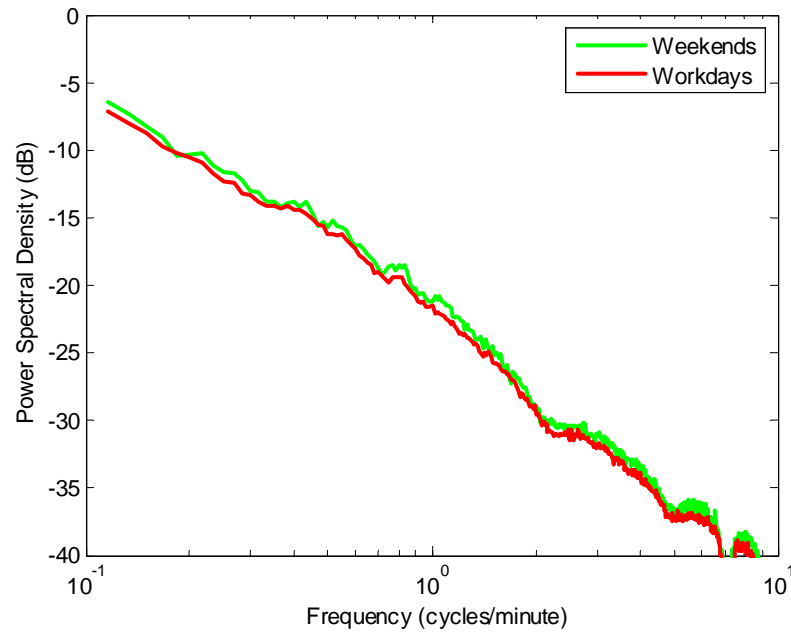


**Figure 6.23.** Benton substation mean PSD of  $I_A$  for summer for workday, weekend (Jun. – Jul. 2005)

Also like the Vista data, time of day loading for the Benton data shows that noise conditions tend to be significantly lower in the evening hours. This is indicated in Figure 6.24.

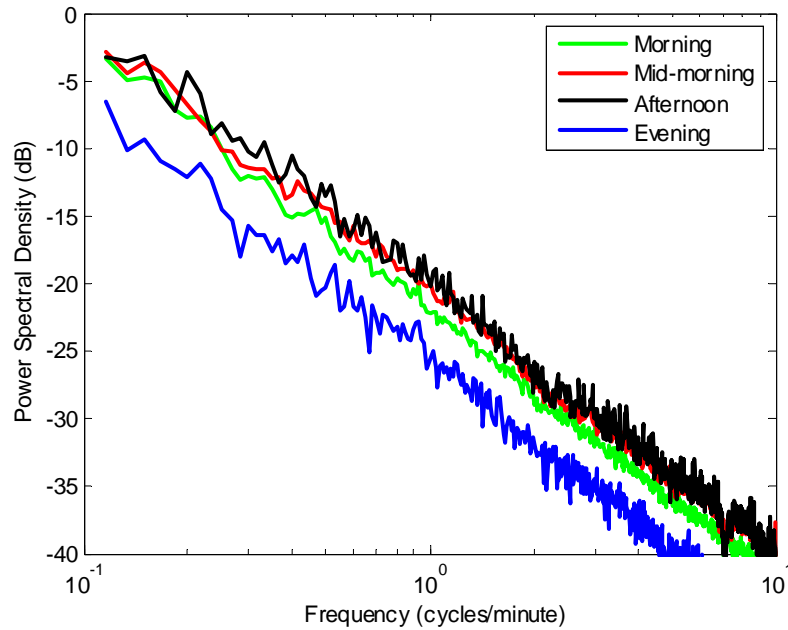


**Figure 6.24.** Benton substation mean PSD of  $I_A$  for winter by time-of-day (17 days Jan. – Feb. 2005)

The properties of the phase-difference currents depend on the method of calculating the phase difference. If one uses  $I_A - I_B$ , the phase-difference current has more noise than  $I_A$ . But, if one uses  $I_A - 0.5I_B - 0.5I_C$ , the phase-difference has less noise. These results are reflected in Figure 6.25 which shows the PSD for  $I_A - 0.5I_B - 0.5I_C$  to be the lowest of the three.

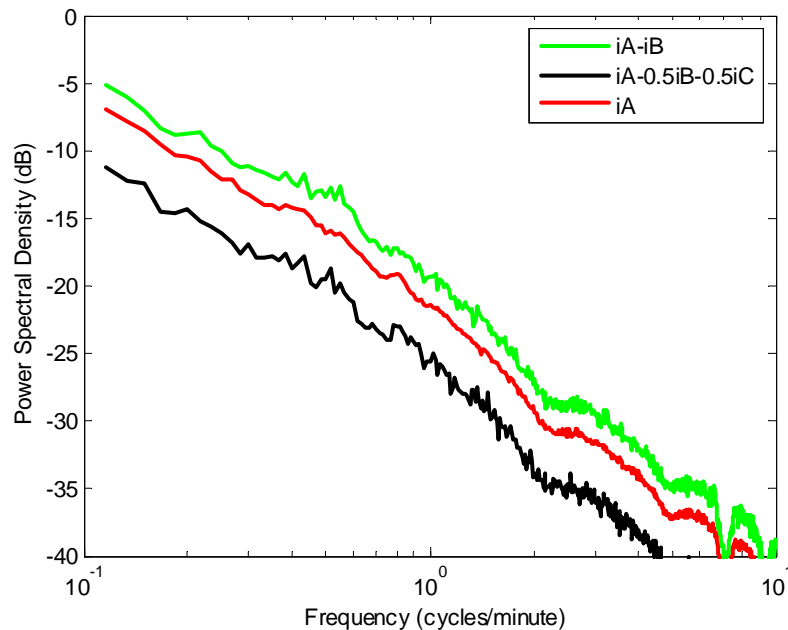


**Figure 6.25.** Benton mean PSD for summer,  $I_A$  versus phase-difference currents (5 days Jun. – Jul. 2005)

Coherency analysis between the 1<sup>st</sup>-half of a day versus the 2<sup>nd</sup>-half of the day for Benton are very similar to the results from the Vista substation data analysis. As shown in Figure 6.26, the coherency is very close to zero.

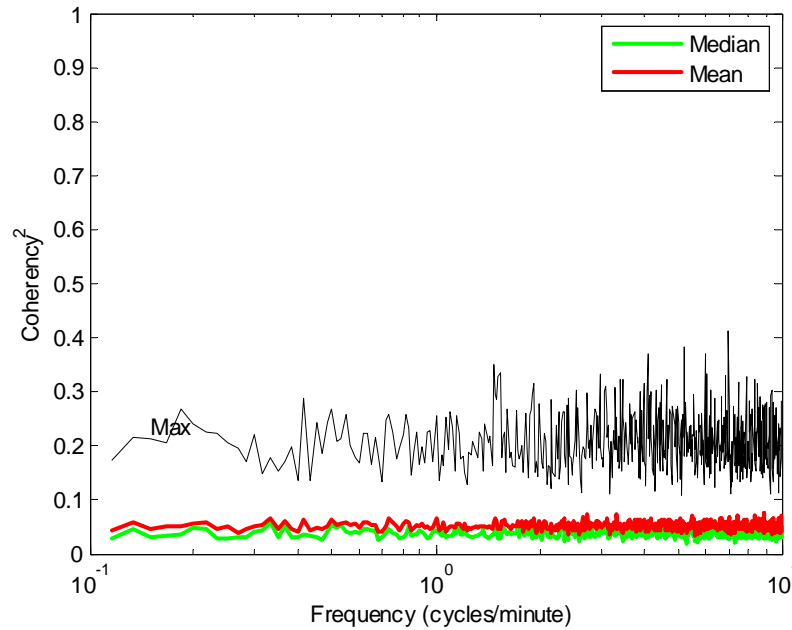


**Figure 6.26.** Benton substation coherency of  $I_A$  for the 1st-half of the day versus the 2nd-half of the day for spring (51 days Mar. – May 2005)

**Figure 6.27** shows a comparison between the Vista and Benton data. Although the Vista PSD tends to be more rounded, both substations have approximately the same level of noise. Remember, the currents have been normalized by the daily averages prior to spectrum analysis. This indicates that the amplitude of the beacon relative to the average feeder loading would have to be the same for both substations.

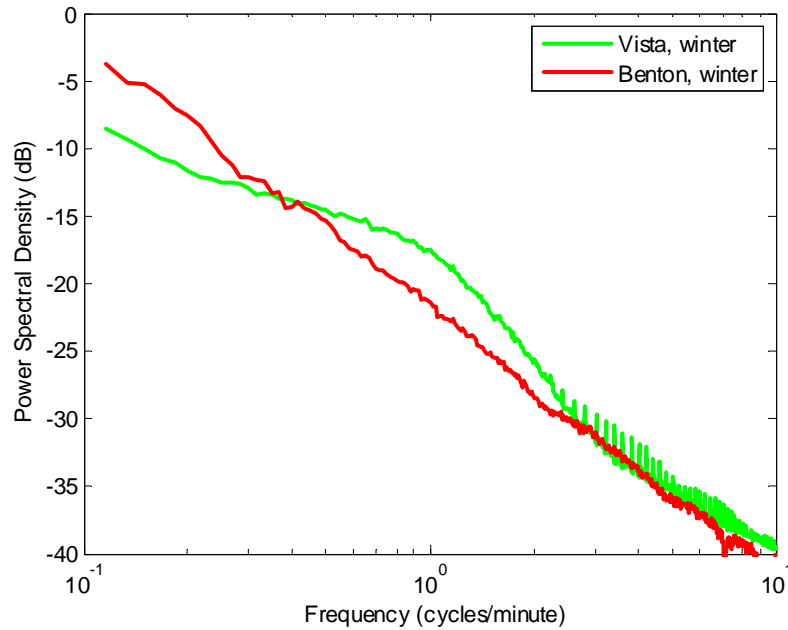


**Figure 6.27.** Mean PSD of  $I_A$ , for Benton versus Vista substations (winter 2004 – 2005)

## 6.4 Riverfront Substation Analysis

We had originally negotiated with Benton PUD for access to data from a large chemical manufacturing plant in Kennewick, Washington. In 2005, we were informed that the plant was inactive, would remain inactive, and would not likely restart. The data from the substation would not be of interest.

Only a limited quantity of data was available from the Riverfront substation, an industrial substation in Prosser, Washington that primarily serves a large food processing plant. Sample PSD of phase currents for a day's data are shown in Figure 6.28. If anything at all can be said about the industrial load, it appears to be flatter, to exhibit lower relative noise to the left of the figures where the frequencies are approximately once per minute. This may have been predicted from the lack of refrigeration and small space heaters that cycle approximately once per minute.

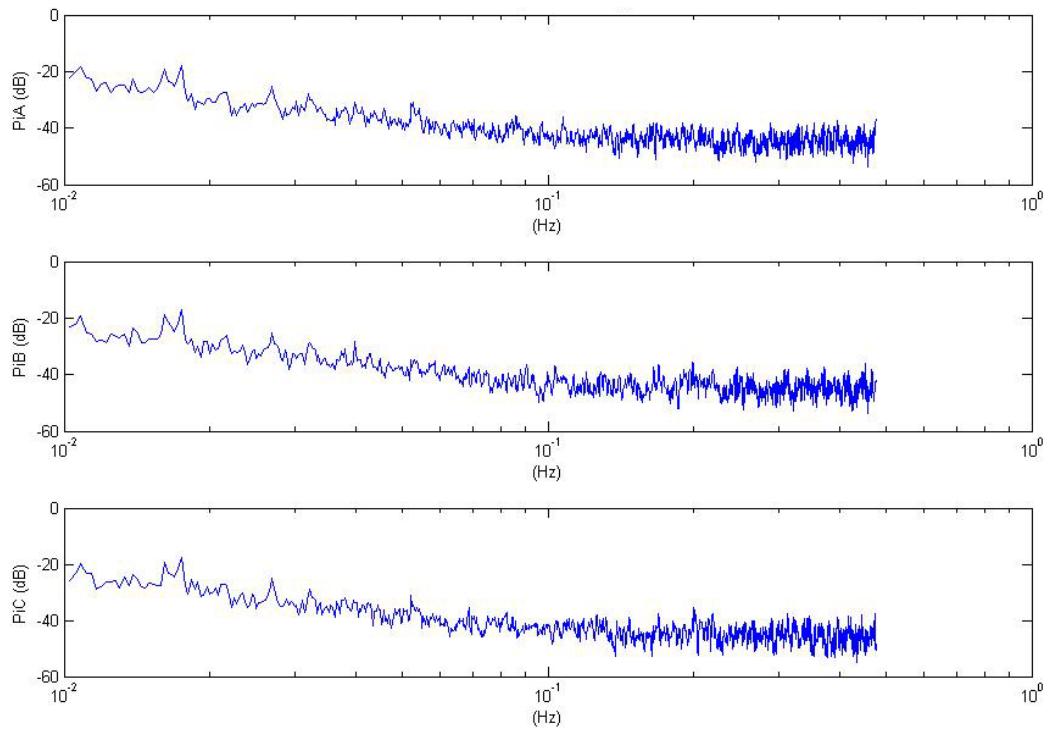


**Figure 6.28.** PSD of Riverfront substation phase currents (full day, Sep. 21, 2005)



## 7.0 Beacon Simulation and Detection

To investigate the potential of beacon detection methodologies, two cases are of special interest. First is the simulation of a beacon. To simulate the effect, a hypothetical beacon signal is added to the field measured ambient data. The second case involves December 1, 2004 of the Vista ambient data. This data set contains a significant periodic switching load that provides insight into potential beacon properties.

### 7.1 Beacon Simulation

As a test case, the Vista substation data from December 4, 2004 is used. The ambient data from this day is typical of the Vista substation. The approximate average daily load for this feeder for December 4 is 4.2 MW.

For the first simulation, a square-wave beacon at a frequency of 3 cycles-per-minute and peak amplitude of 1% of the daily average and a 50% duty cycle is simulated. The beacon signal is shown in Figure 7.1. The beacon signal is added to the ambient data and the resulting  $I_A$  is shown in Figure 7.2. As seen in these figures, the beacon cannot be seen in the time-domain data.

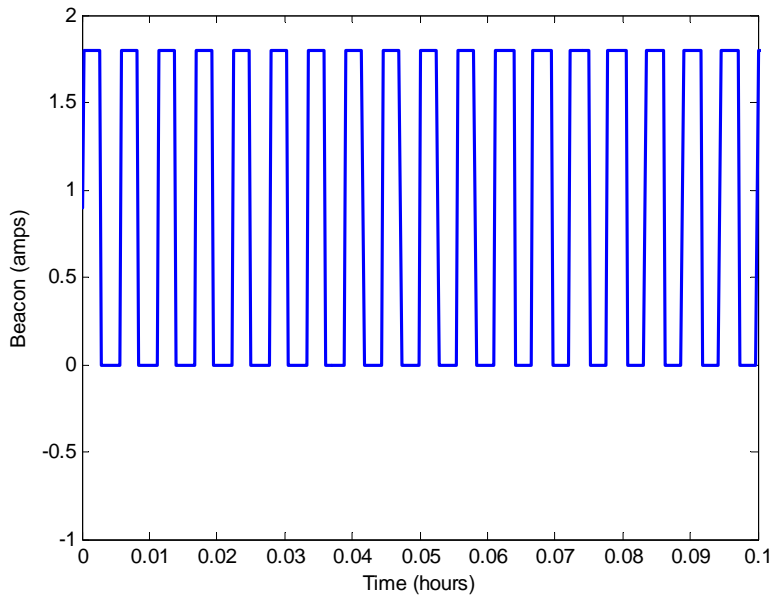


**Figure 7.1.** Beacon square-wave at 3 cycles per minute, beacon amplitude = 1% of average

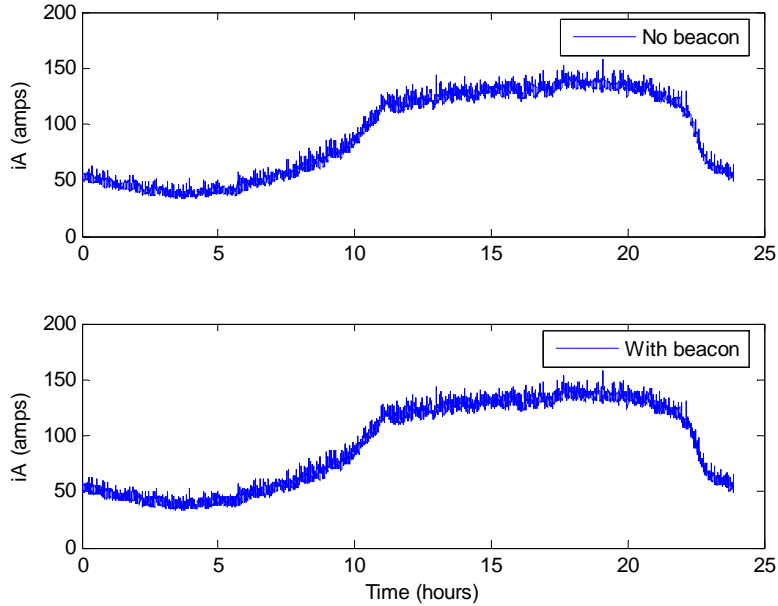


**Figure 7.2.** Beacon simulation  $I_A$  with and without beacon signal (beacon amplitude = 1% average load , Dec. 4, 2005, Vista substation)

Using PSD, the beacon is easily detected, and the power of the beacon can be estimated. Figure 7.3 shows the PSD of the beacon signal alone compared with the PSD of  $I_A$  with the beacon added. Figure 7.4 compares the PSD of the ambient data with the PSD of  $I_A$  with the beacon added. As seen in these plots, the beacon fundamental (1<sup>st</sup> harmonic) is easily observable in the PSD. Also easily detected are the higher harmonics. The PSD of the beacon signal in the first plot shows all the odd harmonics indicating a square-wave signal. The odd harmonics are at 3, 9, and 15 cycles-per-minute. The power at any given harmonic is estimated by

$$P(f) = \frac{10^{PSD_{dB}(f)/10}}{T}, \quad (4)$$

where  $f$  is the frequency of the harmonics,  $P$  is the power in watts,  $T$  is the amount of data used for fft analysis in seconds,  $PSD_{dB}(f)$  is the PSD at frequency  $f$  in dB. In this analysis,  $T = 3600$  seconds. From Figure 7.4, the 1<sup>st</sup> harmonic is estimated to be 32 dB, the 3<sup>rd</sup> harmonic is estimated to be 21 dB, and the 5<sup>th</sup> harmonic is estimated to be 13 dB. Using these values in equation (4) and summing results in a power estimate of 0.48 watts. Note that this is the estimated AC average power consumed by the beacon if the current is passed through a 1- $\Omega$  resistor. The actual AC average power is 0.72 watts. Therefore, the three peaks represent approximately 67% of the energy in the beacon. The difference between the actual and estimated power is caused by signal processing artifacts and truncation at the 5<sup>th</sup> harmonic.

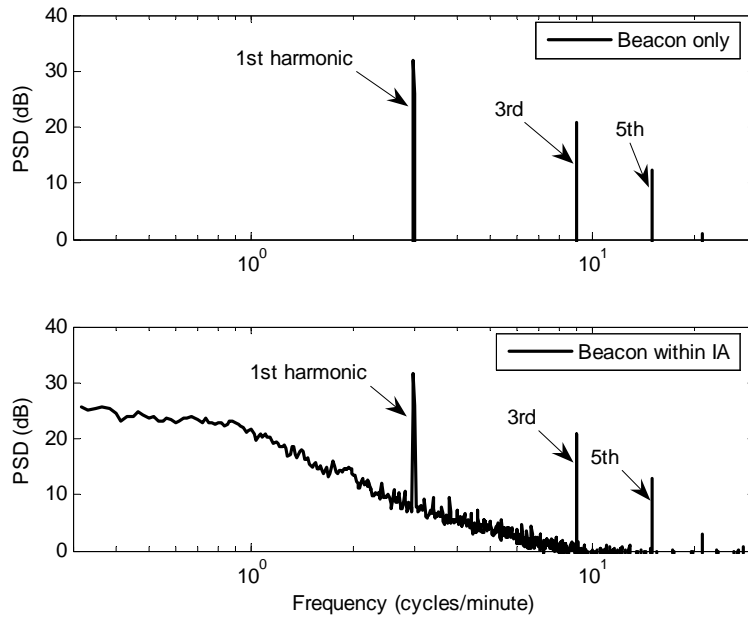


**Figure 7.3.** PSD of beacon alone and  $I_A$  with the beacon added (beacon amplitude = 1%, 24 hours of analyzed data, Dec. 5, 2004, Vista)

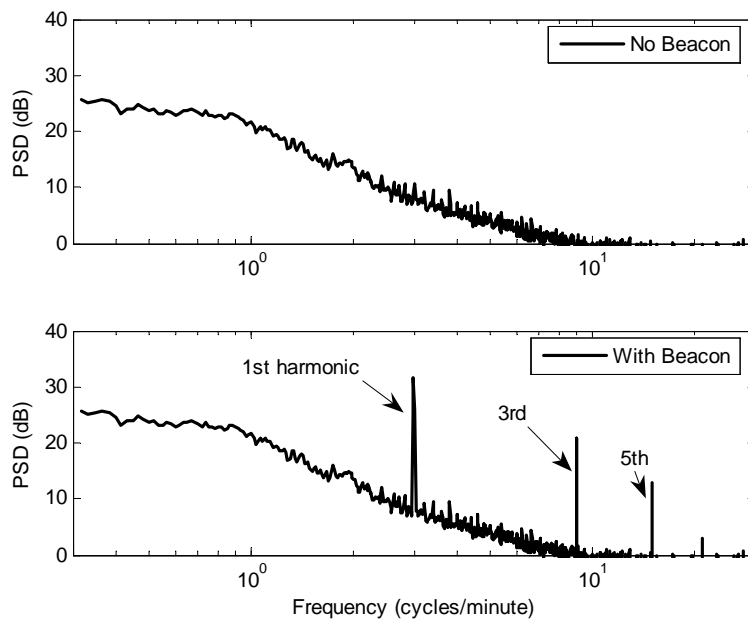


**Figure 7.4.** PSD of  $I_A$  with and without beacon signal (beacon amplitude = 1%, 24 hours of analyzed data, Dec. 5, 2004, Vista)

The PSD for the phase-difference current of  $I_A-I_B$  is shown in Figure 7.5. The beacon is also easily detected in this signal. In fact, it has a larger relative peak than the PSD of  $I_A$  alone because of the lower energy in the ambient  $I_A-I_B$ . The coherency of  $I_A-I_B$  comparing the first-half of the day with the second-

half of the day is shown in Figure 7.6. As with the PSD functions, the coherency clearly shows the presence of the beacon at 3 cycles-per-minute.

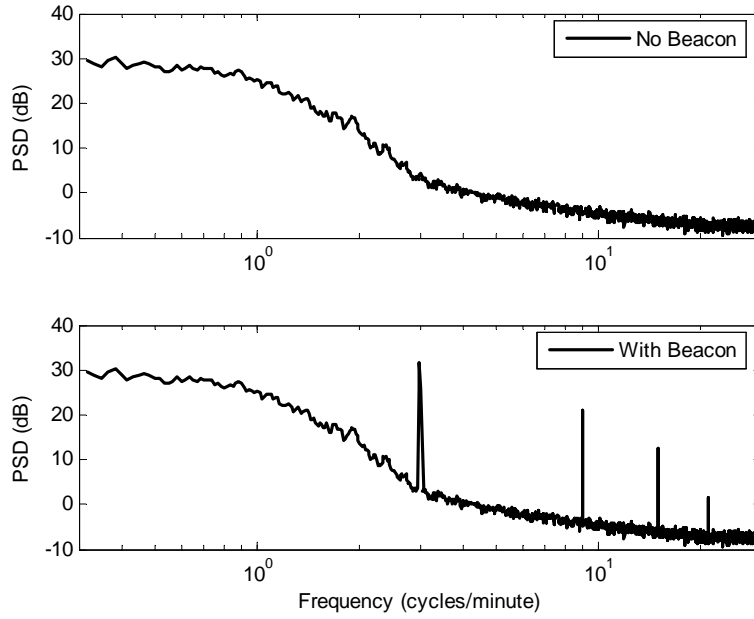


**Figure 7.5.** PSD of  $I_A-I_B$  with and without beacon signal (beacon amplitude = 1%, 24 hours of analyzed data, Dec. 5, 2004, Vista)

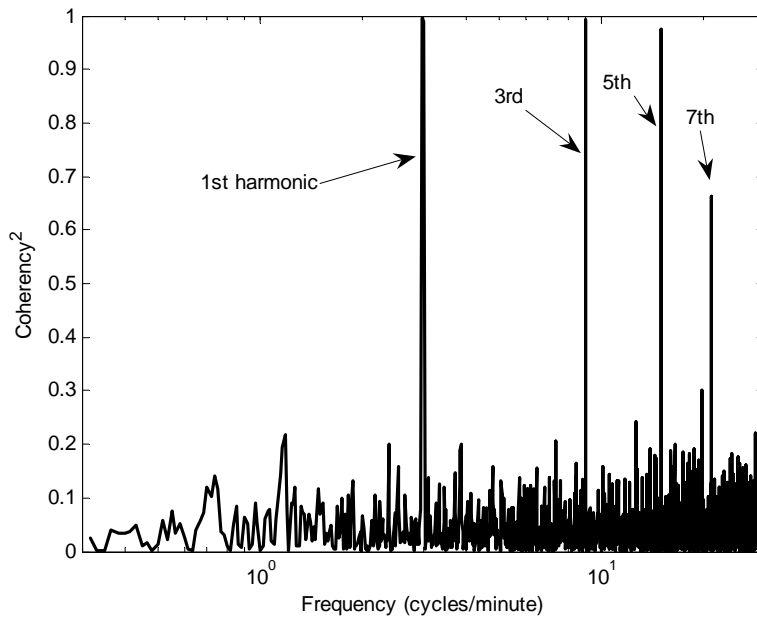


**Figure 7.6.** Coherency of  $I_A-I_B$  for the 1st-half of the day versus the 2nd-half of the day for the beacon simulation example (beacon amplitude = 1%, 24 hours of analyzed data, Dec. 5, 2004)

To detect a very small beacon, one would likely want to select the beacon fundamental frequency to be near the Nyquist frequency. At the higher frequencies, the ambient noise has very low amplitude; therefore, a lower amplitude beacon will be more observable.

As an example, consider a square-wave beacon at a frequency of 10 cycles-per-minute (the Nyquist is just below 30 cycles-per-minute) and a peak amplitude of 0.05% of the daily average (approximately a 2.1-kW load) and a 50% duty cycle. The results are shown in Figure 7.7 and Figure 7.8. As seen, the 1<sup>st</sup> harmonic is easily detected, especially in the coherency. The amplitude is decreased to 0.02% with the result show in Figure 7.9 and Figure 7.10. At this point, the beacon is no longer as easily detected in the PSD but exhibits a significant peak in the coherency.

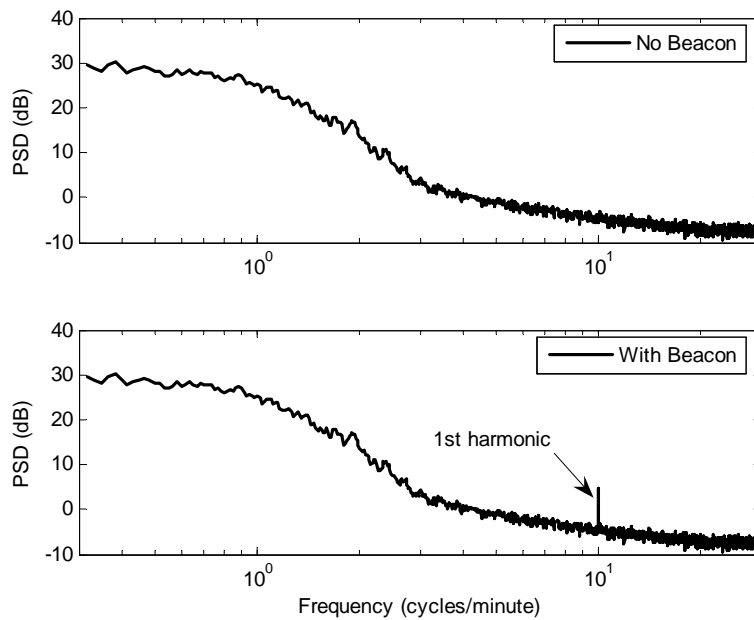


**Figure 7.7.** PSD of  $I_A-I_B$  with and without the beacon signal (beacon amplitude = 0.05%, 24 hours of analyzed data, Dec. 5, 2004, Vista)

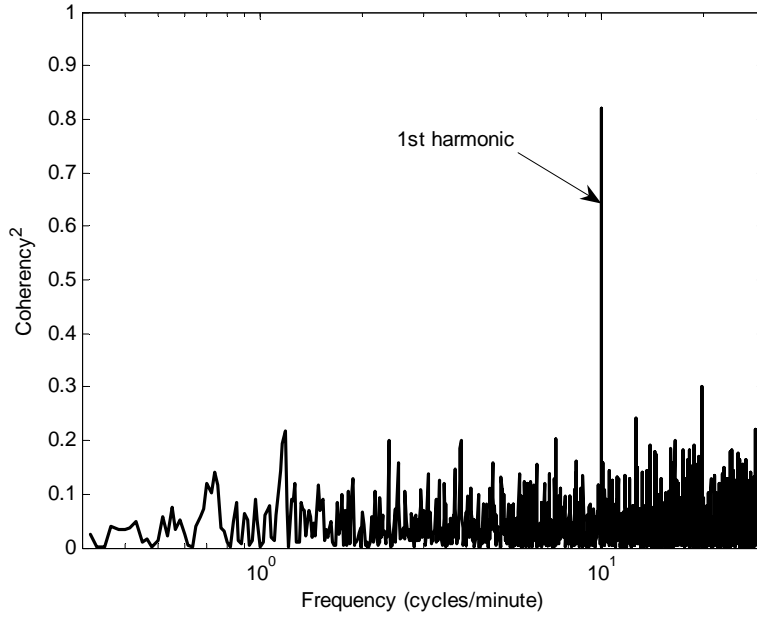


**Figure 7.8.** Coherency of  $I_A-I_B$  for the 1st-half of the day versus the 2nd-half of the day for the beacon simulation example (beacon amplitude = 0.05%, 24 hours of analyzed data, Dec. 5, 2004, Vista)

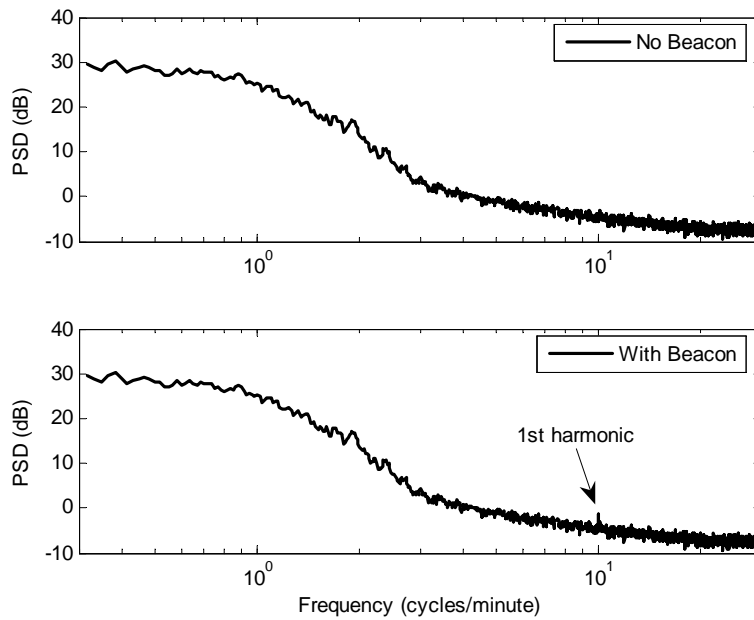


**Figure 7.9.** PSD of  $I_A-I_B$  with and without beacon signal (beacon amplitude = 0.02%, 6 hours of analyzed data, Dec. 5, 2004, Vista)

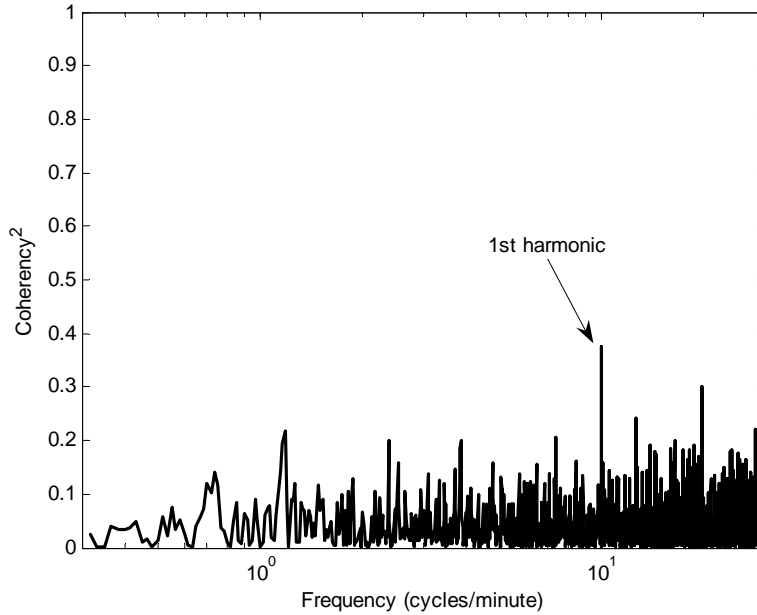


**Figure 7.10.** Coherency of  $I_A-I_B$  for the 1st-half of the day versus the 2nd-half of the day for the beacon simulation example (beacon amplitude = 0.02%, 24 hours of analyzed data, Dec. 5, 2004, Vista)

Another issue to consider is the length of the analysis data. The previous examples in this section all used 24 hours of data to estimate the PSD and coherency functions. If less data is employed, the functions will have more of a random component with possible false peaks. This will then require a larger amplitude beacon. For example, the previous 10 cycle-per-minute, 0.05% amplitude beacon is analyzed first using 12 hours of data and then 6 hours of data. The results are shown in Figure 7.11 through Figure 7.14. In the 12-hour analysis shown in Figure 7.11 and Figure 7.12, the beacon is detectable. But, in the 6-hour analysis in Figure 7.13 and Figure 7.14, the beacon is not longer detectable.

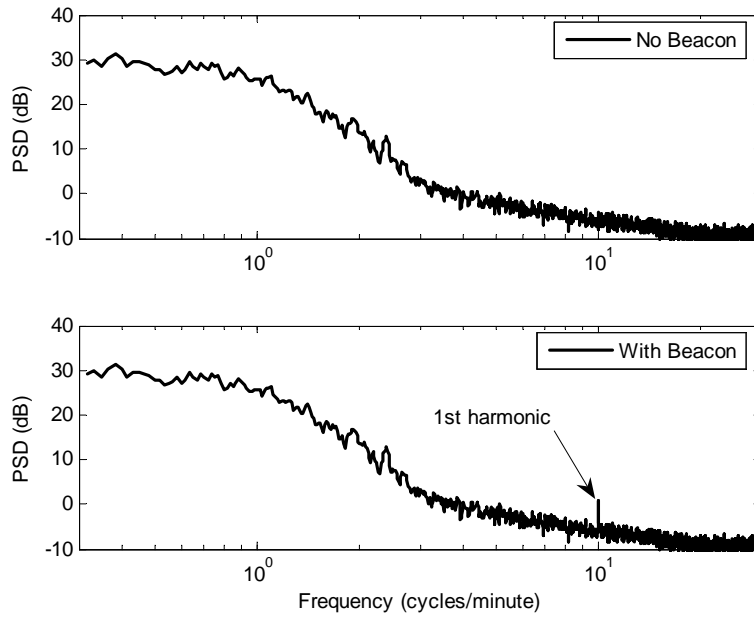


**Figure 7.11.** PSD of  $I_A - I_B$  with and without beacon signal (beacon amplitude = 0.05%, 12 hours of analyzed data, Dec. 5, 2004, Vista)

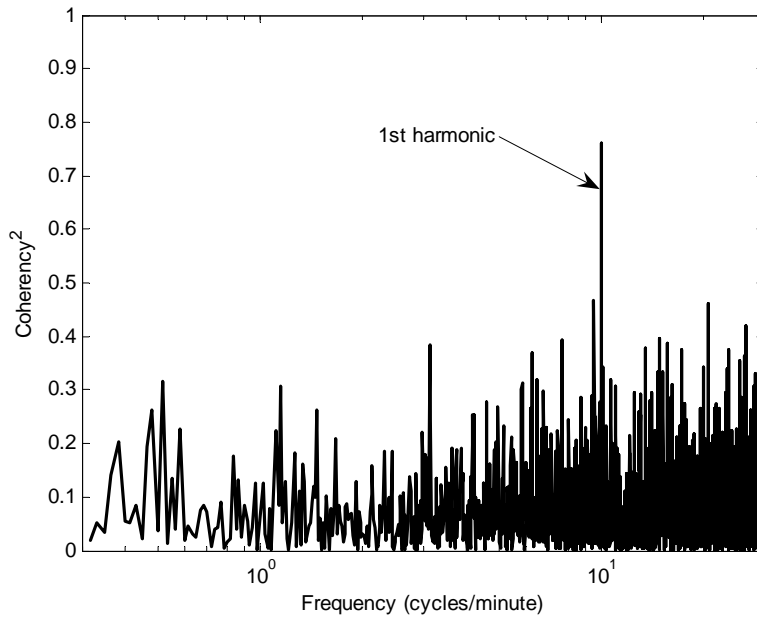


**Figure 7.12.** Coherency of  $I_A - I_B$  for the 1st-half of the data versus the 2nd-half of the data for the beacon simulation example (beacon amplitude = 0.05%, 12 hours of analyzed data, Dec. 5, 2004, Vista)

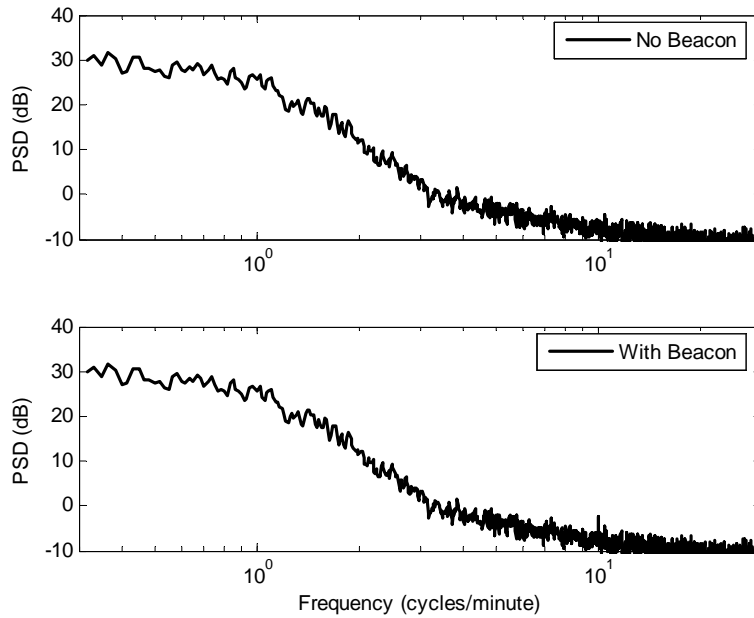


**Figure 7.13.** PSD of  $I_A - I_B$  with and without beacon signal (beacon amplitude = 0.05%, 6 hours of analyzed data, Dec. 5, 2004, Vista)

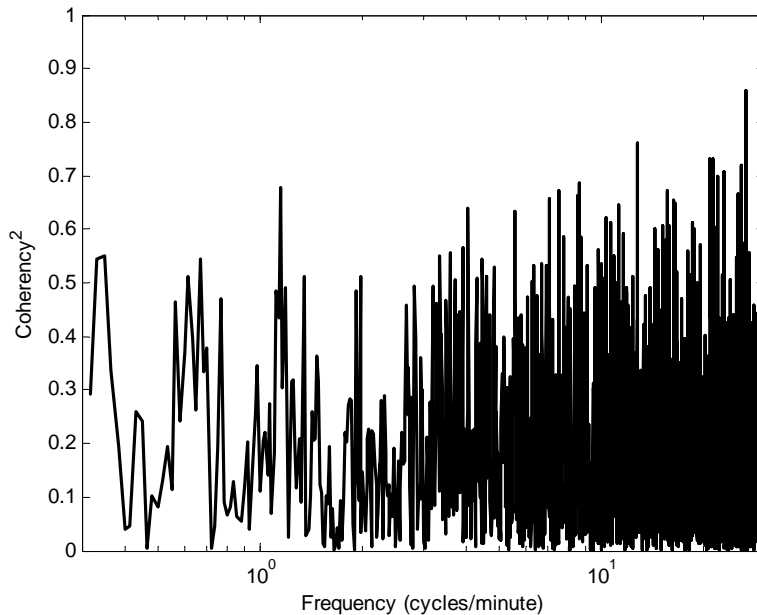


**Figure 7.14.** Coherency of  $I_A - I_B$  for the 1st-half of the data versus the 2nd-half of the data for the beacon simulation example (beacon amplitude = 0.05%, 6 hours of analyzed data, Dec. 5, 2004, Vista)

If the length of the analysis is extended to two days, an even smaller amplitude beacon can be detected. The square-wave beacon amplitude is reduced to 0.02% with 48 hours of total data. The 48-hour average loading is 4.25 MW; therefore, the 0.02% amplitude represents a beacon load of 840 Watts.

The resulting coherency estimate is shown in Figure 7.15. As seen, the 1<sup>st</sup> harmonic is detectable. If the amplitude is further reduced to 0.01%, the beacon is no longer detectable in the 48-hour analysis.

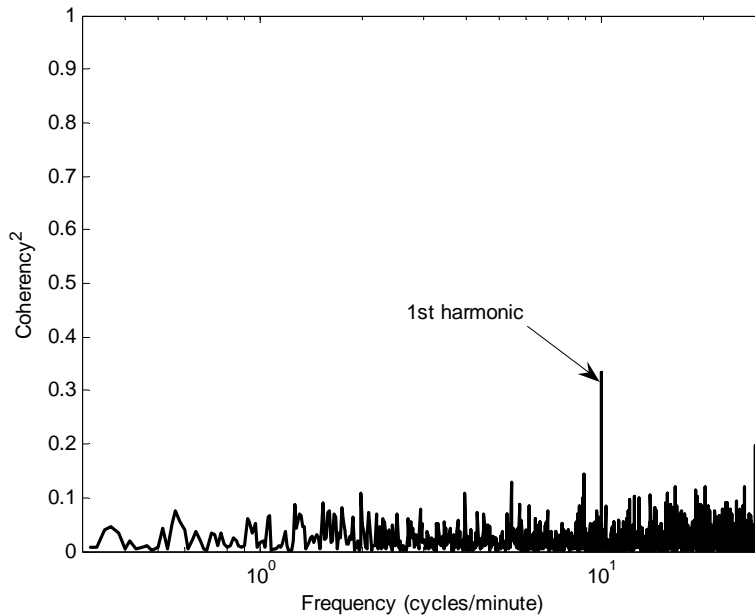


**Figure 7.15.** Coherency of  $I_A-I_B$  for the 1st-half of the data versus the 2nd-half of the data for the beacon simulation example (beacon amplitude = 0.02%, 48 hours of analyzed data, Dec. 5 – 6, 2004, Vista)

## 7.2 December 1, 2004

The Vista data from December 1, 2004 has a periodic signal that also provides some insight into a beacon’s performance. Figure 7.16 shows the a-phase current measured at Vista on December 1-3, 2004. Note that the current on December 1 has noticeably more noise. Figure 7.17 shows the PSD of the December 1 data; this compares with the mean of all other days shown in Figure 6.6. As can be seen in the PSD of Figure 7.17, there is a very large noise content near 3 cycles-per-minute, 6 cycles-per-minute, and 9 cycles-per-minute (all harmonics of 3 cycles-per-minute). This indicates the periodic signal with a fundamental frequency of 3 cycles-per-minute. The energy in the waveform is very large. This observation of an “beacon” that was not inserted by our experiment also points out that there are remote chances that such natural events could confound the efforts to locate an intentionally placed beacon. However, such an event is unlikely given that the vast majority of observed days were well behaved without such nature beacons. Furthermore, it is further unlikely that such a natural beacon would have the same frequency location and anticipated magnitude as for the intentionally placed one.

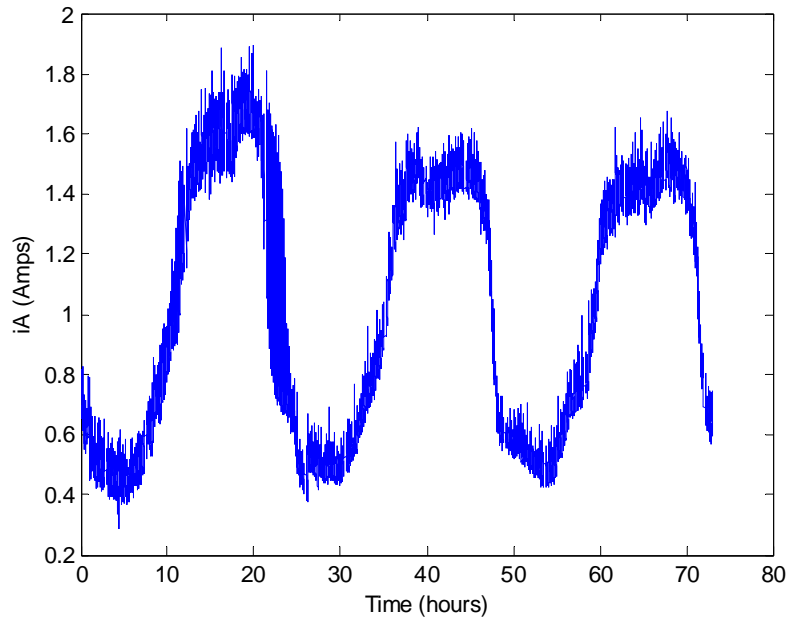


**Figure 7.16.** Normalized  $I_A$  for Vista on December 1-3, 2005

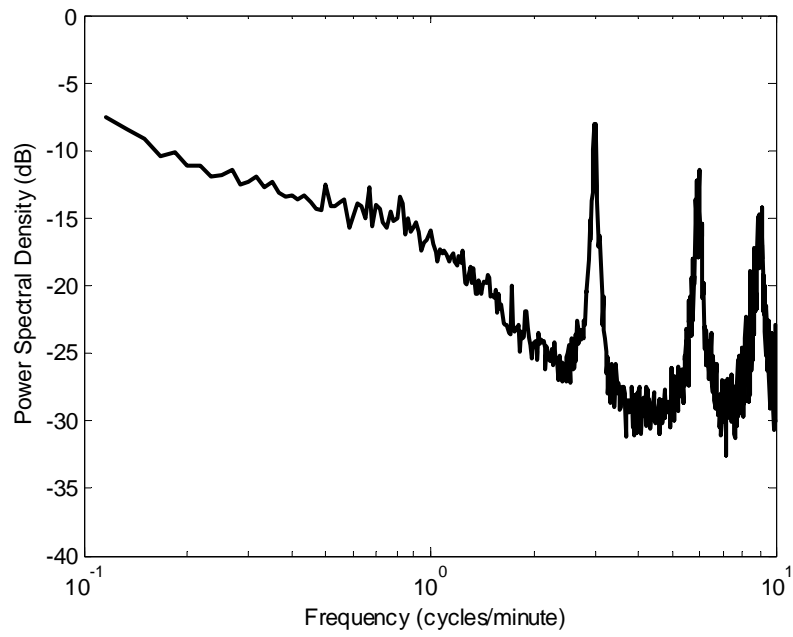


**Figure 7.17.** PSD of Vista  $I_A$ , Dec. 1, 2004



## 8.0 Laboratory Feeder Simulation

A laboratory feeder simulator, shown in Fig.8.1, allowed us to evaluate effects that could not be included easily in our analytical approach. Analyses necessarily ignored the effects of distribution transformers and distance and feeder line impedances. During analysis, beacon signals were mixed with a playback of measured data and detected using an industrial grade SCADA system as if the beacon had been placed in the substation. The laboratory simulator included a distributed feeder impedance model and the approximate electromagnetic coupling that should be anticipated between phases. The laboratory beacon existed at the low-voltage secondary of a transformer, the modeled distribution transformer.

The laboratory model also permits one to perform repeatable experiments that are not easily performed in the field. First, one can easily modify the simulated feeder and can place a beacon at any location on the simulated feeder.

One of the research questions that could not be answered well by either the analysis or field portions of this study concerned the effect that feeder line configuration would have on the observability of a beacon load. Many such configuration questions could be posed:

- How is beacon load observability affected by nearby distribution equipment like capacitor power factor correction banks?
- How does phase placement of a beacon load affect its observability? (*I.e.*, placement on delta vs. wye transformers)
- How is beacon load observability affected by how remotely the beacon load is located on an arterial feeder?
- Is the coupling between multiple feeder phases useful, or detrimental, to the observability of a beacon load?

Of these, we focused on the latter two questions.

### 8.1 Laboratory Feeder Model

The laboratory feeder model was designed to represent a “typical” feeder which was superimposed with recordings of actual feeder noise. The greatest challenge in the design of a laboratory feeder model is designing system scaling factors and impedances that will both emulate the important characteristics of a three phase feeder and maintain the relative accuracies of the SCADA metering equipment.

A decision was made to equally scale both phase voltage and system currents. The consequence of this decision is that system impedances are then the same as for the real field components. The base power of the laboratory feeder model is smaller than the modeled feeder by the square of the scaling factor used for both currents and voltages.

A second decision was made to select the scaled primary feeder voltage as 120VAC. This decision allowed us to use commercially available controllable ac load banks, which are designed to control 120VAC real and reactive loads, in our laboratory model to emulate the switching noise on feeder phases. An unfortunate consequence of this decision is that the modeling of secondary voltages then becomes very challenging when we modeled systems having a moderate or low primary phase voltage. For example, the feeder system shown in Figure 8.1 has a distribution transformer ratio for a 12kV primary. A 2.4kV primary, like that of Benton City substation, would require a very small secondary voltage that could not be accurately modeled and controlled.

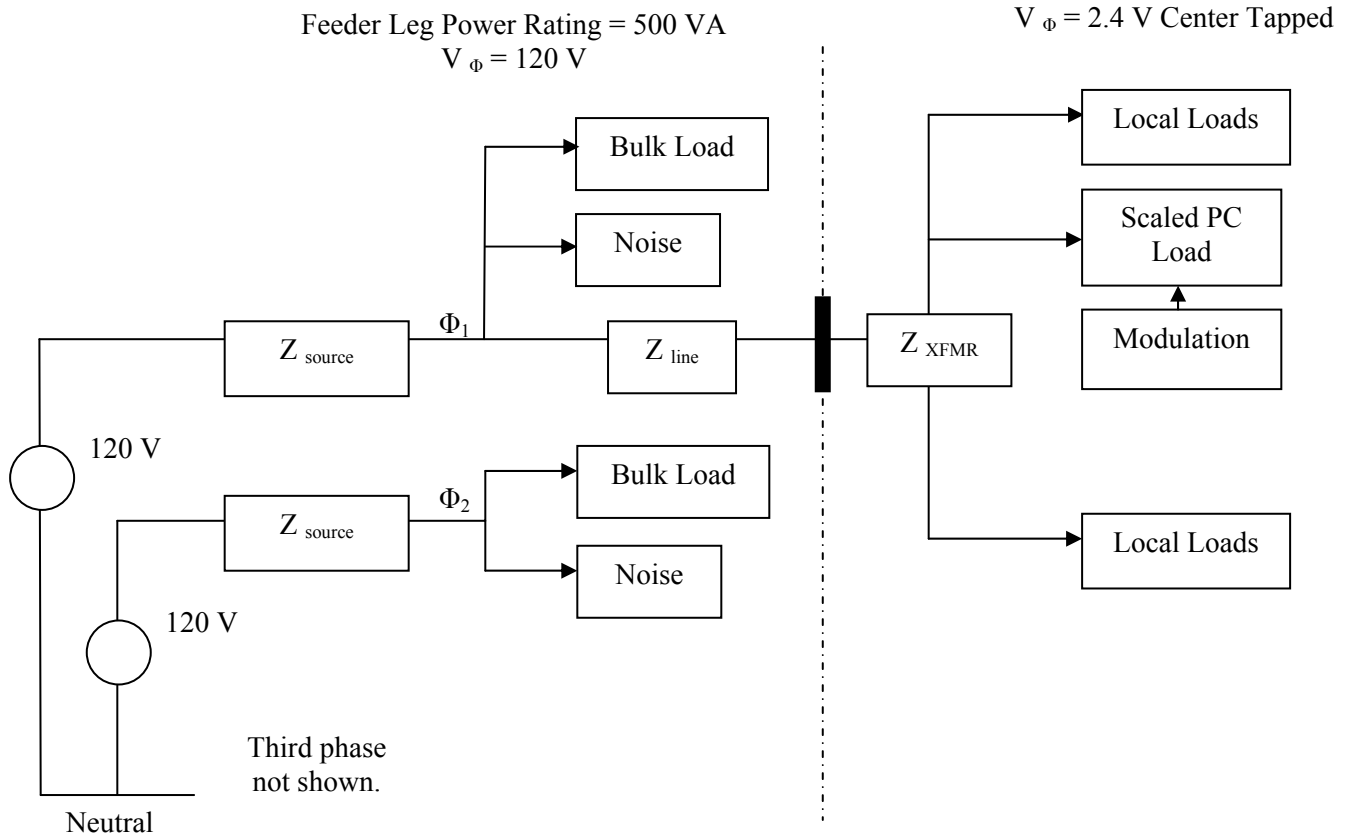


**Figure 8.1.** Laboratory feeder model line diagram

As stated above, the bulk phase loads are created in the laboratory by a combination of “dumb” loads like incandescent bulbs, and sophisticated NHR computer controlled loads. Two of the phases used the NHR loads, through which we played back scripts in real time of phase currents from Vista or Benton substations. The remaining phase used only a bulk, uncontrolled load to model the average phase current for that phase. The quality of the modeled current scripts were acceptable only when the computer controlled loads used more than 100 mA.

The controllable loads and “dumb” loads were electrically located at the extreme terminals of the distribution line emulator. The ac power source “substation” was connected to the other terminals of the distribution line emulator. The three-phase distribution line emulator was constructed of five boards, each representing approximately a mile of distribution line inductive and resistive impedance and mutual coupling between said phase conductors. As is typical for short distribution line models, no capacitive effects were modeled. The boards can be rewired to represent different feeder conductors and distances. A beacon can be moved away from or nearer to the substation by connecting the beacon at the terminals of any of the five emulator boards. While cleverly constructed, the details of the simulated distribution line test proved much less influential than actual feeder tests.

The primary voltage is generated by a three-phase California Instruments ac source. During all studies, the ac voltage was held constant. All feeder noise was emulated at the loads, not at the source.

## **8.2 Data Collection**

A diagram of the laboratory testing environment is shown below. Shown are all three phases, a neutral, and mutual inductance for the distribution feeders. Furthermore, a Schweitzer Engineering Laboratory protective relay (SEL 421) was used to provide the necessary transducers for the current and voltage inputs. The SEL-421 is a transmission line relay, however, it was not being used for any protective actions in this scheme. This relay was chosen instead of purchasing dedicated transducers that are required for the ABB remote terminal unit input. The relay is functionally equivalent to the transducers and such implementations are routinely seen in industry.

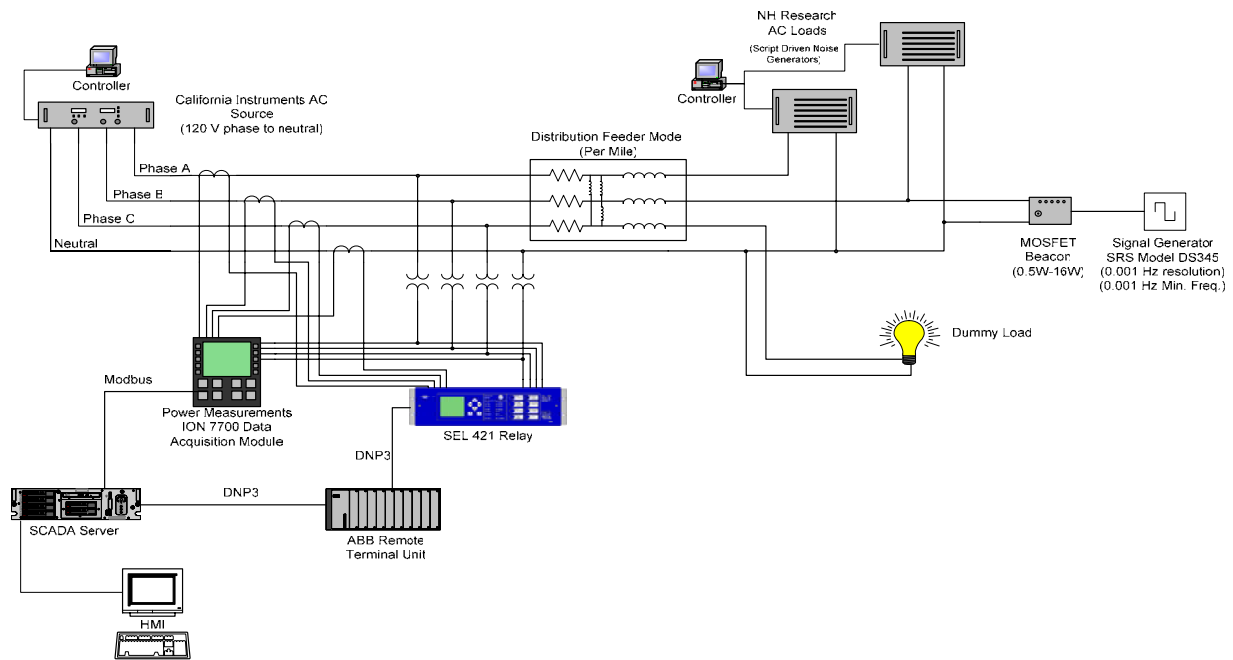


**Figure 8.2.** Laboratory equipment diagram for the scaled laboratory emulation of power grid beacon production and detection

Particular design effort was expended to assure that nominal feeder currents and voltages would register similarly for both a real feeder and for the laboratory model. If this were not the case, a bit of data would represent discrepant range for the real and simulated feeders. This is of greatest import where we desire to observe the smallest observable beacon signals, which must be similarly limited by the resolutions of both the real substation and the laboratory instrumentation. The selection of 120 V as the primary voltage base was fortuitous here because most substation voltage signals are nominally scaled to 120 V. The laboratory primary voltage could therefore be fed directly into the laboratories voltage monitoring equipment.

Similarly, substation current measurements are often scaled to a 5 A measurement scale, so the laboratory currents too could be maintained in a similar range using multiple turns of the primary current through a toroidal 5A current transformer.

The purpose of our selection of laboratory measurement equipment was to obtain laboratory measurements that would have identical bandwidth limitations and precision as can typically be had within a substation. The data path through the SEL-421 and ABB RTU (refer again to Figure 8.2) was thought to have representative capabilities to measurement equipment that would be found in substations. The Power Measurements Ion 7700 data acquisition module was initially included for collection of data at a much higher rate and greater resolution than we would obtain from the laboratory's SCADA data pathway. This distinction proved incorrect: we were able to obtain superior data resolution and speed directly from the SEL-421, especially using the PMU mode of the SEL-421. Neither the resolution of the

SEL-421 nor the data latencies of the RTU SCADA data pathways produced insightful limitations on data measurement in the laboratory. We eventually elected to simply use the PMU sampling function of the SEL-421, and decimated the fast data to represent the approximately 1-s sampling speeds that we had observed in the field at substations.

### 8.3 Laboratory Simulation Results

The simulations described in this section use a laboratory beacon power of about 0.4 W. The nominal primary feeder phase voltage was assigned as constant 120 V, and the average phase currents during the laboratory simulation were about 2 ampere. The two NHR controllable loads were configured to emulate scripts of feeder switching noise on two phases of a recorded Vista substation data script. Therefore, the common voltage and current scale factor in this simulation is about 100 and the beacon load constitutes about 0.06% of the total feeder load. Earlier analysis suggested that this magnitude of beacon load is about 3 times that of the minimum observable beacon load.

Initially, the beacon was switched on and off each 10 seconds (0.1 Hz).

Indeed, the beacon load power was easily observed in the PSD of its b-phase current, as is shown in Figure 8.3. Many odd harmonics of the fundamental are also observable. We observed the beacon power in only one of the three phases because there was no modeled wye-delta transformer that would have caused the beacon power to be spread across any other phases.

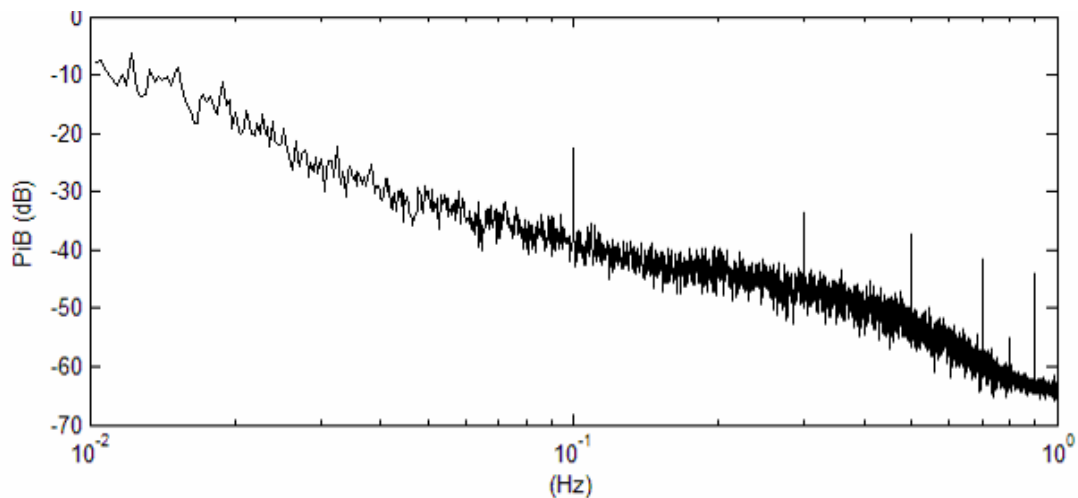


**Figure 8.3.** Laboratory PSD of b-phase data with a 0.1-Hz beacon load and 1 mile of simulated distribution line

Incidentally, the observation that no beacon power was observed in any other phase also suggests that the coupling between the modeled adjacent distribution lines, which we assert is typical for coupling between many distribution lines, was not significant enough to propagate the beacon signal from one phase current to another. We found no evidence that inter-phase magnetic coupling in a distribution line

would be either advantageous or detrimental to the observation of beacon loads of the type investigated here.

We also used this opportunity to exercise several of the differencing tricks that had been suggested during analysis. Figure 8.4 shows PSD plots using not only b-phase, but also several identified phase current differences and sums. Each subfigure shows a clear set of beacon fundamental and harmonic peaks. Note that each of the chosen differences and sums includes the b-phase current.

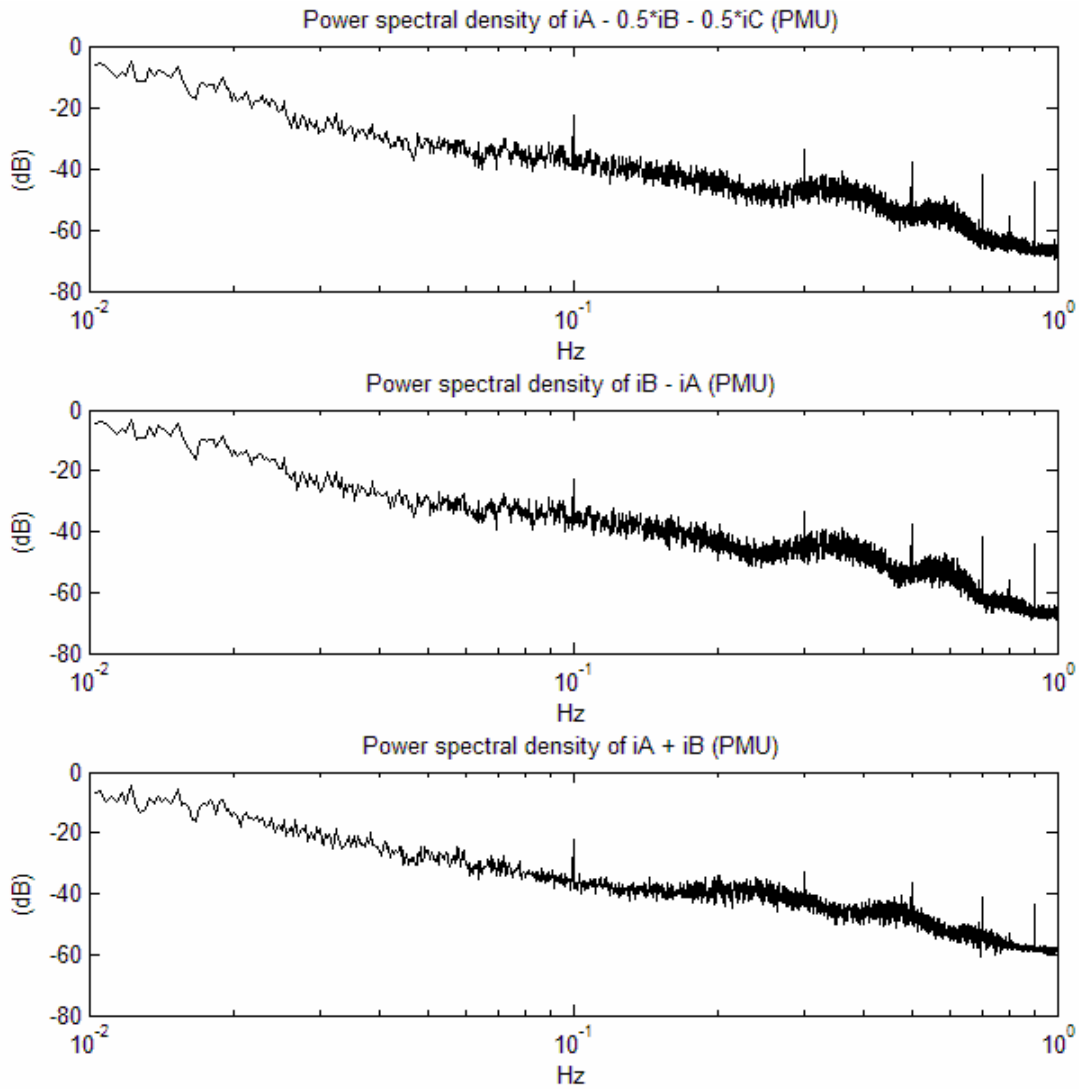


**Figure 8.4.** Laboratory PSD using differences of phase currents with 0.1-Hz beacon load and 1 mile of simulated distribution line

Then the simulated distribution feeder was made 5 times as long by using five of the board that simulate distribution line miles instead of just the one board that had been used in Figure 8.3 and Figure 8.4. The simulation was otherwise run identically using the same feeder load data. The results of this simulation are shown in Figure 8.5 and Figure 8.6. It appears that relative distribution line distance neither significantly degrades nor improves our ability to observe beacon loads of the type investigated here. This is a predictable outcome. A beacon load affects the bulk phase current. The switching of the beacon load is small, even when compared to slow SCADA data sampling rates. Furthermore, the impedances of distribution lines are small, so the effects of adding and removing small loads would not likely create interesting secondary effects.

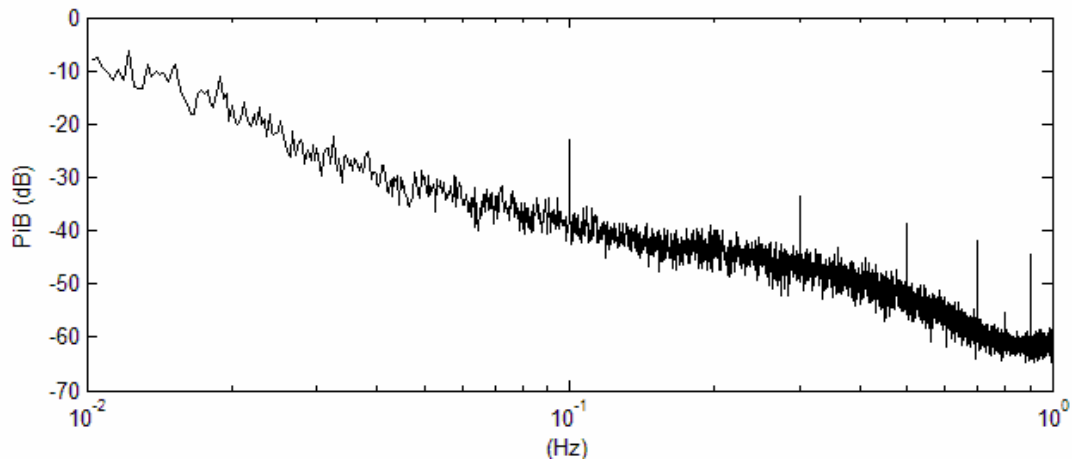


**Figure 8.5.** Laboratory PSD of phase data with a 0.1-Hz beacon load and 5 miles of simulated distribution line

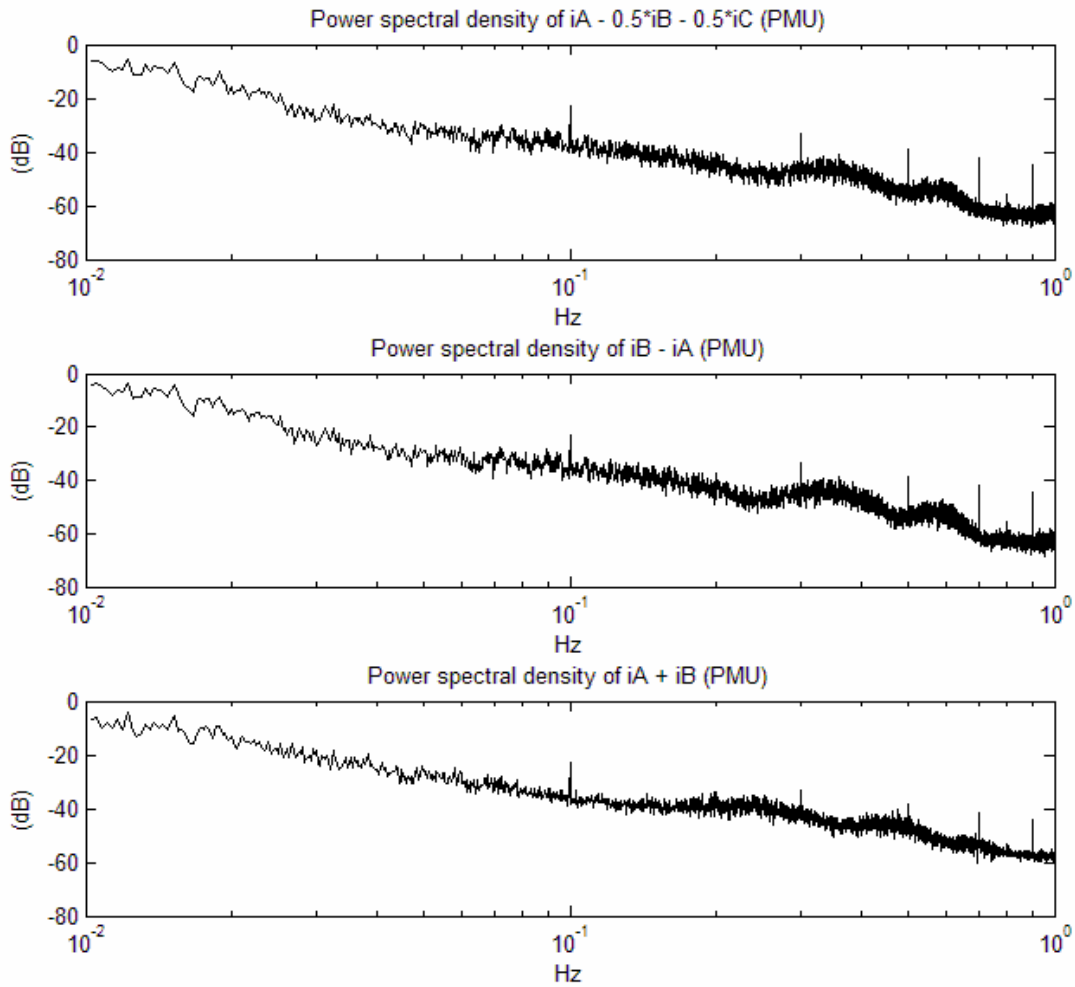


**Figure 8.6.** Laboratory PSD using differences of phase currents with 0.1-Hz beacon load and 5 miles of simulated distribution line

The simulation beacon load frequency was then doubled. Again, all other parameters and data scripts remained constant. The results are shown in PSD plots in Figure 8.7 and Figure 8.8. Except for the expected shift in the beacon load frequency and its harmonics, no other noteworthy observations can be made. A 0.2-Hz beacon load frequency was successful using the laboratory data collection equipment. This beacon frequency appears to adequately exceed the Nyquist frequency for this system.

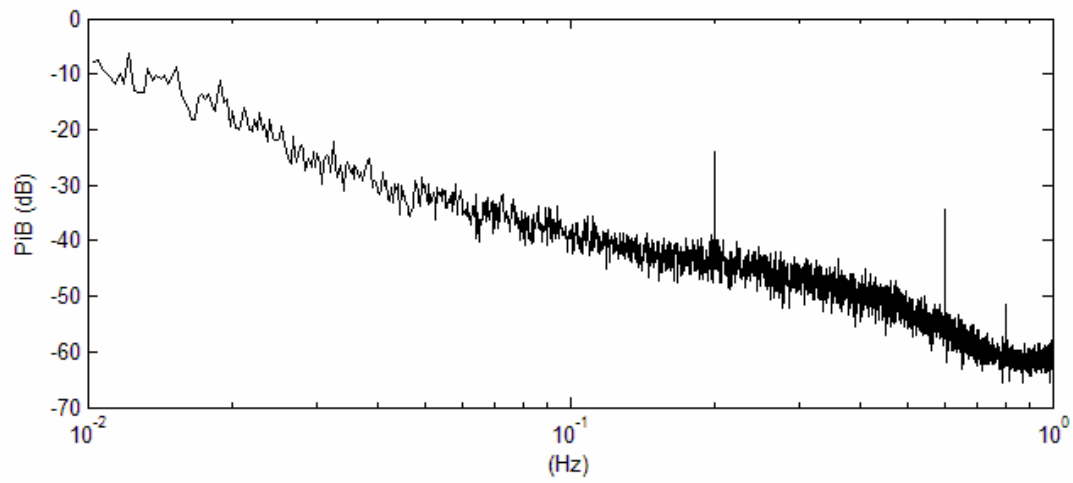


**Figure 8.7.** Laboratory PSD of b-phase current with a 0.2-Hz beacon load and 5 miles of simulated distribution line

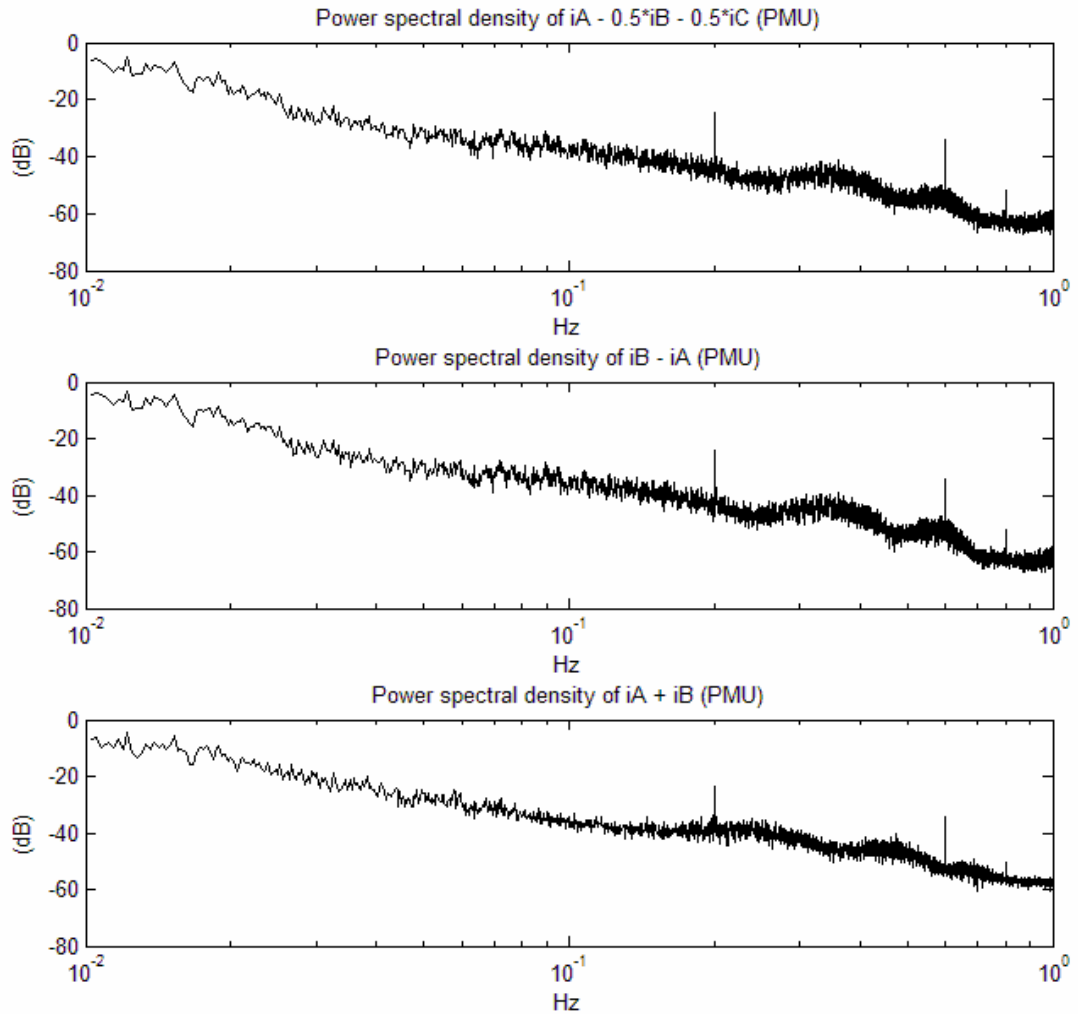


**Figure 8.8.** Laboratory PSD using differences of phase currents with a 0.2-Hz beacon load and 5 miles of simulated distribution line





## 9.0 Field Beacon Load Tests

Field tests were conducted in February and March of 2006 to verify four of the predictions that had resulted from our analytical study.

1. The analytical study had predicted that a beacon should be observable if its magnitude is approximately 0.02% of the average three-phase feeder load or larger. However, this prediction was tied to assumptions about the duration of the observation.
2. The analytical study had predicted that one's ability to detect a beacon among feeder noise is affected by the duration over which one is allowed to collect data. The longer one is able to collect data, the greater will be the likelihood that ambient current loads on the feeder will be uncorrelated and will cancel themselves out to reveal the coherent beacon. The estimate from the analytical study was that durations of a day are needed to reliably detect beacons of magnitude 0.02% of the average feeder load.
3. The analytical study had predicted that our ability to detect a beacon will be improved if we use a higher beacon frequency, as long as one does not operate too close to the Nyquist frequency of the data collection equipment.
4. The analytical study had predicted that differencing of phase currents might prove useful for improved detection of a beacon load.

A set of experiments was conducted to address each of these predictions.

### 9.1 The Field Beacon

Two field beacons were constructed for our field research. The first, constructed prior to analysis, was a 200W circuit that used a rectifier and an IGBT power electronic switch. This device was constructed because it emulated the types of power loads of interest to our project client. Specifically, it included an internal dc power bus as its power supply. After analysis, we concluded that this subtle distinction would not be important. Further, we also learned that our load must consume more power than could be generated by this circuit.

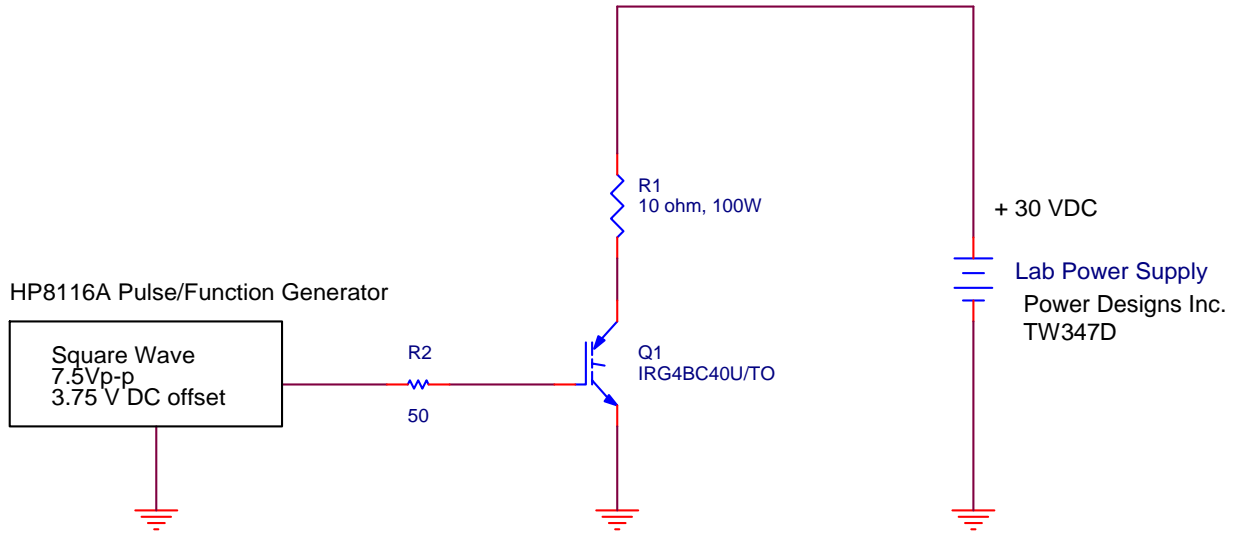


**Figure 9.1.** Original field beacon circuit with IGBT switch

It was determined that the beacon loads would need to control as much as 0.1% of a feeder's load. A beacon load on our Vista substation feeder, whereon much of the earlier analysis was conducted, would therefore need to control up to approximately 2.5kW.

A much simpler, more robust circuit was then constructed using an accurate electronic timer driving an electronic ac circuit relay. The output of the electronic relay was wired to a conventional 120V ac load receptacle flush mounted on the switch's enclosure. Portable space heaters were used as the switched ac beacon loads, which could be ganged in parallel at the receptacle to achieve various load magnitudes. This circuit worked well and could be safely operated at occupied buildings with confidence.

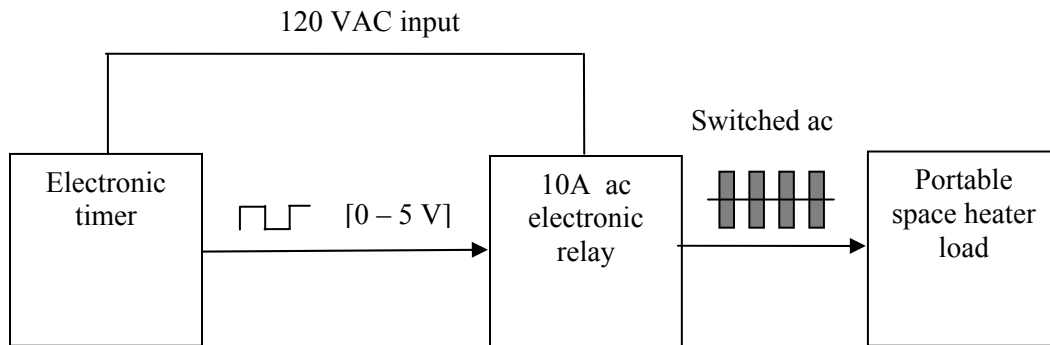


**Figure 9.2.** Final beacon load switch with function generator, electronic relay, and portable heater load



**Figure 9.3.** Picture of opened field-scale beacon load controller showing ac load plugs

The proprietor of a commercial shop at the Columbia Center Mall, served by the Vista substation feeder, permitted the beacon load to be placed in a custodian’s closet at his establishment. Placard warning signs were placed on the experimental apparatus to warn building occupants not to touch or unplug the beacon. The beacon load was permitted to operate unattended for extended periods of time and, to our knowledge, was never disturbed. Every several days, the beacon load magnitude or frequency were changed and recorded. Twice, the beacon load was turned off to again observe the quiescent background noise without the beacon load. This background serves as our comparison.

## 9.2 Data Collection

Data was collected remotely using the same Vista substation feeder radio telemetry equipment with which we had acquired the data used earlier for analysis. (Refer to Figure 4.1.) Unfortunately, the repeater telemetry from Vista substation had degraded during this period, and we had to acquire this data by wireless radio download from the substation gate instead of at our laboratory radio. Regardless, the use of Vista substation permitted us to perform field beacon detection work that was directly comparable to our analysis data at the same substation.

### 9.3 Field Results

At least twice during the field testing period, the field beacon load was turned completely off, and data was collected without a beacon to simply provide a background comparison. As one would expect, the characteristics of these PSD and coherency plots are similar to the data analyzed earlier for 12 hours worth of data at Vista substation. Note that the frequency scales here are represented in the unit  $s^{-1}$ , or Hz.

Figure 9.4 shows the simple PSD for each of the phase load currents calculated as for the earlier analysis. The data represents 12 hours of data during the spring day March 11, 2006 as measured at the Vista substation. Some frequency peaks are present. For example, a small peak appears near .11 Hz in all phases. The cause of this natural peak is not known. Such peaks will be shown later to be easily distinguished from beacon load peaks.

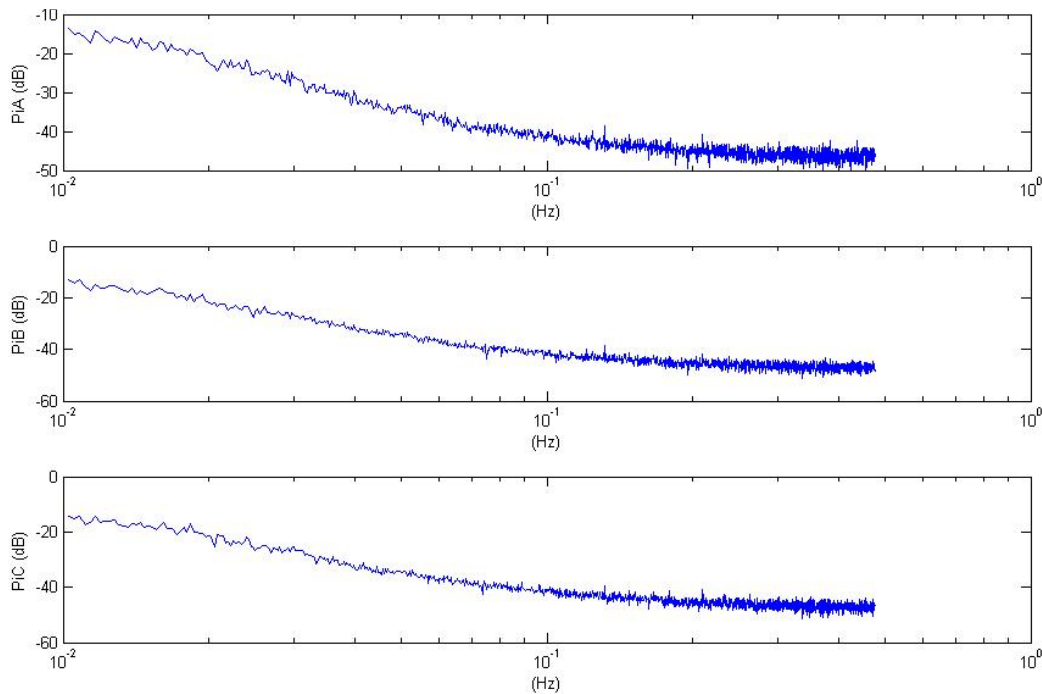


**Figure 9.4.** PSD of Vista field current data for each of the three phase currents without a beacon load (12-hour duration, March 11, 2006)

Figure 9.5 presents some of the power spectral density analysis techniques that had been applied earlier. It is not evident from these PSD plots that any significant reduction in common mode noise occurred that would be advantageous in practice. The data display no evident frequency peaks or other noteworthy artifacts.

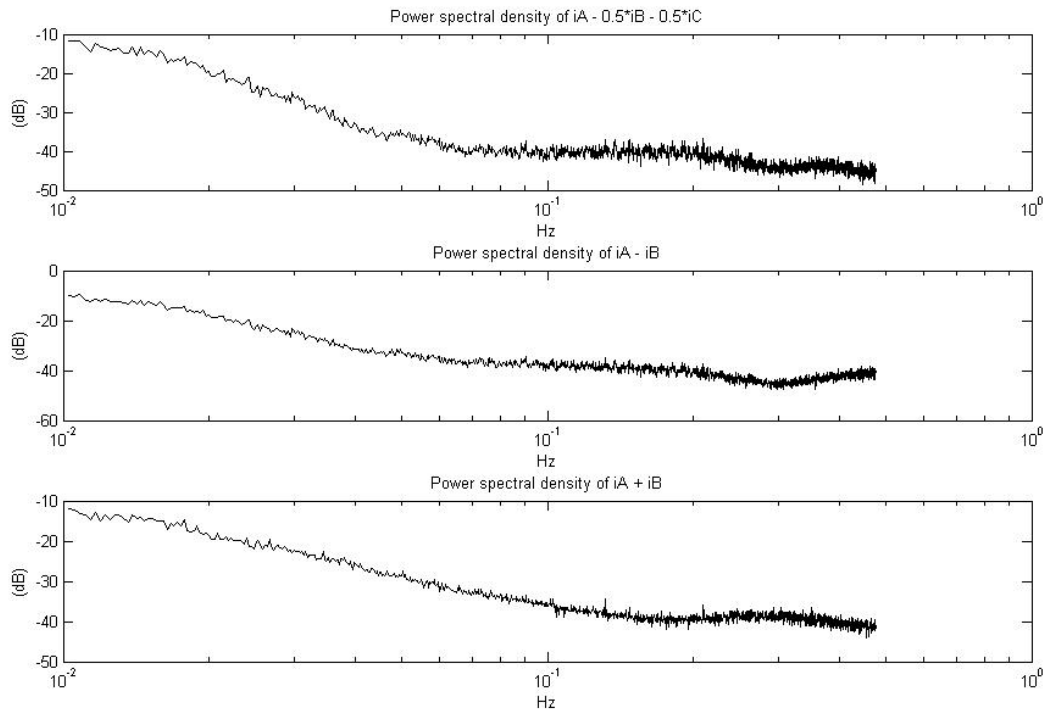
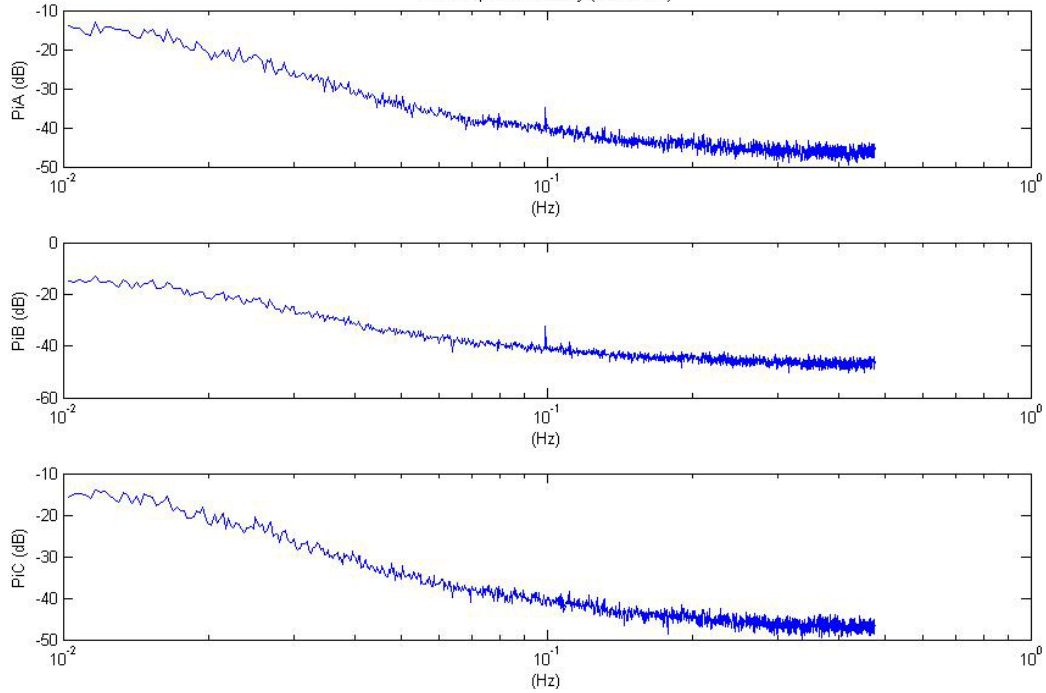


Figure 9.5. PSD of differential currents at Vista substation without a beacon load (24 hour duration, Mar. 11, 2006)

One of the first beacon loads applied in the field was created by using the beacon load controller of Figure 9.3 to switch a 1500-W portable heater load on and off every 10 seconds (0.1Hz). The magnitude 1500 W is approximately 0.04% of the average Vista feeder load and is therefore twice as large as analysis predicted it must be to be observed. The beacon frequency is near the 10 per minute frequency that was used frequently during analysis. The PSD was again calculated for each of the load currents from the Vista substation data for periods during which the beacon was active, as shown in Figure 9.6. We observe that the beacon peak appears in both a-phase and b-phase. This is thought to result from the use of a wye-delta distribution transformer configuration that distributes a single phase's current equally between two of the feeder's phases.

The next Figure 9.7 shows the power spectral densities for various sums and differences of phase current magnitudes as was suggested during analysis. The differencing of two phase currents had been advantageous during analysis, and we hypothesized that the differencing eliminated much of the uncorrelated noise. Here, we see a surprising result that the differencing of a- and b-phases also cancelled out the beacon power. The approach of differencing phase currents can therefore be fooled where the beacon power appears in both phases. There is no advantage for viewing the beacon in either of the plots using differencing in Figure 9.7, but the beacon was easily seen in the plot using the *sum* of a- and b-phase currents. This is an interesting observation. The sum of the incoherent noise in two or more phases should still be incoherent. Therefore, using sums of currents might prove beneficial where there is a possibility for the beacon to appear in multiple phases.



**Figure 9.6.** PSD of Vista substation currents with 1500-W, 0.1-Hz beacon load revealed on a- and b-phases (12-hour duration, Feb. 24, 2006)

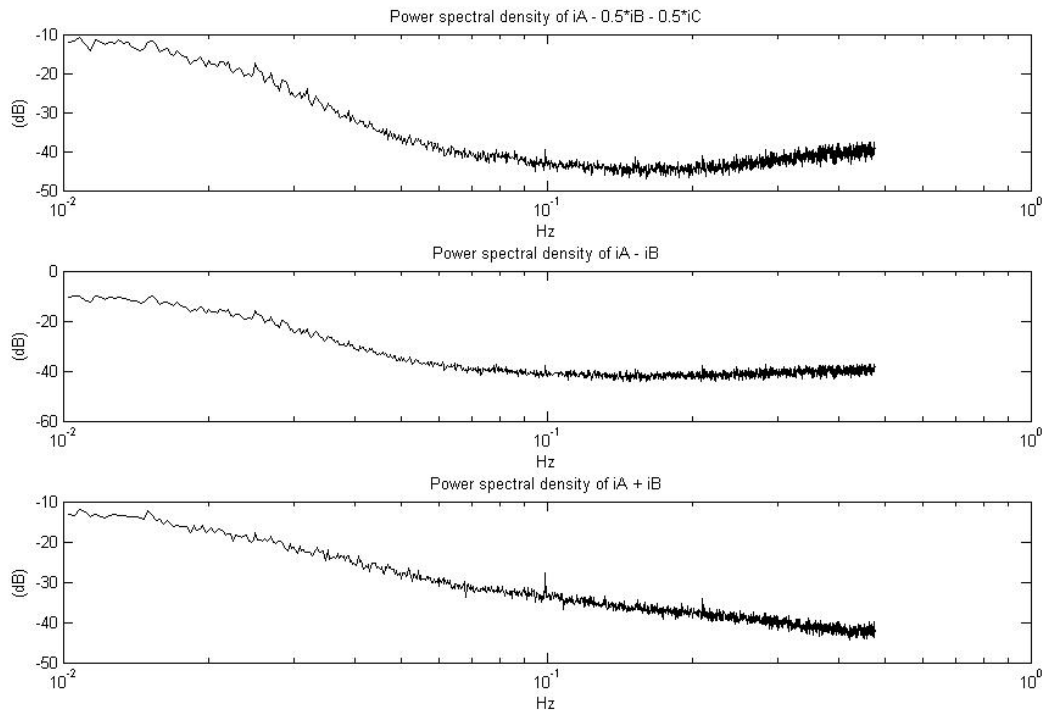


**Figure 9.7.** PSD of various phase current differences at Vista substation with a 1500-W, 0.1-Hz beacon load (24-hours duration, Feb. 24, 2006)

Next the experiment was repeated with half the beacon load at the same location. That is, the beacon's peak power was reduced to 750 W, approximately 0.02% of the average load. The PSD plots for the phase currents under these conditions are shown in Figure 9.8. Observe that beacon power is still evident, but it is revealed in b- and c-phases rather than a- and b-phases, as was observed earlier. We concluded, and later confirmed, that the beacon had become plugged into a different receptacle, one served by different phases, for this experiment.

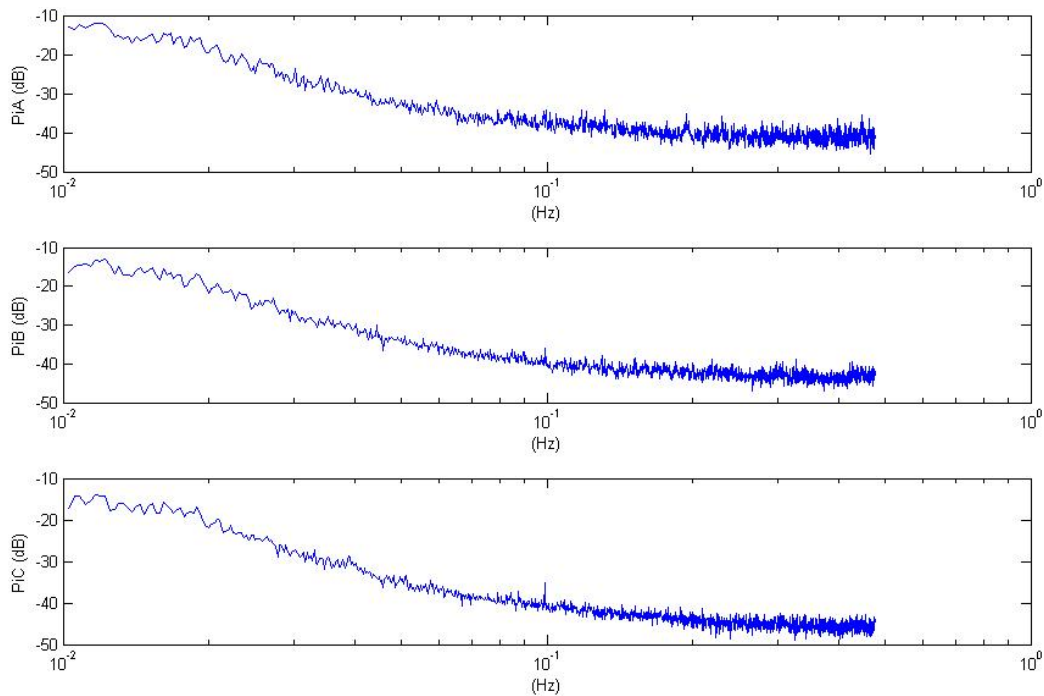


**Figure 9.8.** PSD for phase currents at Vista substation using a 750-W beacon at 0.1 Hz (12-hour duration, Mar. 18, 2006)

Another interesting anecdote occurred when the portable heating load for this experiment was inadvertently set on its “fan only” setting, which consumes only 30-W. No beacon peaks were evident for this condition, and technicians were sent back to the beacon to conduct troubleshooting.

The results shown in Figure 9.8 were observed to be repeatable, as is demonstrated in Figure 9.9, for which the same experiment was repeated with data from the following day. In this figure we observe similar beacon power peaks at similar spectral locations.

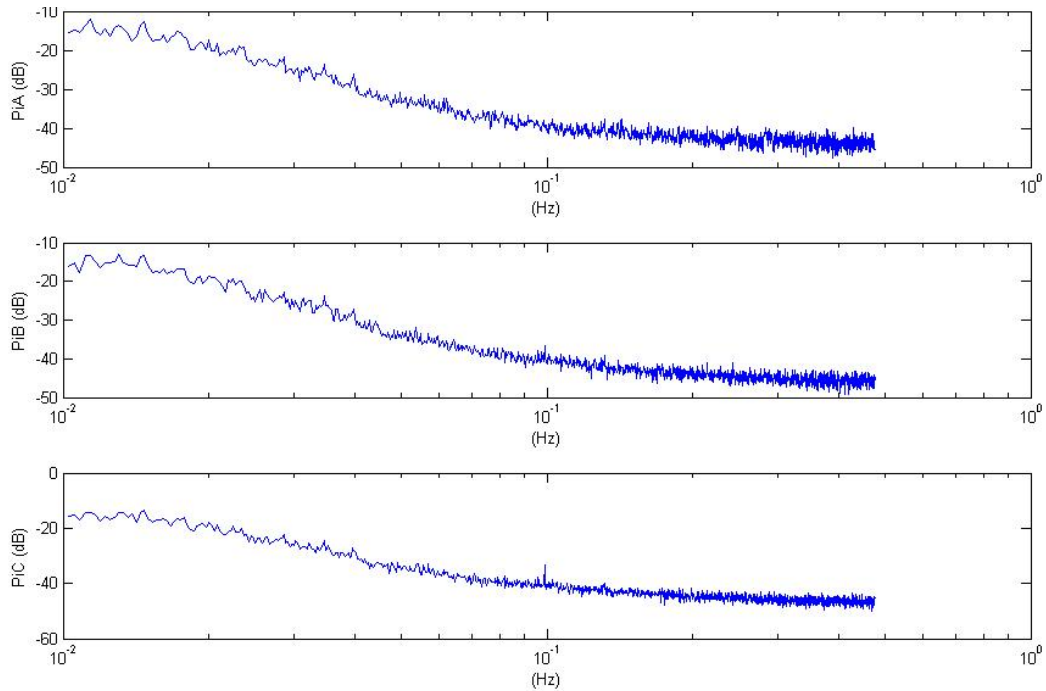


**Figure 9.9.** PSD for phase currents at Vista substation using a 750-W beacon at 0.1 Hz (12-hour duration, Mar. 19, 2006)

Next, we used smaller duration blocks of the data from Figure 9.9 to help us estimate a minimum duration over which data could be collected. Analysis had suggested that at least 12 to 24 hours would be needed for beacon observation. The PSD diagrams are shown as the data duration decreases from 12 hours to 6 hours and 3 hours in Figure 9.9 through Figure 9.11, respectively. While the beacon power peak is easily observed in the 6-hour data collection window of Figure 9.10, it is not clearly observable using the 3-hour data collection window. This series of figures illustrates the tradeoff between beacon magnitude and data collection window. A small beacon can be observed if one uses a long data collection window; a short data collection window will work if one uses a large beacon.

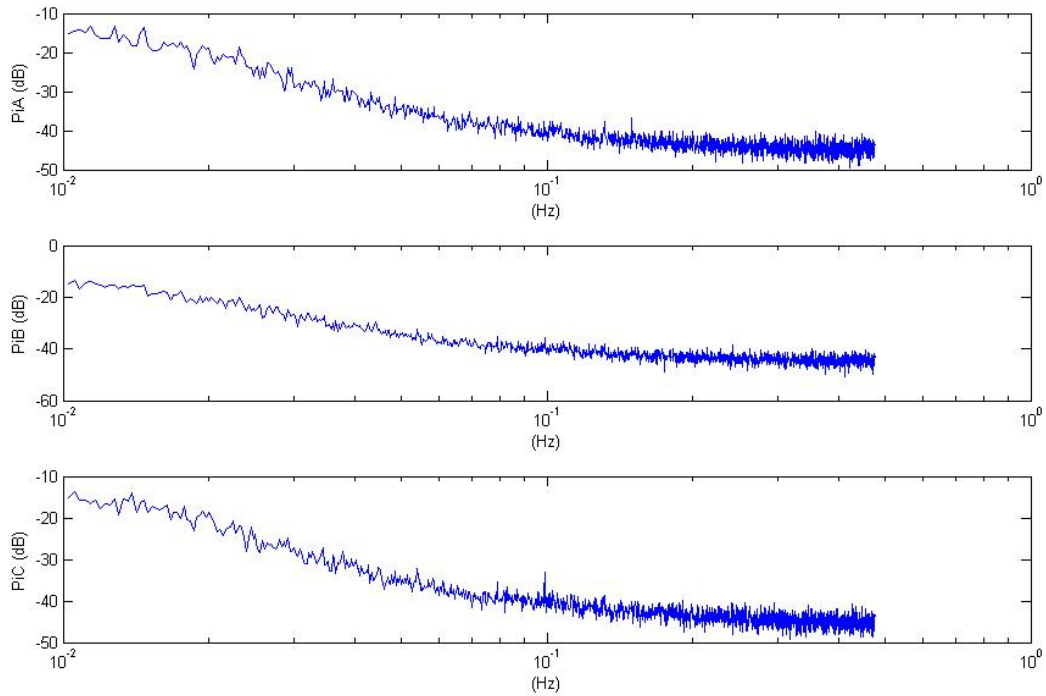


**Figure 9.10.** PSD for phase currents at Vista substation using a 750-W beacon at 0.1 Hz using reduced data collection duration (6-hour duration, Mar. 19, 2006)

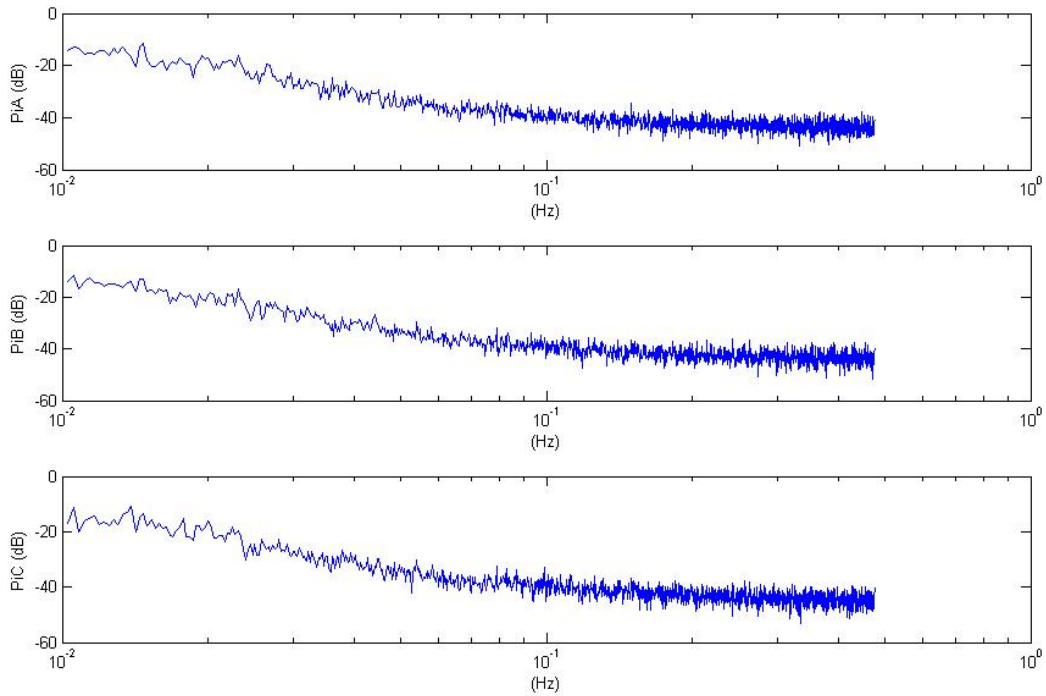


**Figure 9.11.** PSD for phase currents at Vista substation using a 750-W beacon at 0.1 Hz using reduced data collection duration (3-hour duration, Mar. 19, 2006)

The beacon load was again modified to double its switching frequency from 0.1 Hz (1 cycle every 10 seconds) to 0.2 Hz (1 cycle every 5 seconds). Our analysis had suggested that beacon frequency should be as high as possible, as long as the beacon's frequency remains well above the measurement equipments' Nyquist frequency. A series of PSD figures is now presented to show the higher frequency beacon as, again, the data collection duration is reduced from 12 hours to 3 hours.

The beacon is evident in at least the b-phase in Figure 9.12, for which 12 hours of data were used. The beacon power peak is marginally evident for the 6-hour (Figure 9.13) and 3-hour (Figure 9.14) data durations.

While the background PSD does indeed continue to diminish with increasing frequency, the uncertainty in its measurement also increases. That is, the PSD exhibits wilder, less predictable power excursions that begin to mask the beacon. These excursions become even wilder and less predictable with decreasing data window, and the beacon begins to become lost among the noise.

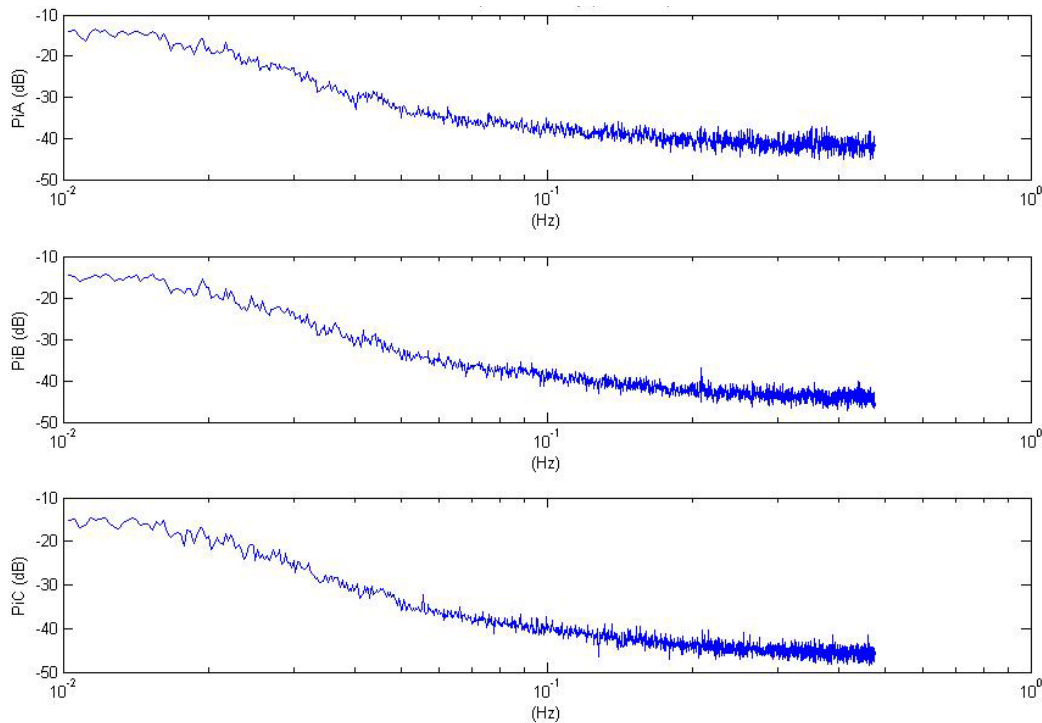


**Figure 9.12.** PSD for Vista substation currents using a 750-W, 0.2-Hz beacon load (12-hour duration, Mar. 22, 2006)

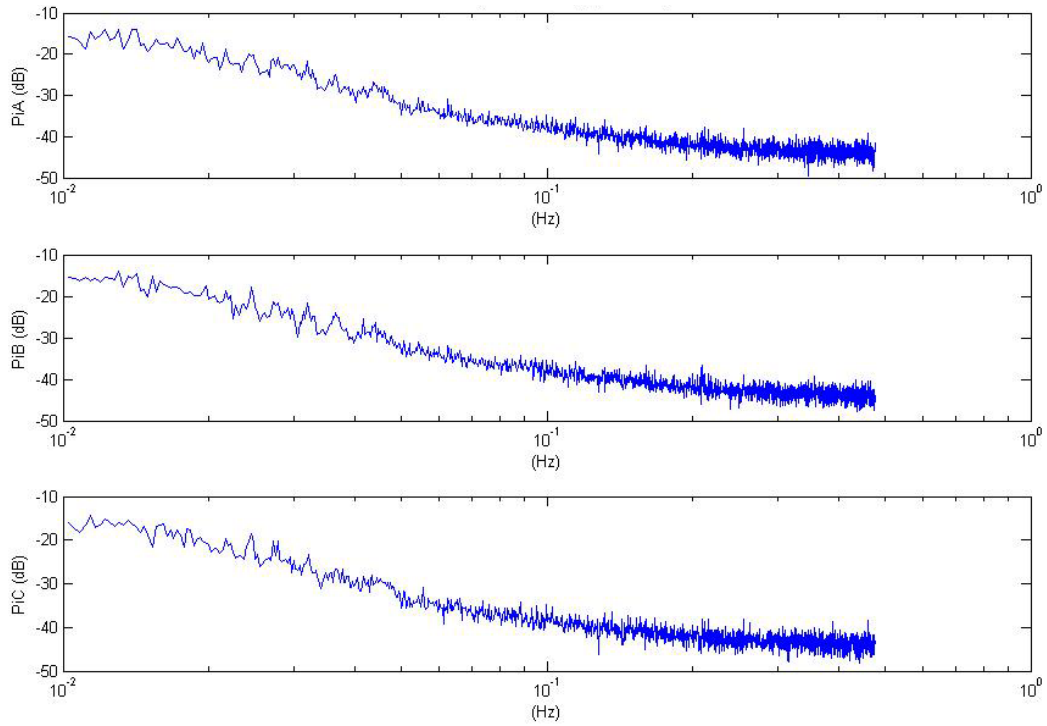


**Figure 9.13.** PSD for Vista substation currents using a 750-W, 0.2-Hz beacon load and reduced data collection duration (6-hour duration, Mar. 22, 2006)

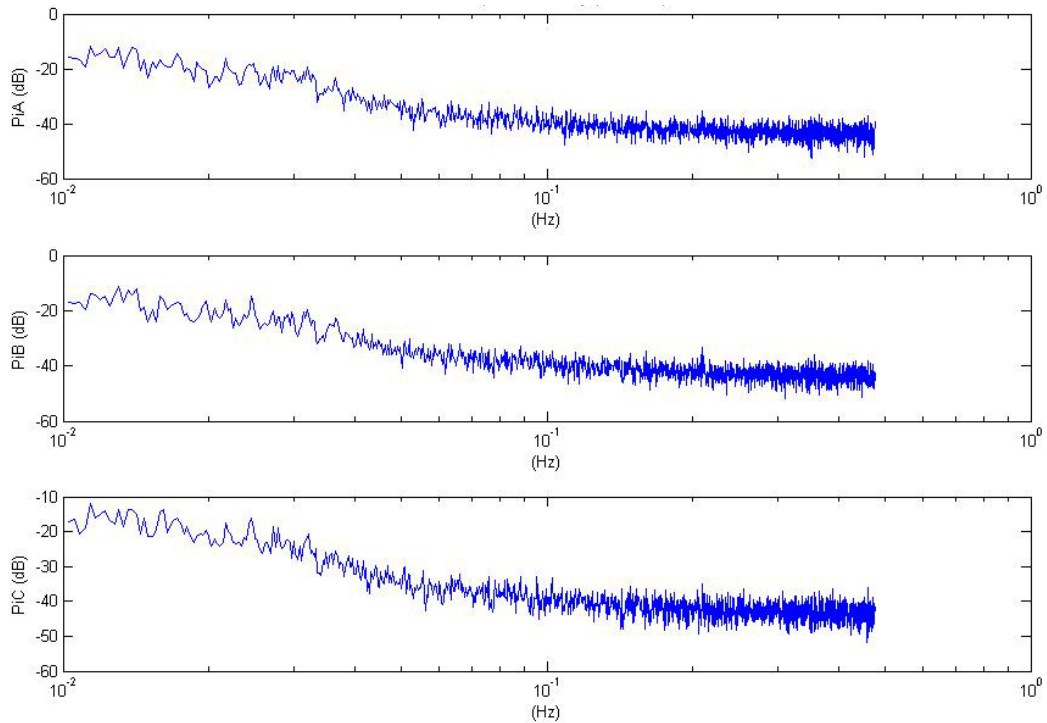


**Figure 9.14.** PSD for Vista substation currents using a 750-W, 0.2-Hz beacon load and reduced data collection duration (3-hour duration, Mar. 22, 2006)



## 10.0 Conclusions

This study has revealed several unique and pertinent properties of power system load feeder data. It is important to recognize that the conclusions are based on the data analyzed and observed through laboratory simulation and a specific field study.

1. Initial beacon simulations demonstrated the potential for using statistical spectral analysis to detect a periodic beacon. Both the power spectral density and correlation of time-separated signals proved to detect beacon signals.
2. There is no significant difference in the noise content of the phase current when comparing seasons (winter, spring, summer, and fall) based on the analyses of Vista and Benton City substation data that represent commercial and residential feeders. We lack adequate data to make this claim for agricultural or industrial feeders.
3. All noise tends to roll off at a rate of approximately  $-20\text{dB/decade}$  in the power spectrum. This finding was remarkably constant for all feeder data analyzed.
4. There is only a slight difference in the normalized noise content during light loading conditions versus heavy loading. Therefore, it is likely that if one can detect a beacon having a peak power  $0.05\%$  of the feeder's loading under a heavy loaded condition, then one could also detect a comparable beacon under a light loaded condition.
5. There is no significant difference between workday and weekend noise content for the analyzed feeders. This finding was unexpected.
6. When comparing time of day loading, the noise tends to be significantly less during the evening or nighttime hours. Therefore, smaller beacons could be detected during the nighttime hours.
7. At higher frequency, the phases tend to have significant common-mode noise. Calculating a phase difference or sum using  $I_A - 0.5I_B - 0.5I_C$  or  $I_A - I_B$  seems to provide the improved common-mode rejection. During field testing, it was observed, however, that the successful application of these differences depended upon transformer configurations between the substation and beacon. Beacon signals can be canceled too if the beacon appears on two phase currents because of a delta-wye transformer connection. Then the sum  $I_A + I_B$  becomes promising. Almost all combinations would need to be tried by trial and error unless one possesses detailed information about the exact phase connections in the feeder.
8. There is no measurable correlation between significantly time-shifted versions of the phase current. The time shift needs to be several hours. Because of this property, coherency analysis between time-shifted versions of the data may be an excellent detection tool. The use of coherency was not yet adequately assessed in laboratory simulations or field experiments.
9. The two analyzed substations have very similar noise amplitudes when comparing the normalized phase currents. After normalization of the feeder currents, the differences between feeders by

type, season, and time-of-day will likely become unimportant. Only the relative magnitude of the beacon load and its frequency are then important.

10. There is a trade off between the length data being analyzed versus the amplitude of the beacon that can be detected. For simulations conducted on the Vista substation data, a beacon amplitude of 0.02 - 0.05% of the feeder's average load is detectable if a one-half to one full day of data is collected and analyzed. But, if the analysis data is reduced to 6 hours or less, beacon powers in this range are difficult or impossible to detect. This observation, based on analysis, was later tested and proven using the full-scale beacon in the field.
11. We were able to obtain 1-s data bandwidth for load currents sampled at 3 of the 4 substations where we collected data. This data sample rate was perhaps 5 times faster than the rate that would be available centrally through existing SCADA. At the residential Benton City substation, data collection was limited to about 0.05 Hz by other communications equipment at the substation that was competing for metering resources.
12. A switched beacon load as small as 750 W, representing approximately 0.02% of the feeder load, was detected from substation data in the field using 6 – 12 hours of phase current data. As suggested by analysis, detection of this beacon became questionable as the data duration and beacon magnitude were reduced.
13. Beacons having cycle periods 5 and 10 seconds were detected in the field. Contrary to prediction, there was no clear benefit for using the higher frequency beacon load.
14. Based on laboratory simulation, the distance between the substation and beacon load does not seem to influence the beacons observability. There is some evidence that the beacon load current will not be appreciably coupled from one phase to another simply by distribution line magnetic coupling over distance.

## 11.0 Recommendations

In this section we propose further investigation that should be conducted to confirm findings. We also propose new, interesting directions to proceed with this line of research:

1. It has been concluded that the beacon frequency should be as high as possible given the bandwidth and sampling limitations of the data acquisition. To do this, one must know the bandwidth properties of the data acquisition. It is recommended that a study be conducted to characterize the bandwidth properties of typical sensor and data acquisition systems.
2. This study has employed statistical signal processing methods primarily based on fft averaging. Other signal detection methods used in combination with fft averaging or as an alternative to fft averaging may provide improved performance. It is recommended that a study be conducted to review and test state-of-the-art detection methods and base-line them against the methods used in this report. Such methods might allow detection of even signals that could not be detected by eye in this report.
3. Additional field beacon load studies should be conducted at a variety of locations and at different types of substations.
4. Potential applications of this technology should be suggested and verified. The present study did not emphasize applications for this technology.
5. The field study should be extended to determine whether the remotely obtainable SCADA data from a feeder, the type of data that is already routinely collected, can be used equally effectively. In this study, we assumed that we would have access to the substation, where one can often obtain higher-bandwidth data than is available centrally by SCADA.



## 12.0 References

Bendat J and A Piersol. 1993. *Engineering Applications of Correlation and Spectral Analysis*. John Wiley & Sons, Inc., New York.



## Distribution

No. of  
Copies

No. of  
Copies

OFFSITE (via email)

ONSITE

Client

(7) Pacific Northwest National Laboratory

Benton County Public Utility District  
Attn: Bryan Coyne  
Supervisor of Operations  
1500 S. Ely St.  
P.O. Box 6270  
Kennewick, WA 99336-0270

CA Bonebrake	K5-20
PA Boyd	K5-20
DP Chassin	K1-85
RT Guttromson	K1-85
DJ Hammerstrom	K5-20
N Lu	K5-20
JM Shaw	K5-20

Montana Tech  
Attn: Dr. Dan Trudnowski  
General Engineering Department  
1300 West Park Street  
Butte, MT 59701-8997